



Review

Review of high efficiency and clean reactivity controlled compression ignition (RCCI) combustion in internal combustion engines

Rolf D. Reitz ^{a,*}, Ganesh Duraisamy ^b^a Engine Research Center, Department of Mechanical Engineering, University of Wisconsin-Madison, 1018A Engineering Research Bldg, 1500 Engineering Drive, Madison, WI 53706, USA^b Department of Mechanical Engineering, Anna University, Chennai 600025, India

ARTICLE INFO

Article history:

Received 19 January 2014

Accepted 20 May 2014

Available online 3 August 2014

Keywords:

RCCI

HCCI

Fuel efficiency

Combustion

In-cylinder fuel blending

PCCI

NO_x

ABSTRACT

This article covers key and representative developments in the area of high efficiency and clean internal combustion engines. The main objective is to highlight recent efforts to improve (IC) engine fuel efficiency and combustion. Rising fuel prices and stringent emission mandates have demanded cleaner combustion and increased fuel efficiency from the IC engine. This need for increased efficiency has placed compression ignition (CI) engines in the forefront compared to spark ignition (SI) engines. However, the relatively high emission of oxides of nitrogen (NO_x) and particulate matter (PM) emitted by diesel engines increases their cost and raises environmental barriers that have prevented their widespread use in certain markets. The desire to increase IC engine fuel efficiency while simultaneously meeting emissions mandates has thus motivated considerable research. This paper describes recent progress to improve the fuel efficiency of diesel or CI engines through advanced combustion and fuels research. In particular, a dual fuel engine combustion technology called “reactivity controlled compression ignition” (RCCI), which is a variant of Homogeneous Charge Compression Ignition (HCCI), is highlighted, since it provides more efficient control over the combustion process and has the capability to lower fuel use and pollutant emissions. This paper reviews recent RCCI experiments and computational studies performed on light- and heavy-duty engines, and compares results using conventional and alternative fuels (natural gas, ethanol, and biodiesel) with conventional diesel, advanced diesel and HCCI concepts.

© 2014 The Authors. Published by Elsevier Ltd. This is an open access article under the CC BY-NC-ND license (<http://creativecommons.org/licenses/by-nc-nd/3.0/>).

Contents

1. Introduction	14
2. Experimental engine and computational models	16
2.1. ERC engine specifications	16
2.1.1. Heavy-duty engine data acquisition systems and hardware	16
2.1.2. Light-duty engine data acquisition systems and hardware	16
2.1.3. ERC computational models	18
2.1.4. Fuel and injector details	19
2.1.5. Fuel introduction strategies	19
3. Results and discussion	19
3.1. Dual fuel HCCI and PCCI combustion using in-cylinder fuel blending	19
3.1.1. Selection of baseline fuel reactivity and EGR	20
3.1.2. Dual-fuel operation	20
3.1.3. Comparison of dual fuel combustion modes	21
3.2. Comparison of low temperature combustion strategies	22
3.2.1. Baseline operating conditions	23
3.2.2. Intake temperature sensitivity and controllability: primary reference fuels	24

* Corresponding author. Tel.: +1 608 262 0145; fax: +1 608 262 0167.

E-mail address: reitz@engr.wisc.edu (R.D. Reitz).

3.2.3.	Intake pressure sensitivity and controllability: primary reference fuels	24
3.2.4.	Combustion phasing sensitivity and controllability: pump fuels	25
3.3.	Fuel reactivity controlled RCCI combustion – HD engines	26
3.3.1.	Effect of first and second main injection timings (SOI-1 and SOI-2)	26
3.3.2.	Effect of SOI-1 fuel quantity	27
3.3.3.	Effect of IVC timings (effective compression ratio)	27
3.3.4.	Mixing and auto-ignition processes in RCCI combustion	31
3.4.	RCCI combustion using fuel additives (single fuel strategy)	32
3.5.	Comparison of single and dual fuel strategies	35
3.5.1.	Dual fuel – gasoline/diesel light load operation	35
3.5.2.	Comparison of injection strategies	37
3.5.3.	Intake temperature effects	38
3.5.4.	RCCI operation at idle	38
3.6.	RCCI- A pathway to controlled high efficiency and clean combustion	38
3.6.1.	Dual direct injection RCCI combustion to control UHC and CO emissions	41
3.6.2.	Comparison of conventional diesel and RCCI combustion	43
3.7.	RCCI operation toward 60% thermal efficiency	44
3.8.	RCCI operation with conventional and alternative fuels (mid and high loads)	48
3.8.1.	Reactivity reduction and enhancement strategies	48
3.8.2.	Engine operating condition and charge preparation strategies	49
3.8.3.	Gasoline–diesel (G/D) and E85–diesel (E85/D) strategies	49
3.8.4.	Mid load G/D and E85/D comparisons	49
3.8.5.	Combustion and emission comparisons	50
3.8.6.	Methanol/diesel reactivity controlled compression ignition (RCCI) engine	51
3.8.7.	Hydrogen addition to DME/CH ₄ dual fuel RCCI engine	52
3.9.	Extension of RCCI to LD engines	52
3.9.1.	Comparisons of RCCI combustion between HD and LD engines	52
3.9.2.	Methods to reduce heat transfer losses in LD engines	53
4.	RCCI For improved efficiency and low emissions on a multi-cylinder LD diesel engine	55
4.1.	Dual fuel modeling and experiments	55
4.1.1.	RCCI multi-cylinder experiments	55
4.2.	Effect of alternative fuels on RCCI performance and emissions	56
4.2.1.	Heavy-duty engine natural gas – diesel RCCI operation	56
4.2.2.	Use of E85–diesel in a light-duty multi-cylinder engine	57
4.2.3.	Effect of DI fuel (diesel & 3% 2-EHN doped gasoline) properties on engine gross thermal efficiency	59
4.3.	Piston bowl optimization for RCCI combustion in a LD multi-cylinder engine	60
4.3.1.	Cylinder balancing with RCCI	60
4.3.2.	RCCI piston design	61
4.3.3.	Experimental results of optimized LD RCCI pistons	62
4.4.	Efficiency and emissions mapping of RCCI in the LD diesel engine	64
4.5.	Use of low pressure direct injection for RCCI LD engine operation	64
4.6.	Effect of biodiesel blends on RCCI combustion in an LD multi-cylinder diesel engine	66
4.7.	RCCI combustion phasing control during load transitions	66
5.	Conclusions and scope for future work	67
5.1.	Scope for future work	68
	Acknowledgments	69
	References	69

Abbreviations

aTDC	after top dead center	DTBP	di-tertiary butyl peroxide
AHRR	apparent heat release rate	DPF	diesel particulate filter
BMEP	brake mean effective pressure	EPA	environmental protection agency
BDC	bottom dead center	ERC	engine research center
BTE	brake thermal efficiency	FTP	federal test procedure
CO	carbon monoxide	FSN	filter smoke number
CDC	convention diesel combustion	gIMEP	gross indicated mean effective pressure
CI	compression ignition	GDI	gasoline direct injection
CN	cetane number	GTE	gross thermal efficiency
CA50	crank angle of 50% heat released	GIE	gross indicated efficiency
CFD	computation fluid dynamics	GDBF	gasoline/diesel blend fuels
CRI	common rail injection	HCCI	homogeneous charge compression ignition
CAD	crank angle degree	HT	heat transfer
DI	direct injection	HTHR	high temperature heat release
		HTR	high temperature reaction
		HD	heavy-duty

HCII	homogeneous charge induced ignition	PFI	port fuel injection
IC	internal combustion	PLIF	planer laser induced fluorescence
ISFC	indicated specific fuel consumption	PRF	primary reference fuel
IVC	intake valve closing	PRR	pressure rise rate
LDEF	Lagrangian-drop and Eulerian fluid	rpm	revolution per minute
LTHR	low temperature heat release	R	gas constant
LNT	lean NO _x trap	RCCI	reactivity controlled compression ignition
LTC	low temperature combustion	RCM	rapid compression machine
LTR	low temperature reaction	RI	ringing intensity
LD	light-duty	SCR	selective catalytic reduction
MPRR	maximum pressure rise rate	SCOTE	single cylinder oil test engine
MFB50	50% mass fraction burned	SOI	start of injection
MCE	multi-cylinder engine	SI	spark ignition
NMEP	net mean effective pressure	TDC	top dead center
NO _x	oxides of nitrogen	UHC	unburned hydrocarbon
OEM	original equipment manufacturers	VGT	variable geometry turbine
PM	particulate matter	°CA	degree crank angle
PCCI	premixed charge compression ignition	γ	specific heat ratio
PCI	premixed compression ignition	2-EHN	2-ethylhexyl nitrate
PDPA	phase Doppler particle analyser		

1. Introduction

Diesel engines are widely used for transportation and power-generation applications because of their high fuel efficiency. However, diesel engines can cause environmental pollution owing to their high NO_x and soot emissions. Considerable effort has thus been devoted toward reducing these pollutant emissions as these have adverse effects on the environment and human health [1]. Revolutionary in-cylinder combustion strategies and exhaust emission aftertreatment systems are required to meet stringent emission regulations. Emission aftertreatment devices, however, have problems in terms of their cost and durability. Since emission aftertreatment systems such as Diesel Particulate Filters (DPF), Lean NO_x Trap (LNT) and Selective Catalytic Reduction (SCR) systems also often increase fuel consumption, in-cylinder technologies for emission reduction have therefore been the focus of intense research [2]. Indeed, the US National Science Foundation (NSF) and Department of Energy (DOE) have formed a partnership for a program targeting a 25–40% improvement in fuel economy in light duty vehicles and the attainment of 55% brake thermal efficiency in heavy-duty engine systems. Developing engine technologies to achieve these targets while meeting emission mandates will require substantial research progress, even beyond that made so far. The NSF/DOE program solicitation [3] provides more information on “big picture” challenges that may be the focus of research in the next few years.

From the above discussion it is inferred that to maximize overall engine efficiency, an engine should minimize the need for after-treatment emission reduction. Accordingly, reduction of NO_x and soot in-cylinder has been investigated by many researchers. Most of the current strategies can be placed in the category of premixed Low Temperature Combustion (LTC). Lower combustion temperatures result in NO_x reduction due to the high activation energy of the NO formation reactions [4]. In addition, utilizing long ignition delay times allows adequate time for mixing prior to the start of combustion; thus, rich regions in the combustion chamber are reduced and soot formation is inhibited.

In an effort to reduce NO_x and soot emissions in-cylinder, while maintaining high thermal efficiency, many new compression ignition combustion strategies have been proposed. One of the simplest methods of achieving low NO_x and soot emissions in a CI engine is HCCI combustion. Although HCCI combustion appears to be

thermodynamically attractive, the controllability challenge (ignition timing control and rate of heat release control) raised by the HCCI concept over conventional engines, which results from the near constant volume combustion, leads to very rapid rates of heat release and hence a very rapid rates of pressure rise. In order to maintain control over the combustion process on a cycle-to-cycle basis, coupling between the fuel injection event and the combustion event is desired [5]. This has prompted a trend in the engine research community to study PCCI combustion, which is a hybrid between HCCI and conventional DI CI combustion. In order to maintain the coupling between the start of fuel injection and the start of combustion, in the case of PCCI the fuel is injected early during the compression stroke to promote fuel-air mixing before ignition and thus can avoid high NO_x and soot formation rates.

Many researchers have shown that HCCI and premixed charge compression ignition (PCCI) concepts are promising techniques for simultaneous NO_x and soot reduction [6–12]. In addition to significant NO_x and soot reductions, premixed LTC operation can provide fuel efficiency advantages due to reduced combustion duration and lower heat transfer (HT) losses. But HCCI and PCCI combustion generally suffer from high levels of carbon monoxide (CO) and unburnt hydrocarbon (UHC) emissions. However, in recent years several researchers have demonstrated that boosted HCCI and PCCI combustion can exhibit nearly 100 per cent combustion efficiency [13,14]. These improvements came through the use of piston designs featuring minimum crevice volumes, as well as use of high intake pressures.

A recent review of the fundamental phenomena governing HCCI operation is given by Saxena et al. [15] who placed particular emphasis on high load conditions. Emissions characteristics were discussed, with suggestions on how to inexpensively enable low emissions of all regulated emissions. First, a review of hydrocarbon fuel decomposition was presented, including the chemical pathways for low and intermediate temperature chemistry and hot ignition. The characteristics of different fuels were discussed, with focus on single- and two-stage ignition, the influence of molecular structure on fuel vaporization, and the fuel characteristic referred to as ϕ sensitivity. Next, the importance of the in-cylinder charge conditions was discussed. This included a review of different types of EGR and its effects, and the importance of thermal and mixture stratification. The operating limits that govern high load operation were also discussed in detail, and finally a review of recent

research, which expands the high load limits of HCCI, was discussed. Although this article focused on the fundamental phenomena governing HCCI operation, it was also useful for understanding the fundamental phenomena in other kinetically controlled combustion concepts, including reactivity controlled compression ignition (RCCI), partial fuel stratification (PFS), partially premixed compression ignition, spark-assisted HCCI, and all forms of low temperature combustion (LTC).

Saxena et al. [15] systematically identified the fundamental phenomena influencing operation at high load and concluded that, despite the substantial improvements to LTC engines in recent years, additional research challenges still remain. They pointed out that more research is required to translate promising high load operating strategies to cover the full engine load and speed ranges, while simultaneously addressing the control complexities that occur in multi-cylinder engines. Better understanding is required of the chemical kinetic processes leading to intermediate temperature heat release with certain fuels, and better explanations are required to understand the reported qualitative observation that fuels that exhibit Low Temperature Heat Release (LTHR) tend to be more sensitive to equivalence ratio (ϕ -sensitivity). As ringing (large amplitude pressure oscillations) is one of the principal constraints that dictate high load limits, better fundamental understanding is required of this phenomena. Research efforts to improve the ringing intensity correlation are underway, and better quantitative understandings of how ringing impacts heat loss being obtained. Unburned hydrocarbon and carbon monoxide emissions from certain LTC operating regimes are also a problem that requires further research, and aftertreatment technologies must be developed to address this problem while considering the lower exhaust gas temperatures from LTC and HCCI engines. Finally, Saxena et al. [15] concluded that beyond simply expanding the load limits, better integration of LTC engines in power generation or vehicle powertrain systems is required. To cite a specific example, practical deployment of high load LTC or HCCI engines will require turbochargers that are designed for the unique operating conditions of these engines.

Musculus et al. [16] described recent research in optically accessible engines and combustion chambers, and proposed conceptual models for low temperature combustion (LTC). The models are based on multiple optical diagnostic observations and homogeneous reactor simulations using detailed chemical kinetic mechanisms. The models describe low-load, single-injection, partially premixed compression ignition conditions with high EGR rates (oxygen concentrations in the range of 10–15%), and consider the spray formation, vaporization, mixing, ignition, and pollutant formation and destruction mechanisms that are consistent with experimental observations in LTC diesel engines. Two separate subcategories were offered for either heavy-duty, large-bore or for light-duty, small-bore engines. Relative to the conventional diesel conceptual model of Dec et al. [17], the features of LTC conceptual models include longer liquid-fuel penetration, an extended ignition delay that allows more premixing of fuel, a more distinct and temporally extended two-stage ignition, more spatially uniform second-stage ignition, reduced and altered soot formation regions, and increased over-mixing, leading to incomplete combustion.

Extensive research has also been conducted on diesel PCCI at Lund University [18], which has revealed that the traditional NO_x – soot trade-off that exists in conventional diesel combustion can be defeated by diesel PCCI with high EGR rates in excess of 65% and use of a reduced compression ratio (e.g., 12.4). The high levels of EGR required the reduced compression ratio and, in addition, wall wetting issues associated with early injection of diesel fuel (due to its high boiling point) showed that diesel fuel is not an ideal candidate for PCCI operation. Kalghatgi et al. [19] discovered that,

for a given set of operating conditions and the same combustion phasing, operation with less reactive gasoline produced a much longer ignition delay, which facilitates premixed combustion, resulting in lower NO_x and soot emissions. Accordingly, gasoline PCCI has been studied by many engine researchers (e.g., Dec et al. [20], and Dempsey and Reitz [21]).

Indeed, experiments conducted by Bessonette et al. [22] suggested that the best fuel for HCCI-type operation may have auto-ignition qualities between those of diesel fuel and gasoline. Gasoline's resistance to auto-ignition can be exploited to extend the pre-combustion mixing time, but at low load the poor auto-ignition qualities of gasoline can make it difficult to achieve combustion. Conversely, diesel fuel has better auto-ignition qualities, but requires high levels of EGR for appropriate combustion phasing as the engine load increases.

Similarly, Park et al. [23] also investigated the effect of blending gasoline with diesel on fuel properties, droplet atomization, combustion performance, and exhaust emission characteristics of gasoline–diesel direct blended fuels in a four-cylinder diesel engine with a common rail system. In this study it was found that the gasoline fraction decreased the fuel density, kinematic viscosity, and surface tension. The droplet size of the fuel was measured using a phase Doppler particle analyser (PDPA). Park et al.'s investigation revealed that addition of gasoline reduced the temperature of the 10% distillation point and decreased the droplet size due to increased droplet instability due to decreased surface tension. The results also indicated that the addition of gasoline extended the ignition delay and thus provided a more homogeneous mixture. These combustion characteristics caused the simultaneous reduction in NO_x and Soot emission. Thus, the investigation provided valuable insights about the effect of blending gasoline with diesel.

An experimental investigation was carried out by Valentino et al. [24] to study the performance and emissions of a high speed diesel engine fueled with *n*-butanol/diesel blends on a turbocharged, water cooled, DI diesel engine, equipped with a common rail injection system. This work aimed at achieving simultaneous reduction in NO_x and smoke emissions, without significant penalties on engine efficiency using fuel blends with a low cetane number and high resistance to auto ignition under premixed low temperature combustion conditions. In that context, *n*-butanol was identified as a fuel for blending with diesel. The higher volatility and high resistance to auto ignition quality of *n*-butanol-diesel (20% and 40% of *n*-butanol by volume) blends improved engine emissions with a low penalty on fuel consumption.

Inagaki et al. [25] investigated dual-fuel (premixed iso-octane and direct injected diesel) premixed compression ignition (PCI) operation with the objective of reducing the EGR requirements of PCI strategies. In that investigation, they were able to operate up to 12 bar IMEP in the PCI mode. From these studies it can be concluded that different fuel blends could be required at different operating conditions, i.e., a high cetane fuel at light load and a low cetane fuel at high load. Thus, it is desirable to have the capability to operate with fuel blends covering the spectrum from neat gasoline to neat diesel fuel, depending on the operating regime. Accordingly, one strategy proposes the injection of low cetane number (CN) fuel (low reactivity fuel) in the intake port, and early cycle DI of high cetane number fuel (high reactivity fuel). This has been called RCCI by Kokjohn et al. [26]. RCCI is a dual fuel engine combustion technology that uses in-cylinder fuel blending with at least two fuels of different reactivity, and multiple injections to control the in-cylinder fuel reactivity to optimize the combustion phasing, duration and magnitude. The process involved in RCCI includes the introduction of a low reactivity fuel into the cylinder to create a well-mixed charge of low reactivity fuel, air and recirculated gases. The high reactivity fuel is then injected before ignition of the

premixed fuel using single or multiple injections directly into the combustion chamber.

The RCCI concept has been shown to provide better control of combustion compared to other strategies, such as dual fuel HCCI, dual fuel PCCI and single fuel PPC, and high thermal efficiencies approaching 60% have been demonstrated with this concept. Thus, the present review emphasizes experimental and computational works on RCCI using a variety of fuel combinations, including gasoline–diesel (G/D), ethanol–diesel (E/D), gasoline–biodiesel and gasoline–gasoline with small additions of cetane number improver (2-EHN and DTBP). In this paper gasoline–gasoline doped with 2-EHN or DTBP is also referred to as a “single fuel” strategy since so little additive is required, and other fuel combinations are referred to as dual-fuel strategies.

2. Experimental engine and computational models

RCCI combustion has been investigated on Heavy-Duty (HD) and Light-Duty (LD) engines at the Engine Research Center (ERC) of UW-Madison and at the Oak Ridge National Laboratory (ORNL). The heavy-duty engine is a 2.44 L Caterpillar 3401 single cylinder oil test engine (SCOTE) and the light-duty engines include single cylinder and four-cylinder General Motors (GM) 1.9-L common rail diesel engines. The HD engine EGR system comprises an electrically driven supercharger and a diesel particulate filter (DPF), to prevent fouling of the EGR cooler and supercharger. The EGR supercharger was implemented as a pump to maintain constant EGR levels with constant surge tank pressures as the DPF fills. Conversely, the use of the supercharger in this manner allows experimentation with more than practical turbocharger efficiency levels, especially if the pressure difference between the intake and exhaust surge tanks is small. However, effort was made to avoid such conditions. The multi-cylinder LD engine is also equipped with a variable geometry turbocharger (VGT), and an electronic EGR valve with a high pressure loop EGR cooling system. The HD and LD engine geometries are shown in [Tables 1 and 2](#) and the experimental set ups are shown in [Figs. 1 and 2](#).

2.1. ERC engine specifications

2.1.1. Heavy-duty engine data acquisition systems and hardware

In the ERC's heavy duty engine the cylinder pressure was measured with a Kistler model 6043 Asp/6061C water-cooled pressure transducer in conjunction with a Kistler model 510 charge amplifier. Acquired cylinder pressure traces were averaged for 500 cycles. Intake air flow was measured using choked flow orifices. To obtain choked flow for a variety of engine operating conditions, combinations of six different sized orifices were used to gain the desired intake air flow rate. The intake air was heated with two immersion-style heaters with PID control to ± 1 °C. Both the intake and exhaust system surge tank pressures were equipped with PID control to ± 0.7 kPa. PM measurements were performed with an AVL model 415S smoke meter. PM measurements of FSN, mass per volume (mg/m^3), and specific emissions (g/kWh) were related with the factory AVL calibration and averaged between five samples of a 2 L volume each with paper-saving mode off. All gaseous emissions measurements were performed with a five gas emissions bench. The EGR rate was determined through the ratio of intake CO_2 to exhaust CO_2 levels. Gaseous emissions were averaged for 30 s after attaining steady state operation.

2.1.2. Light-duty engine data acquisition systems and hardware

In the ERC and ORNL LD engines high speed combustion data was acquired using Kistler model 6058A pressure sensors installed in the glow plug ports of all 4 cylinders. Individual Kistler type 5010

Table 1
HD engine geometry [8].

Base engine type	Caterpillar SCOTE
Bore × stroke	13.72 × 16.51 cm
Connecting rod length	26.16 cm
Squish height	0.157 cm
Piston pin offset	None
Displacement	2.44 L
Geometric comp. ratio	16.1:1
Swirl ratio	0.7
Bowl type	Open crater
Number of valves	4
IVO	-335° aTDC
IVC	-85° and -143° aTDC
EVO	130° aTDC
EVC	-355° aTDC

dual-mode amplifiers were used to process the pressure signals and a combustion package from National Instruments (Drivven) was used to process the data. Cylinder pressure was pegged to the intake manifold pressure near the end of the intake stroke. Pressure was taken at 0.2° crank angle intervals and resolved for 500 cycles. Engine performance and emissions data were sampled at 1 Hz within the Dyne Systems Cell Assistant data acquisition program. Diesel fuel flow measurement was carried out using a Micro Motion CMF type Coriolis mass flow sensor. Gasoline fuel flow was measured gravimetrically using a Sartorius CP34001S weighing balance connected to the low speed data acquisition system. Steady state engine-out carbon monoxide (CO), carbon dioxide (CO_2), hydrocarbon (HC), oxides of nitrogen (NO_x), and oxygen (O_2) concentrations were measured using California Analytical gas analyzers. PM emissions were monitored by measuring the filter smoke number (FSN) using the AVL model 415s smoke meter.

The engine and injection controls were managed using the National Instruments Labview based Drivven control unit, which was equipped with the injector drivers for both direct injection (DI) of diesel fuel and port fuel injection (PFI) of gasoline. The same controller was able to simultaneously manage both injection systems while running the engine map. The Drivven system allows for full user control over engine parameters and was programmed to allow individual injection control for start-of-injection (SOI) timing, number of injection events and injection duration for each DI diesel injector, as well as injection duration for each PFI gasoline injector. This setup allowed the operator to manually adjust the fueling duration and timing for cylinder-to-cylinder balancing. This setup also allows for dual-fuel operation in a single or a few cylinders, while traditional diesel-only operation can be maintained in the other cylinders, aiding in diagnostic and troubleshooting. Boost pressure was controlled by demanding a boost set point using vane position controls on the variable geometry turbocharger. The intake

Table 2
LD engine geometry [94].

Engine type	GM DI diesel engine
No. of cylinders	4
Displacement	1.9 L
Boe × Stroke	82 × 90.4 mm
Compression ratio	17.5
No. of Valves/Cyl.	4
Injection system	Common rail
Injector location	Centrally mounted
Rated power	110 kW @ 4000 rpm
Rated torque	315 Nm @ 2000 rpm
IVO	361° aTDC
IVC	588° aTDC
EVO	112° aTDC
EVC	356° aTDC

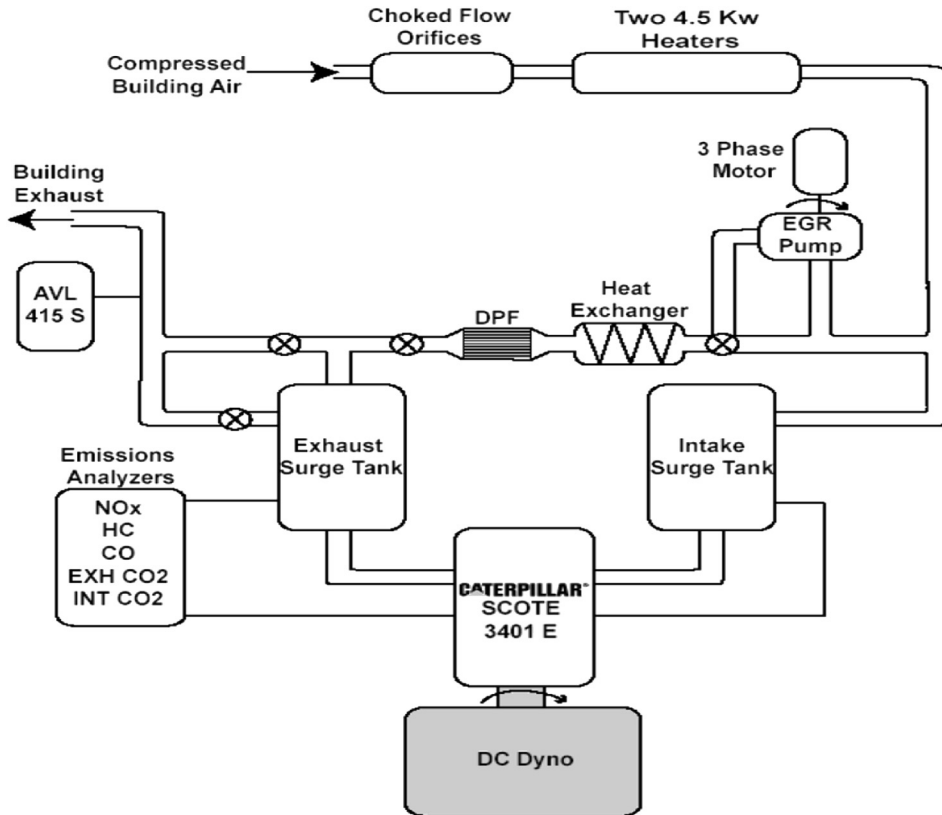


Fig. 1. HD engine set up [8].

charge temperature was controlled by adjusting the amount of process water to an air-to-water charge air cooler. This was done manually using a ball valve on the inlet side of the charge air cooler allowing the intake temperature to be controlled to within a few

degrees. The test engine was equipped with a variable swirl actuator in one of the intake ports. A fully open swirl valve (minimum swirl ratio) and a fully closed valve (maximum swirl ratio) correspond to a swirl valve angle of 0° and 90° , respectively.

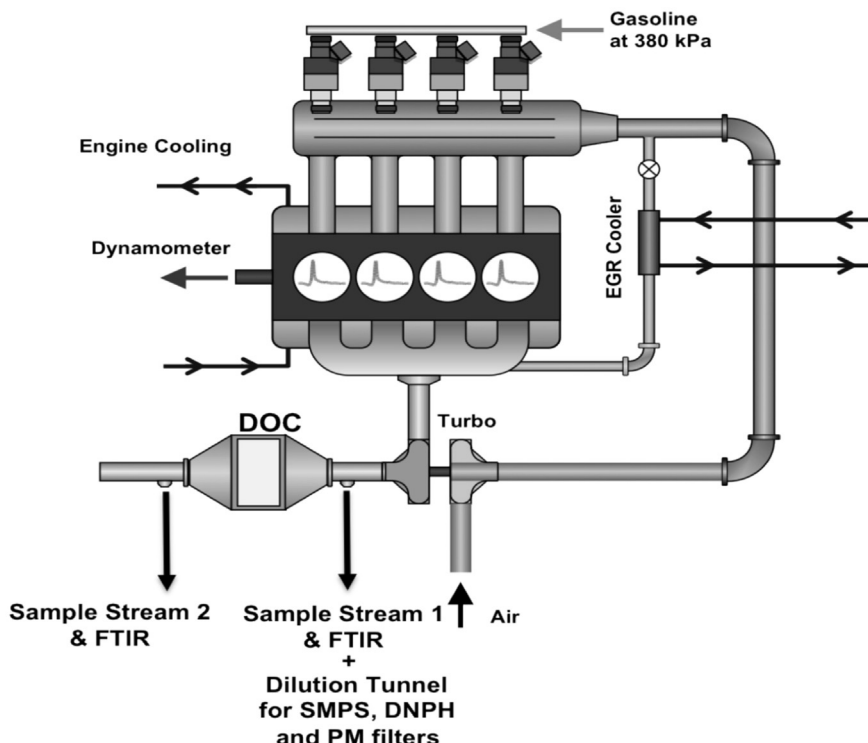


Fig. 2. Multi-cylinder LD engine set up [94].

The intake manifold was modified to allow the PFI injectors to spray directly into the non-swirl actuated intake port of the engine. The gasoline PFI injectors at cylinders 2, 3 and 4 were positioned similar to traditional PFI installations, however, the position of the cam-driven high pressure fuel pump necessitated the installation location of the PFI injector for cylinder 1 to be on top of the intake manifold and aimed at the intake port as shown in Fig. 3. This was preferred rather than modifying the high-pressure fuel pump for the diesel fuel injection system, since cylinder 1 is located at the end of the intake manifold and the PFI injector has a narrow spray angle such that the fuel should get into the port without much mass transfer to the other cylinders.

An automotive fuel pump and a custom fuel rail were installed to meet the needs of the PFI gasoline system. The fuel rail was mounted on a support near the engine and connected to each injector with braided metal covered fuel lines. An automotive pressure regulator was used to maintain the correct rail pressure of 380 kPa. Fig. 4 shows the installed gasoline fuel system. The return flow from the gasoline fuel rail was cooled and returned to the supply line downstream of the fuel flow meter.

2.1.3. ERC computational models

Engine combustion simulations were performed using the KIVA-3v release 2 code [27] with improvements to many physical and chemistry models, which have been developed at the ERC [28–31]. The KIVA-3v code was coupled with the CHEMKIN II solver for detailed chemistry calculations. In the models the chemistry of gasoline and diesel fuel were represented by iso-octane and *n*-heptane, respectively. A reduced reaction mechanism made up of 45 species and 142 reactions [32] described the combined oxidation of *n*-heptane and iso-octane, since many studies (e.g., Ra and Reitz [33]) have shown that the combustion characteristics of gasoline and diesel are closely represented by iso-octane (i.e., PRF 100) and *n*-heptane (i.e., PRF 0), respectively. This approach has also been shown to yield acceptable agreement for blends of gasoline and diesel fuel (e.g., Kokjohn et al. [8], Hanson et al. [34], and Splitter et al. [35]).

The physical properties of diesel fuel for spray and mixing processes were represented by tetradecane. Of course, the multicomponent vaporization of the actual diesel fuel used in the experiments was not captured by this approach (i.e., the distillation curve of diesel fuel is not reproduced). Therefore, it is possible that differences between single and multicomponent vaporization result in differences in the fuel distribution prior to and during combustion. Indeed, PCCI combustion has been shown to be very

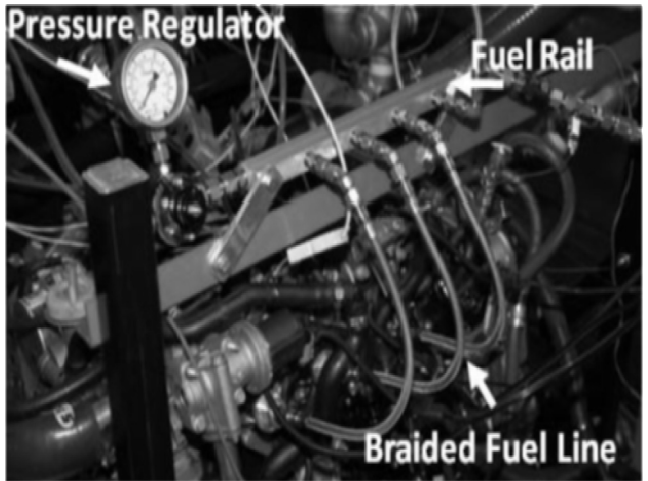


Fig. 4. Installed gasoline PFI system [90].

sensitive to the mixture preparation details (e.g., Opat et al. [12]); therefore, the use of simplified fuel models should be borne in mind when assessing observed differences between simulations and experiments.

Soot was predicted using a phenomenological soot model based on the approach of Hiroyasu and Kadota [36]. The soot model used acetylene as an inception species, which allows the soot model to be coupled to the chemistry solver through the addition of 13 reactions involving acetylene. NO_x emissions were predicted using a reduced NO mechanism [37] consisting of four additional species and 12 reactions. The spray model used the Lagrangian-drop and Eulerian Fluid (LDEF) approach. In order to reduce the grid size dependency of the LDEF spray model and to allow accurate spray simulation on a relatively coarse grid, the gas-jet model of Abani et al. [29,30] was used to model the relative velocity between the droplets and gas phase in the under-resolved near-nozzle region. Their approach assumes that the relative velocity between a droplet and the gas phase is equal to that between the droplet and a turbulent gas-jet with the same mass and momentum of that of the injected fuel.

Droplet breakup was modeled using the hybrid KH–RT model described by Beale and Reitz [28]. The droplet collision model was based on O'Rourke's model [38]; however, a radius of influence method is used to determine the possible collision partners to further reduce mesh dependency [39]. In addition, the collision model was expanded by Munnannur [40] to include a more comprehensive range of collision outcomes. The implementation of the droplet collision model considered the effects of bounce, coalescence, and fragmenting and non-fragmenting separations. Droplet interactions with the wall were considered through a wall



Fig. 3. Modified intake manifold for PFI [90].

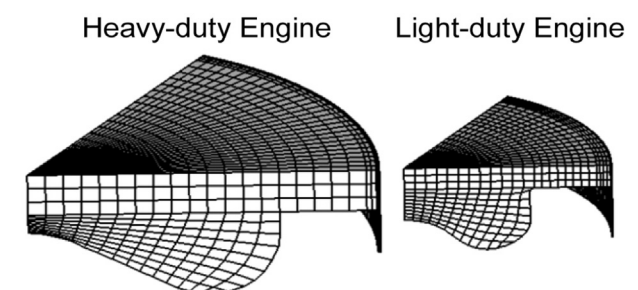


Fig. 5. Computational grids [88].

Table 3
Port fuel injector specifications [26,96].

HD engine	LD engine
Steady flow rate at 3 bar	12.5 cc/s
Included spray angle	15°
Fuel pressure	5.17 bar
Number of holes	3
Steady flow rate	2.74 g/s
Included spray angle	15°
Fuel pressure	3.8 bar
Number of holes	4

film sub-model, which included effects associated with splash, film spreading, and motion due to inertia. The simulations were performed using the three-dimensional computational grids shown in Fig. 5. To reduce the computational burden, a 60° sector mesh that considers a single nozzle hole of a six nozzle hole injector with periodic boundaries was used. Notice that the region above the top piston ring is resolved; however, ring motion and flows past the compression rings are not included.

2.1.4. Fuel and injector details

The ERC and ORNL RCCI engine experiments were performed using port fuel injection of gasoline/ethanol and early direct injection of diesel/B20/gasoline-with-DTBP/and gasoline-with-2-EHN using a conventional (i.e., wide angle, large nozzle hole) common-rail injector and a GDI injector. The properties of the fuels and specifications for the port fuel, common rail and GDI injectors used in the engines are given in Tables 3–7, respectively.

2.1.5. Fuel introduction strategies

The RCCI engine experiments were performed using port fuel injection of a lower reactivity fuel and early direct injection of a higher reactivity fuel with a conventional solenoid operated common rail injector. A lubricity additive was added at around 500 ppm to the common rail fuel system during “single fueling” strategies (i.e., gasoline and gasoline doped with 2-EHN/DTBP) to provide adequate injector lubrication. In the RCCI studies, gasoline was injected very early in the cycle and the reactive fuel was injected using a double injection strategy later in the cycle. An example of the injection timing windows of the DI event is shown in Fig. 6. The DI strategy utilized only early injection to raise the reactivity of the fuel in the squish region near the cylinder liner and a second injection closer to top dead center (TDC) to increase the reactivity in the center of the cylinder. The timings, duration and fuel quantity varies with the operating conditions.

3. Results and discussion

Low Temperature Combustion investigations carried out on the ERC and ORNL engines described above over wide ranges of operating conditions are reviewed. The use of CFD modeling to guide the experimental work is also discussed.

3.1. Dual fuel HCCI and PCCI combustion using in-cylinder fuel blending

The potential of controlling premixed charge compression ignition (PCCI and HCCI) combustion strategies by varying fuel

Table 4
Common rail injector specifications [26,96].

HD engine	LD engine
Steady flow rate at 100 bar	33.3 cc/s
Included spray angle	145°
Injection pressure	600–800 bar
Number of holes	6
Hole diameter	250 μm
Steady flow rate	14.67 cc/s
Included spray angle	143°
Maximum inj. pressure	1500 bar
Number of holes	7
Hole diameter	154 μm

Table 5
GDI injector specifications [26,102].

HD engine	LD engine
Steady flow rate at 100 bar	12.8 cc/s
Included spray angle	60°
Number of holes	6
Hole diameter	165 μm
Included spray angle	142°/120°
Number of holes	6
Hole diameter	150 μm

Table 6
Properties high reactivity fuels and Cetane Improvers.

Diesel (ULSD) [26]	Biodiesel (B20)- Soy methyl eater (SME) [103]
Lower heating value (MJ/kg)	42.912
Specific gravity	0.8452
H (Weight %)	13.2
C (Weight %)	86.8
Aromatic (Weight %)	29.3
Sulfur (ppm)	9.9
Initial boiling point (°C)	189
Final boiling point (°C)	344
Cetane number	46
Viscosity @ 40 °C	2.71 cSt

Cetane Improvers [50,55]	
	2-EHN
Lower heating value (MJ/kg)	27.364
H/C ratio	2.125
O/C ratio	0.375
Specific gravity @15.6 °C	0.96
DTBP	0.704

reactivity was investigated by Kokjohn et al. [26]. In-cylinder fuel blending was proposed as the fuel delivery and blending strategy to adjust the fuel reactivity on a cycle-to-cycle basis by changing the injected quantities of gasoline and diesel fuel to optimally accommodate engine load and speed changes. A preliminary experimental study at an engine load of 6 bar IMEP was performed in the HD engine using port fuel injection of gasoline and direct injection of diesel fuel near BDC using a low pressure GDI injector. The operating conditions are given in Table 8. Fig. 7 shows the cylinder pressure and heat release rates over an EGR sweep at 6 bar IMEP and 1300 rev/min. The simulations were run from IVC to EVO using

Table 7
Properties of low reactivity fuels.

Gasoline [26]	85% Ethanol and 15% gasoline (E85) [78]
Distillation curve	ASTMD86
Initial boiling point (°C)	38.89
Temperature 10% evaporated (°C)	69.4
Temperature 50% evaporated (°C)	105
Temperature 90% evaporated (°C)	16056
Final boiling point (°C)	215.56
Lower heating value (MJ/kg)	4322
MON	87.8
RON	95.6
[(RON + MON)/2]	91.6
Ethanol (%)	0
H/C ratio	1.88
Specific gravity @15.6 °C	0.7
[(RON + MON)/2]	[(RON + MON)/2]
Ethanol (%)	4.6
MON	MON
RON	RON
[(RON + MON)/2]	[(RON + MON)/2]
Lower heating value (MJ/kg)	39.642
Ethanol (%)	19.8
MON	90.5
RON	101.2
[(RON + MON)/2]	95.9
Specific gravity @15.6 °C	0.755

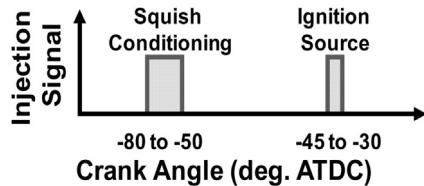


Fig. 6. Injection timing window [60].

a two-dimensional sector grid representation of the combustion chamber. At IVC a homogeneous mixture of iso-octane, *n*-heptane, residuals/EGR, and air was assumed. The simulations captured the combustion characteristics reasonably well. However, the peak cylinder pressure and AHRR were slightly over predicted due to the neglected spatial inhomogeneity in fuel/EGR/air mixture. But, the results were extremely useful to provide guidelines for the selection of combustion strategies, as described next.

3.1.1. Selection of baseline fuel reactivity and EGR

The KIVA-CHEMKIN code and a reduced PRF mechanism were used to find optimized fuel blends and EGR combinations for HCCI operation at several engine loads. The study found that a minimum fuel consumption could not be achieved using either neat diesel fuel or neat gasoline alone, and that the optimal fuel reactivity required decreased with increasing load [13,14]. Fig. 8 shows the simulation results at 6 bar IMEP, and it is seen that when PRF 70 was used, the optimal combustion phasing could be achieved with no EGR. Thus, the reduced fuel reactivity could significantly reduce the burden on the air handling system. Furthermore, the ability to operate at low EGR rates may be beneficial for combustion phasing control during transient LTC operation. The optimal CA50 combustion phasing for 6 bar IMEP operation was found to be between 4 and 6° aTDC. Similarly, Fig. 9 shows simulation results at 11 bar IMEP that indicates that low ISFC can be achieved using PRF blends ranging from 60 to 90, depending on the EGR level. The minimum ISFC coincided with a CA50 of ~6° ATDC. Furthermore, as load was increased, operation had to be shifted to higher EGR levels in order to reduce the rate of heat release and to meet the PRR constraint. It was observed that, even with combustion phasing after TDC, the PRR was excessive (~20–30 bar/deg) due to the volumetric heat release, and it was inferred that stratification may be useful to control the rate of heat release.

3.1.2. Dual-fuel operation

The outcome of the preliminary study conducted to select baseline PRF and EGR levels indicated that it is possible to improve fuel economy by optimizing the fuel reactivity for each specific operating condition. The investigations assumed a perfectly

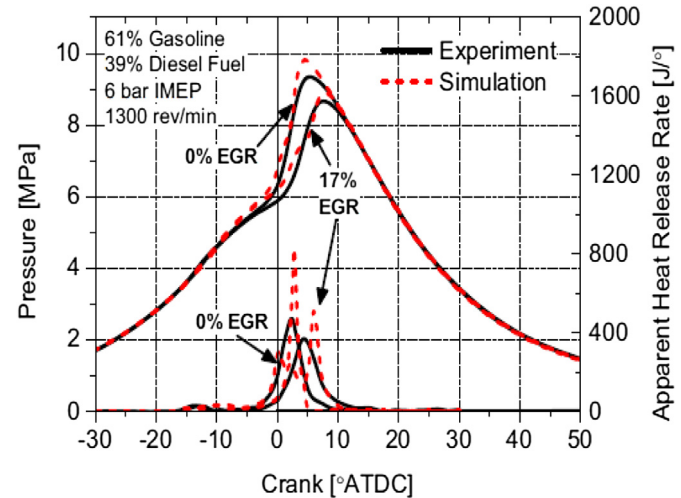


Fig. 7. Comparison of measured and predicted cylinder pressure and heat release rate for dual-fuel HCCI [26].

homogeneous mixture, which is likely to be unrealistic. However, similar results were achieved using production-type hardware for this engine. Dual-fuel operation was explored using port fuel injection of gasoline and early multiple injection of diesel fuel with a conventional diesel injector. The experimental results confirmed that an extension of the PCCI operating regime was possible when optimized fuel blends were used. The operating conditions for the dual-fuel PCCI operation at 6 and 11 bar IMEP are shown in Table 9.

Fig. 10 shows the measured and simulated cylinder pressure and heat release rate for dual-fuel PCCI operation at 6 bar IMEP. It is seen that the model predicted the combustion characteristics well at this condition. It was thought that the over prediction of the ignition delay was due to uncertainties in the initial and boundary conditions, rather than due to short comings of the physical models. The performance and emissions results are shown in Table 10. Comparisons of the predicted and measured emissions show that the models were able to predict NO_x, CO and ISFC extremely well. However, significant under prediction of soot was observed due to the inhomogeneities at IVC (not modeled), which may have contributed to the differences in the predicted and measured soot levels. Note however that the soot levels are extremely low.

The results confirmed that the use of optimized fuel reactivity provides control of the combustion phasing and spatially stratified reactivity extends the combustion duration. Thus, the ability of the strategy to extend the operating range of low emission, high efficiency PCCI combustion to higher engine loads (e.g., 11 bar IMEP) was explored. Fig. 11 shows the cylinder pressure and heat release rates over a gasoline percentage sweep. The simulations agree very well with the experimental cylinder pressures and heat release rates. The heat release rate curves show evidence of a cool flame reaction from the diesel fuel, followed by two distinct bumps on the high temperature heat release. It was thought that the first bump corresponds to high temperature oxidation of CO formed from oxidation of the diesel fuel and the second bump corresponds to oxidation of CO formed from the gasoline breakdown.

The performance and emissions of dual-fuel operation at 11 bar IMEP is shown in Fig. 12. The simulations were able to predict NO_x emissions very well, but soot was significantly under predicted. However, the soot levels in the experiments were well below US 2010 heavy-duty limits. The CO prediction shows reasonable agreement, but HC was slightly overpredicted. However, the trend

Table 8
HD Engine operating conditions for dual fuel study [26].

Nominal IMEP	6 bar				
Engine speed	1300 rev/min				
EGR rate (%)	0	7	11	17	25
Equiv. ratio	0.3	0.32	0.34	0.36	0.4
Intake Temp.	32 °C				
Intake press.	1.38 bar				
Total fuel	67 mg/cycle				
Gasoline by mass	61%				
Gasoline by energy	61.4%				
Mass of diesel fuel	26.1 mg/cycle				
Mass of gasoline	40.9 mg/cycle				
Diesel Injection pressure	100 bar				
Diesel SOI	−140 °aTDC				
Diesel injection duration	13.7 °CA				

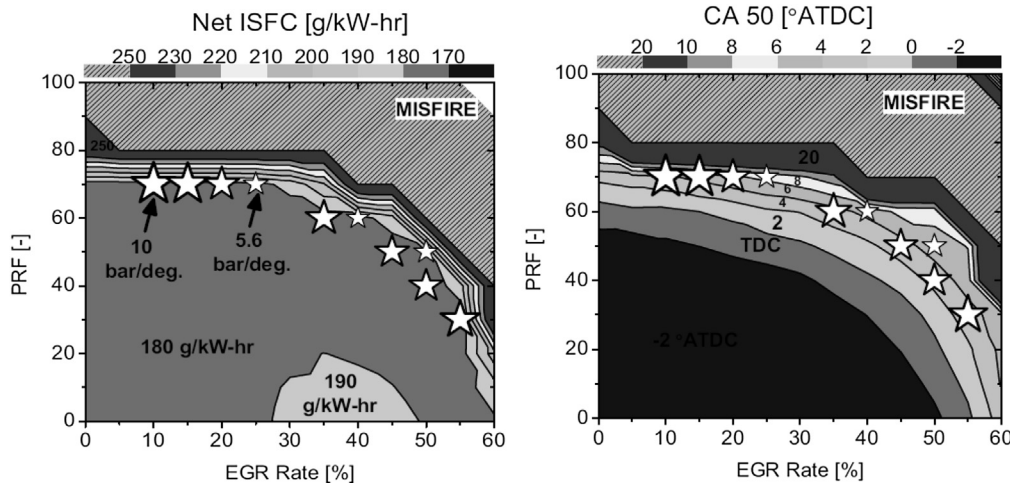


Fig. 8. Predicted ISFC and CA50 contours as function of fuel reactivity (PRF) and EGR at 6 bar IMEP [26].

of increasing HC with increasing gasoline percentage was captured. The increase in HC emissions with increasing gasoline percentage may be due to the increase in fuel trapped in the piston liner crevice as more gasoline is premixed.

The key feature of the dual fuel approach is the ability to control the combustion process by optimizing the reactivity of the blended fuels. This led to the terminology “reactivity controlled compression ignition” or RCCI, to differentiate the combustion process from HCCI or PCCI.

3.1.3. Comparison of dual fuel combustion modes

Yu et al. [41] compared their so-called Gasoline Homogeneous Charge Induced Ignition (HCII) combustion and Gasoline/Diesel Blend Fuels (GDBF) combustion modes. In the HCII mode port fuel injection of gasoline was used to form a homogeneous charge and direct injection of diesel fuel served as the ignition source, while in the GDBF mode a premixed blend of diesel-gasoline was directly injected into the cylinder for combustion. The results of this study demonstrated that the above two methods may integrate the advantages of gasoline and diesel fuels to achieve high thermal efficiency and low emission targets. Yu et al. investigated these two

combustion modes on a high-pressure common rail single-cylinder diesel engine. The results show that both HCII and GDBF modes can achieve higher thermal efficiency than gasoline SI combustion and a similar or even higher thermal efficiency than diesel CI combustion due to near constant volume combustion. It was noticed that an increase in gasoline ratio improved the fuel-air mixing and shortened the combustion duration significantly in both the HCII and GDBF modes, which, in turn, resulted in a 90% reduction in soot emissions. Overall, the study demonstrated that in both HCII and GDBF combustion modes extremely low soot and NO emission is possible with use of large amounts of EGR.

Yang et al. [42] performed numerical simulations and experiments to explore the differences in combustion and emissions characteristics between dual-fuel Highly Premixed Charge Combustion (HPCC, including Early-HPCC and Late-HPCC) and blended-fuel Low Temperature Combustion (LTC) modes with gasoline and diesel. Their results illustrate that most of the mixture in E-HPCC is uniform in both concentration and reactivity, while there are various degrees of mixture stratification in Late-HPCC and LTC. Based on the in-cylinder charge distributions, the combustion occurs in the very center area of the combustion chamber and in the

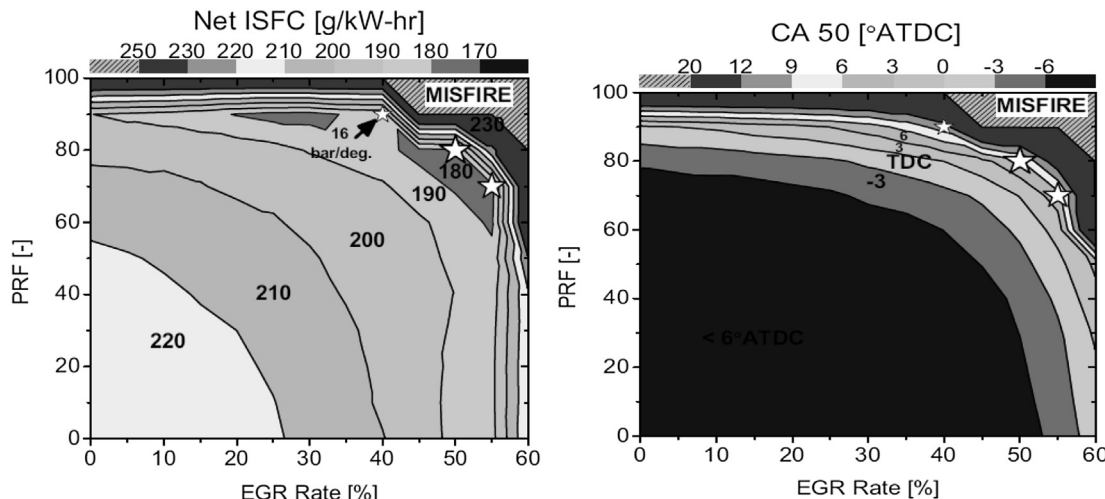


Fig. 9. Predicted ISFC and CA50 contours as function of fuel reactivity (PRF) and EGR at 11 bar IMEP [26].

Table 9

Engine operating conditions for dual-fuel PCCI operation at 6 and 11 bar IMEP [26].

Nominal IMEP (bar)	6	Nominal IMEP (bar)	11
Engine speed (rev/min)	1300	Engine speed (rev/min)	1300
EGR rate (%)	0	EGR rate (%)	45.5
Equivalence ratio	0.29	Equivalence ratio	0.77
Intake Temperature (°C)	32	Intake Temperature (°C)	32
Intake pressure (bar)	1.38	Intake pressure (bar)	2.0
Total fuel (mg/cycle)	66.2	Total fuel (mg/cycle)	128
Percent gasoline by mass (%)	69	Percent gasoline by mass (%)	78
Percent gasoline by energy (%)	69.3	Percent gasoline by energy (%)	78.3
Mass of diesel fuel (mg/cycle)	20.7	Mass of diesel fuel (mg/cycle)	28.2
Mass of gasoline (mg/cycle)	45.5	Mass of gasoline (mg/cycle)	99.8
Diesel Injection pressure (bar)	600	Diesel Injection pressure (bar)	800
Diesel SOI 1 (°aTDC)	-55	Diesel SOI 1 (°aTDC)	-67
Diesel SOI 2 (°aTDC)	-30.7	Diesel SOI 2 (°aTDC)	-33
Fraction of diesel fuel in pulse 1	0.68	Fraction of diesel fuel in pulse 1	0.65
Diesel injection duration1 (°CA)	5.9	Diesel injection duration1 (°CA)	5.9
Diesel injection duration 2 (°CA)	2.7	Diesel injection duration 2 (°CA)	3.1

area closer to the piston bowl wall in the two HPCCs and LTC respectively, and then the flame spreads to peripheral regions. In the two HPCCs, substantial heat release was noticed due to the oxidation by the OH radical that derived from low temperature reactions of the diesel fuel, and reasonable MPRR values were observed due to the staged reactions of diesel and gasoline. The fuel stratification in the LTC mode resulted in a rapid heat release rate and high MPRR because of the coupled combustion reactions of gasoline and diesel in regions of higher fuel concentration. Yang et al. found that, compared to LTC, the two HPCCs produce more incomplete combustion products, and consequently lower combustion efficiencies, which could be improved by increasing the gasoline-diesel fuel ratio.

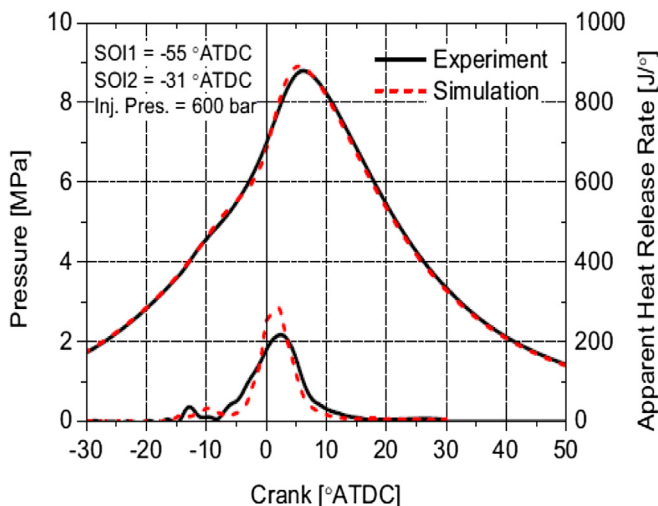
3.2. Comparison of low temperature combustion strategies

Comparisons of various low temperature combustion strategies were investigated by Dempsey et al. [5] with focus on engine performance and emissions, combustion sensitivity to intake conditions, and the ability to control observed sensitivities through the fuel injection strategy. The combustion strategies that were investigated were fully premixed dual fuel HCCI, dual fuel RCCI, and single fuel PPC. The study investigated each combustion strategy's controllability on a cycle-to-cycle basis. The three combustion strategies were first operated using the primary reference fuels: *n*-

heptane and iso-octane, to remove fuel effects from comparisons. In addition, dual fuel RCCI and single fuel PPC were investigated using commercial pump gasoline and diesel fuel to investigate if the findings with the reference fuels were transferable to fuels used in the transportation market today.

The experiments were carried out on a single-cylinder version of the LD diesel engine shown in Fig. 2. The stock-re-entrant piston bowl geometry was replaced with a modified piston that featured a wide shallow bowl, which is shown Fig. 13. In the study the pre-mixing of fuel and air was accomplished with two port fuel injectors mounted in the intake runner upstream of the intake valves. For RCCI and PPC operation, a portion of fuel was injected directly into the cylinder via the centrally mounted common rail injector. During the HCCI experiments, the injector was replaced with a solid plug that had the same dimensions as the injector, so as to maintain the same geometric compression ratio. The specifications of the injectors used are given in Tables 3 and 4. Table 11 shows the physical and chemical properties of the fuels used. The different fueling strategies used in the study are described in Table 12. Prior to the sensitivity study, the engine's response to changes in the input fuel system parameters, such as the global fuel reactivity, premixed fuel amount, and DI timing were studied. First the effect of varying the premixed fuel amount was demonstrated.

As shown in Fig. 14, when operated on primary reference fuels, both HCCI and RCCI have a very pronounced ability to target a given CA50 via slight changes of the global fuel reactivity in the combustion chamber. Single fuel PPC operated on PRF 94 gasoline demonstrated some level of control, but over a much wider range of premixed fuel percentage. In addition, when the premixed fuel percentage was low, the NO_x emissions began to increase due to the existence of high equivalence ratio regions in the combustion chamber at the start of combustion. PPC and RCCI displayed very similar trends with pump fuels compared to the primary reference fuels, as shown in Fig. 14. However, pump fuel RCCI showed less controllability and increased NO_x emissions compared to operation with the primary reference fuels due to the reduced reactivity gradient between the premixed and direct injected fuels.

**Fig. 10.** Pressure traces at 6 bar IMEP [26].**Table 10**

Experimental (Exp) and Simulated (Sim) performance and emissions for dual-fuel operation [26].

	NO _x g/kWh	Soot g/kWh	CO g/kWh	HC g/kWh	Max PRR bar/°	Net ISFC g/kWh
Sim	0.016	0.0005	12	14	8.4	179
Exp	0.013	0.01	14	6	6.1	179

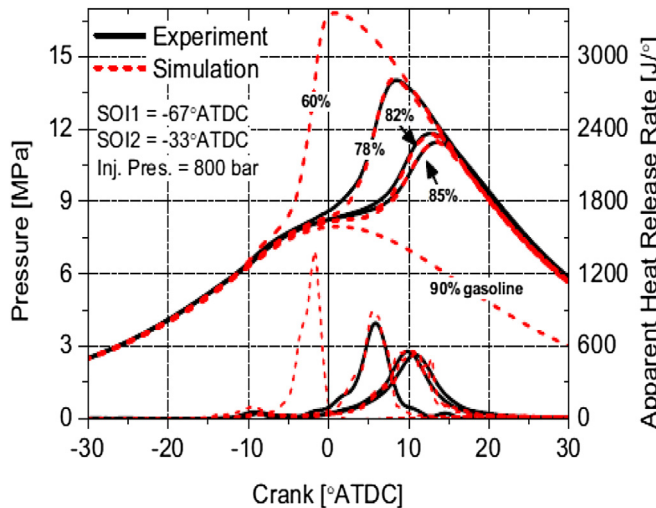


Fig. 11. Pressure and AHRR traces [26].

One of the major advantages of a partially premixed combustion strategy is the added control flexibility allowed by varying the direct fuel's injection timing. For both single fuel PPC and dual fuel RCCI with pump fuel, a single direct injection with DI timing closer to TDC was used, which resulted in an advance in combustion phasing at the cost of increased NO_x emissions due to the lower volatility of gasoline compared to diesel fuel. As the DI timing was advanced beyond -50° aTDC, combustion phasing control was diminished with the PRF fuel for both combustion strategies. This finding was very consistent for single fuel PPC operation with pump gasoline. However, for RCCI operation with pump fuels, the combustion phasing continued to respond to changes in DI timing for timings earlier than -50° aTDC, most likely due to the low volatility of diesel fuel. The study clearly demonstrated that the three

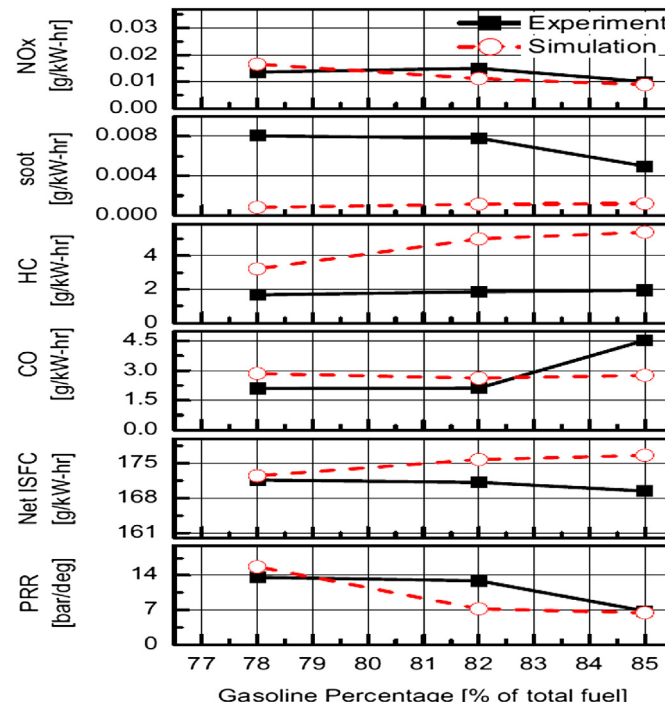


Fig. 12. Emissions and performance trends [26].

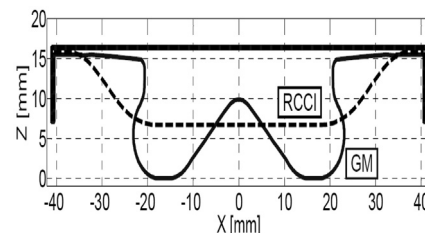


Fig. 13. GM stock piston (solid line) and Modified RCCI piston (dotted line) [5].

combustion strategies allow combustion phasing control via the fuel delivery details, and the results obtained from the study were used as a guide to control combustion phasing via intake conditions.

3.2.1. Baseline operating conditions

The investigations of Dempsey et al. [5] were continued to study the sensitivity and controllability of HCCI, RCCI and PPC combustion for engine conditions. A mid-load operating condition of 5.5 bar gIMEP and 1500 rev/min was chosen. This condition is representative of an operating condition that would be experienced in an LD diesel engine application (Kokjohn, Reitz, [82]), and at this operating condition the NO_x target was ~ 0.1 g/kWh (0.6 g/kg-fuel). An intake pressure of 1.3 bar absolute was used for all three combustion strategies and a intake temperature of 50 °C was used for HCCI and RCCI, whereas a slightly higher intake temperature of 70 °C was used for PPC to achieve the target combustion phasing of interest 0 to 5° aTDC. Fig. 15 shows the cylinder pressure and apparent heat release rate and Table 13 summarizes the performance of all the three baseline operating points shown in Table 14.

RCCI operation with the primary reference fuels yielded a longer combustion duration and lower peak pressure rise rates compared to HCCI and PPC. The combustion efficiency of RCCI was the lowest among the three strategies when operated with PRF fuel. However, despite the lower combustion efficiency, the gross indicated efficiency (GIE) of RCCI was slightly higher due to lower heat transfer losses stemming from the lower PPRR. As could be noticed from the pump fuel results, when the reactivity of the premixed fuel was increased via the 87 AKI gasoline, the combustion efficiency for RCCI operation was improved to the same level as for PPC. Fully premixed HCCI and single fuel PPC displayed very high PPRR. This is somewhat surprising, but a similar observation was explained by Dec et al. [17] at low intake pressures ($\sim < 1.6$ bar) when comparing fully premixed HCCI with partially stratified charge. They found that the ignition delay of these fuels (conventional gasoline, iso-octane, and PRF 94) has very little sensitivity to the mixture equivalence ratio for equivalence ratios less than 0.5. Thus, for even relatively large amounts of direct injected fuel, the combustion

Table 11
Fuel properties of PRF and commercially available pump fuels [5].

Descriptions	n-Heptane	Iso-octane	Diesel fuel	Gasoline
Chemical Formula	C ₇ H ₁₆	C ₈ H ₁₈	CH _{1.76}	CH _{2.0}
Lower heating value (MJ/kg)	44.6	44.3	42.6	43.4
RON	0	100	—	91.4
MON	0	100	—	83.1
[(RON + MON)/2]	0	100	—	87.3
Cetane number	56	—	42	—
Liquid density @ 25 °C (g/cc)	0.684	0.692	0.859	0.741
Enthalpy of vaporization (kJ/kg)	316	272	>270	>300
Initial boiling point (°C)	98	99	174	34
Temperature 50% evaporated (°C)	98	99	262	99
Final boiling point (°C)	98	99	350	217

Table 12

Fueling strategies for three combustion modes [5].

Primary reference fuels			Pump fuels			
Fuel injector	HCCI	PPC	RCCI	Fuel injector	PPC	RCCI
Port fuel injector –1	PRF 75	PRF 94	PRF 100	Port fuel injector –1	87 AKI Gasoline	87 AKI Gasoline
Port fuel injector –2	PRF 100	PRF 94	PRF 100	Port fuel injector –2	87 AKI Gasoline	87 AKI Gasoline
Direct fuel Injector	—	PRF 94	PRF 0	Direct fuel Injector	87 AKI Gasoline	42 CN Diesel fuel

duration remains nearly unchanged from HCCI at this baseline operating condition.

3.2.2. Intake temperature sensitivity and controllability: primary reference fuels

The three strategies displayed significant combustion sensitivity to changes in the intake temperature. This was expected considering that the strategies are sufficiently premixed and predominantly controlled by chemical kinetics, which is driven by the mixture temperature. Fig. 16 shows the intake temperature sensitivity for the primary reference fuels. An intake temperature sensitivity correction for dual fuel HCCI was done by varying the fuel reactivity using the two port injectors, and the baseline combustion phasing was easily recovered for both hotter and colder intake temperatures through slight modifications of the global fuel reactivity (the DI timing was kept constant). The major difference with dual fuel HCCI and RCCI was the resulting PRRR. RCCI yielded significantly lower PRRR than HCCI.

In the case of single fuel PPC with PRF 94 gasoline, for the hotter intake temperature the baseline combustion phasing was unrecoverable, despite increasing the premixed fraction from 79.1% to 95.2%. As mentioned before, the baseline operating condition for single fuel PPC yielded approximately the same combustion

duration as fully premixed HCCI. This suggested that the equivalence ratio distribution created by the baseline injection strategy was not broad enough to produce a range of ignition delays. Thus, it was expected that if changes were made to the injection strategy to create a more premixed charge, the ignition delay will be relatively unaffected, as observed for the increased intake temperature case.

On the contrary, for the colder intake temperature, by using a combination of more direct injected fuel and a retarded timing, the baseline combustion phasing was reasonably recovered. However, this came at the cost of increased NO_x emissions.

3.2.3. Intake pressure sensitivity and controllability: primary reference fuels

In addition to intake temperature variations, the sensitivity of the combustion process to the intake pressure also was investigated by Dempsey et al. [5]. This is extremely important for the development of transient operation of a turbocharged engine, because under a speed and load transient, the intake pressure changes more rapidly than the intake temperature. Fig. 17 shows the results of changing the intake pressure by approximately ± 0.1 bar for all three strategies. The same order of sensitivity to the intake pressure was observed for HCCI and PPC as there was to the intake temperature. Interestingly, when the intake pressure was reduced, the

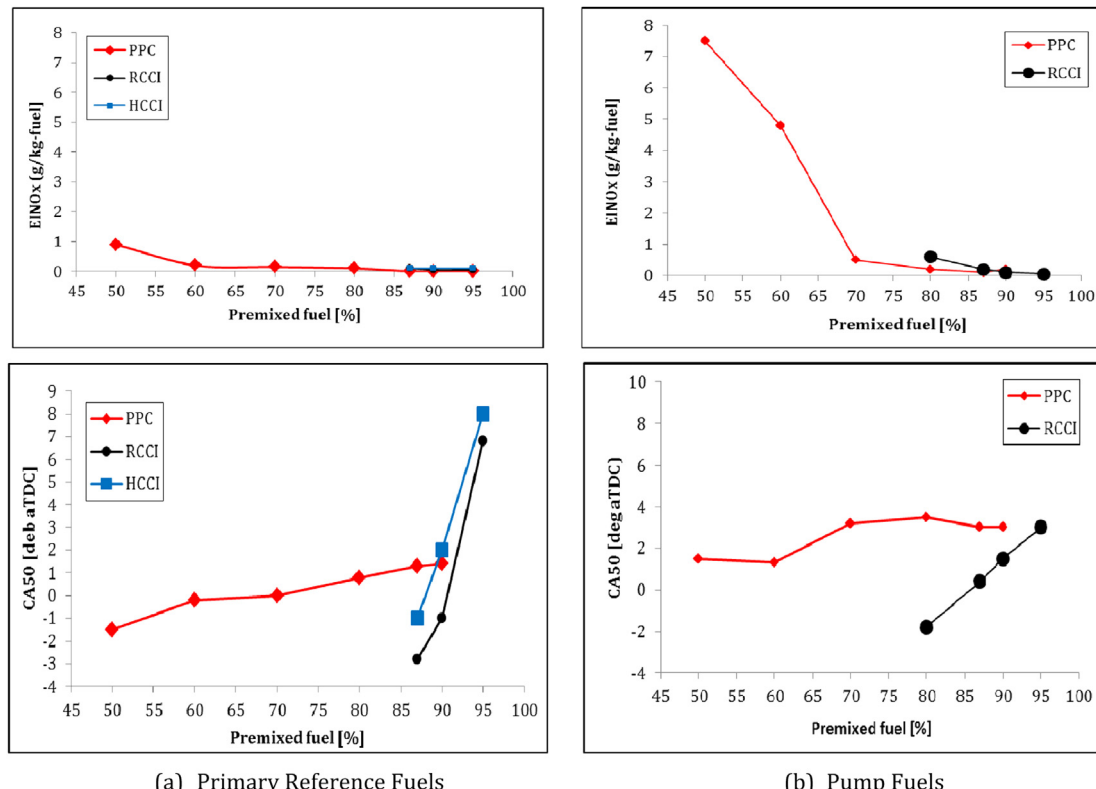


Fig. 14. Combustion phasing response to premixed fuel amount [5].

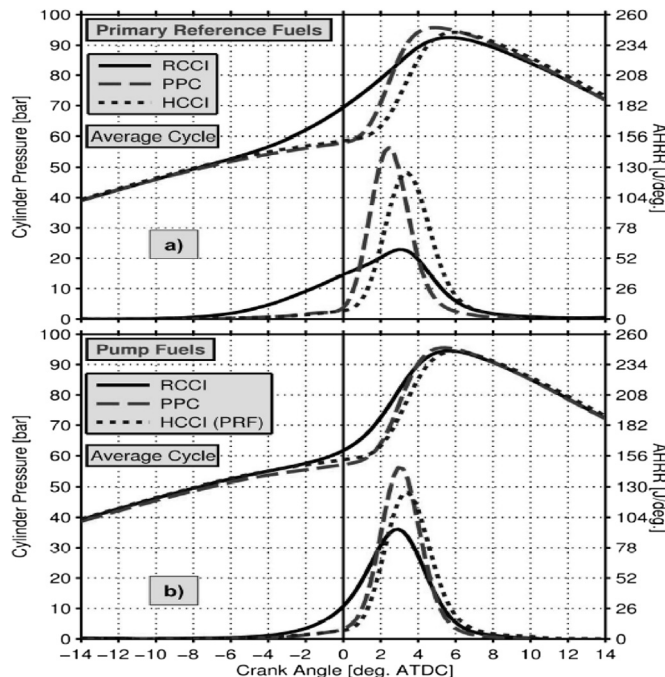


Fig. 15. Cylinder pressure and AHRR for baseline operation [5].

Table 13
Baseline operating conditions [5].

Primary reference fuels				Pump fuels		
Fixed conditions	HCCI	PPC	RCCI	Fixed conditions	PPC	RCCI
Intake pressure [bar]	1.3	1.3	1.3	Intake pressure [bar]	1.3	1.3
Intake temp. [°C]	50	70	50	Intake temp. [°C]	70	50
Premixed fuel [%]	100	79.1	92.6	Premixed fuel [%]	74.5	96.2
Global PRF	92.9	94.0	92.6	Global PRF	—	—
DI timing	—	-65°	-45°	DI timing	-47°	-50°
Global equiv. ratio	0.33	0.33	0.33	Global equiv. ratio	0.33	0.33

combustion phasing retard for PPC operation was greater than that observed for HCCI. In addition, RCCI is not as sensitive to the intake pressure as the other strategies.

For the fully premixed HCCI combustion case, the intake pressure sensitivity correction was again done, just as with the intake temperature compensation, by simply varying the port fuel injection percentage with a fixed DI timing. The baseline combustion phasing was recovered and NO_x emissions remained well below the target level. The results of intake pressure sensitivity for single fuel

PPC with PRF 94 were also extremely consistent with the findings of intake temperature perturbations.

3.2.4. Combustion phasing sensitivity and controllability: pump fuels

In order to confirm that the findings were transferable to readily available market fuels, which contain numerous classes of hydrocarbon species that may not respond in the same fashion as the primary reference fuels, Dempsey et al. [5] investigated all the three strategies in the same manner with pump fuels.

Fig. 18a shows the results of correcting for the observed intake temperature sensitivity for RCCI operation on pump fuels. The baseline combustion phasing was reasonably recovered for both the increased and decreased intake temperature cases. Due to the small gradient in reactivity between the two pump fuels as compared to the primary reference fuels, changes to the DI timing were employed along with changes to the premixed fuel percentage in order to recover the baseline phasing for the increased temperature case. In addition, Fig. 18b also shows the results of perturbing the intake pressure for RCCI operation on pump fuels and subsequently correcting the observed sensitivity. The results were very consistent with the findings for the primary reference fuels, however, pump fuels and the primary reference fuels display slightly different sensitivities, both of which, however, were readily corrected through changes in the fuel injection details.

Fig. 19a shows the results of perturbing the intake temperature approximately ±10 °C for single fuel PPC operation on pump gasoline and subsequently attempting to correct for the observed sensitivity. As can be seen, the sensitivity was very similar between the pump 87 AKI gasoline and PRF 94, and the results were very consistent with the findings for PPC operation with PRF 94. For the increased intake temperature condition, the premixed fuel percentage was increased to 91.5% and the DI timing was advanced to -70° aTDC, and yet the baseline combustion phasing was unrecoverable. For the decreased intake temperature condition, the baseline combustion was recovered by increasing the level of fuel stratification (i.e., decreased premixed fuel percentage and retarded DI timing), but the NO_x emissions increased to 4.3 g/kg-fuel, which is significantly above the target level of 0.6 g/kg-fuel. As can be seen from Fig. 19b, PRF 94 and the 87 AKI gasoline displayed the same level of sensitivity to the increased intake pressure, but responded somewhat differently to the decrease in intake pressure. The ability to correct the combustion phasing sensitivity is very similar to that of PRF 94. With increased intake pressure it is not possible to correct for the advancement in combustion phasing. On the contrary, with decreased intake pressure it is possible to advance the combustion phasing back to the baseline condition, but again with a significant increase in the NO_x emissions.

The results discussed in this section demonstrated that all three advanced low temperature combustion concepts, HCCI, PCCI and RCCI, are sensitive to the intake conditions. This is an expected result because each strategy is governed by chemical kinetics, which is known to be controlled by the mixture temperature and

Table 14
Baseline performance results [5].

Primary reference fuels				Pump fuels		
Fixed conditions	HCCI	PPC	RCCI	Fixed conditions	PPC	RCCI
CA50 ± σ ₅₀ [°aTDC]	3.5 ± 0.5	2.5 ± 0.3	2.2 ± 0.5	CA50 ± σ ₅₀ [°aTDC]	3.2 ± 0.4	2.7 ± 0.9
GIE [%]	47.1	45.6	47.5	GIE [%]	46.9	46.1
Comb. Eff. [%]	92.8	93.1	91.5	Comb. Eff. [%]	93.7	93.2
NO _x [g/kg – fuel]	0.05	0.01	0.04	NO _x [g/kg – fuel]	0.15	0.05
PPRR [bar/deg]	14.0	16.0	5.8	PPRR [bar/deg]	16.4	11.7
COV of IMEP [%]	2.6	2.5	2.6	COV of IMEP [%]	2.5	2.1

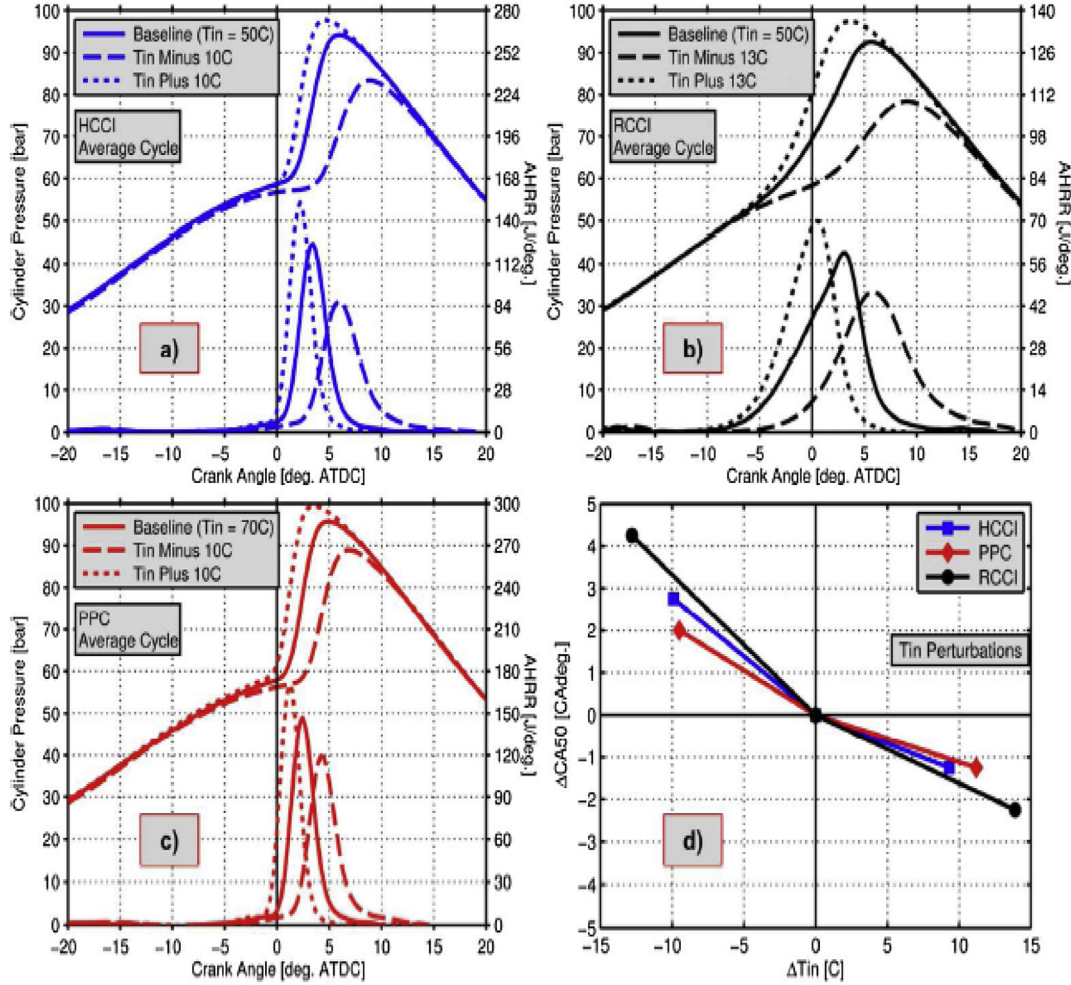


Fig. 16. Intake temperature sensitivity for primary reference fuels [5].

pressure. However, it was demonstrated that the ability to vary the global fuel reactivity (i.e., by using dual fuels) could be an enabler for the control of premixed combustion concepts that yield high thermal efficiency and near zero NO_x and soot emissions, at least at operating conditions considered in the referenced study.

3.3. Fuel reactivity controlled RCCI combustion – HD engines

Hanson et al. [34] investigated the potential of controlling RCCI combustion strategies by varying the fuel reactivity. The parameters used in the study were steered from KIVA-CHEMKIN simulations made with a reduced PRF mechanism, which included injection timing, PFI fuel percentage and intake valve closing (IVC) timings. The engine experiments were conducted on the engine shown in Fig. 1 with a conventional common rail injector, and the results demonstrated control and versatility of dual-fuel RCCI combustion with proper fuel blends, SOI and IVC timings. The objective of the study was to explore fuel blending as a means for extending the RCCI operating regime.

To lower peak cylinder pressures and to aid in combustion phasing control, different methods of modifying IVC timings were implemented by Nevin et al. [43], who used four different custom manufactured camshafts with IVC timings ranging from -143° aTDC (stock) to -85° aTDC in order to lower the effective compression ratio. The intake valve lift profiles are shown in Fig. 20. Initial CFD modeling results suggested that the IVC timing of -85°

aTDC would be optimal, due to the resulting lower TDC temperatures and pressures. However, in the study of Hanson et al. [34], IVC timings closer to those utilized in the production Caterpillar 3406 engine were investigated by using three camshafts with IVC timings of -85° , -115° and -143° ATDC.

3.3.1. Effect of first and second main injection timings (SOI-1 and SOI-2)

The first engine experiments were conducted at 9 bar IMEP and 1300 rev/min with injection timing (SOI-1) sweeps from -55° to -62° aTDC. In this case 73% (by mass of total fuel) gasoline was injected in the intake port and the remaining 27% of diesel fuel was injected into the cylinder. The diesel fuel was injected in two injections with 62% of the diesel fuel quantity in the first injection. The diesel injection durations for first and second pulses were 5.47°CA and 3.12°CA , respectively. The second injection timing, was varied from -29° to -48° aTDC, and the first injection quantity and durations were the same as used in the first case.

As the SOI-1 timing was advanced, it was noticed that combustion phasing was retarded, NO_x and peak pressure rise rates were reduced, and an increase in CO was observed. It is very interesting to note that HC emissions remained relatively flat. The reason for the reduced HC was thought to be due to less spray impingement on the liner with an advance in SOI-1 timing, and this was analysed in detail in the study of Kokjohn et al. [8]. From Figs. 21 and 22 [34], it is noticed that, as SOI-1 timing was advanced,

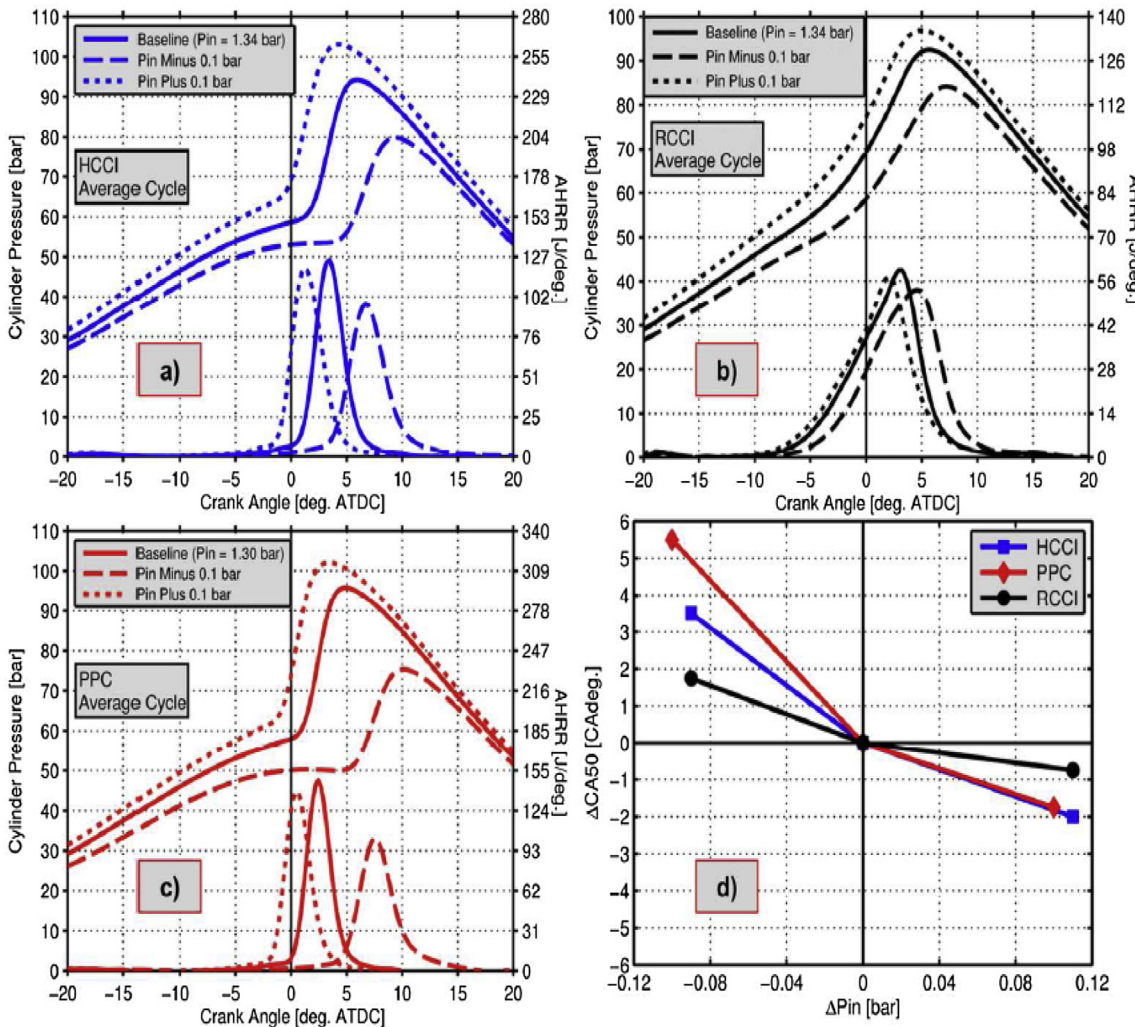


Fig. 17. Intake pressure sensitivity for primary reference fuels [5].

the peak pressure decreases and the combustion phasing is retarded. This results in reduced in-cylinder temperatures, whereas in the case of SOI-2 timings, when the injection timing was retarded, the combustion phasing advanced and peak pressure increased. Due to the advanced combustion phasing and increased peak pressure, the cylinder temperature is high. This increased cylinder temperature is mainly due to the retarded injection timing, since when the time available for mixing is less, fuel rich regions result, which causes increased NO_x and PM emissions. But HC and CO remained unchanged with variation in SOI-2 timings. Fuel consumption (i.e., net ISFC) was also constant due to the similar combustion phasing and combustion efficiency.

The low ISFC of ~170 g/kWh seen in the experiments correlates to a net thermal efficiency of 50%. As SOI-2 was advanced, the pressure rise rates increased due to less mixture stratification, resulting in a more homogeneous charge, which then delayed ignition. Although some differences in the simulated and measured results exist (e.g., HC is over predicted and soot is under predicted, as was explained in the SOI-1 sweep) the agreement in NO_x and combustion phasing provided confidence that the models adequately described the physical processes.

3.3.2. Effect of SOI-1 fuel quantity

After investigating the effects of SOI-1, SOI-2 and IVC timings, the next parameter investigated by Hanson et al. [34] was the fuel

quantity split between the two diesel injections. The percentage of fuel in the first injection was varied, but the overall gasoline/diesel fuel split was kept constant. The fraction of diesel fuel in SOI-1 was varied from 36% to 62% (by mass) of the total fuel injected. From the results of the SOI-1 fuel quantity sweep it was found that CO and HC were relatively unaffected by the first injection fuel quantity. However, NO_x and PM increased significantly with the additional second fuel injection. Similar to the results of the SOI-1 and SOI-2 timing tests, when more diesel fuel was injected later in the cycle, a more stratified mixture was provided, which increased the fuel reactivity. These richer and more reactive regions are likely to ignite earlier, increasing cylinder temperatures, and thus cause NO_x and PM to increase. Fig. 23 shows the measured and simulated pressure traces and heat release rates for SOI-1 fuel fractions of 36, 50 and 62%. As can be seen, a lower percentage of fuel in the first injection advances the High Temperature Heat Release (HTHR) and even gave a distinct two stage HTHR. With additional fuel injected in SOI-1, the two stage HTHR is reduced and combustion phasing is retarded.

3.3.3. Effect of IVC timings (effective compression ratio)

Hanson et al. [34] also investigated the effect of IVC timing on dual fuel operation. First, dual fuel operation was investigated at the three IVC timings, -143°, -115° and -85° aTDC, while the combustion phasing was held fixed by varying the gasoline

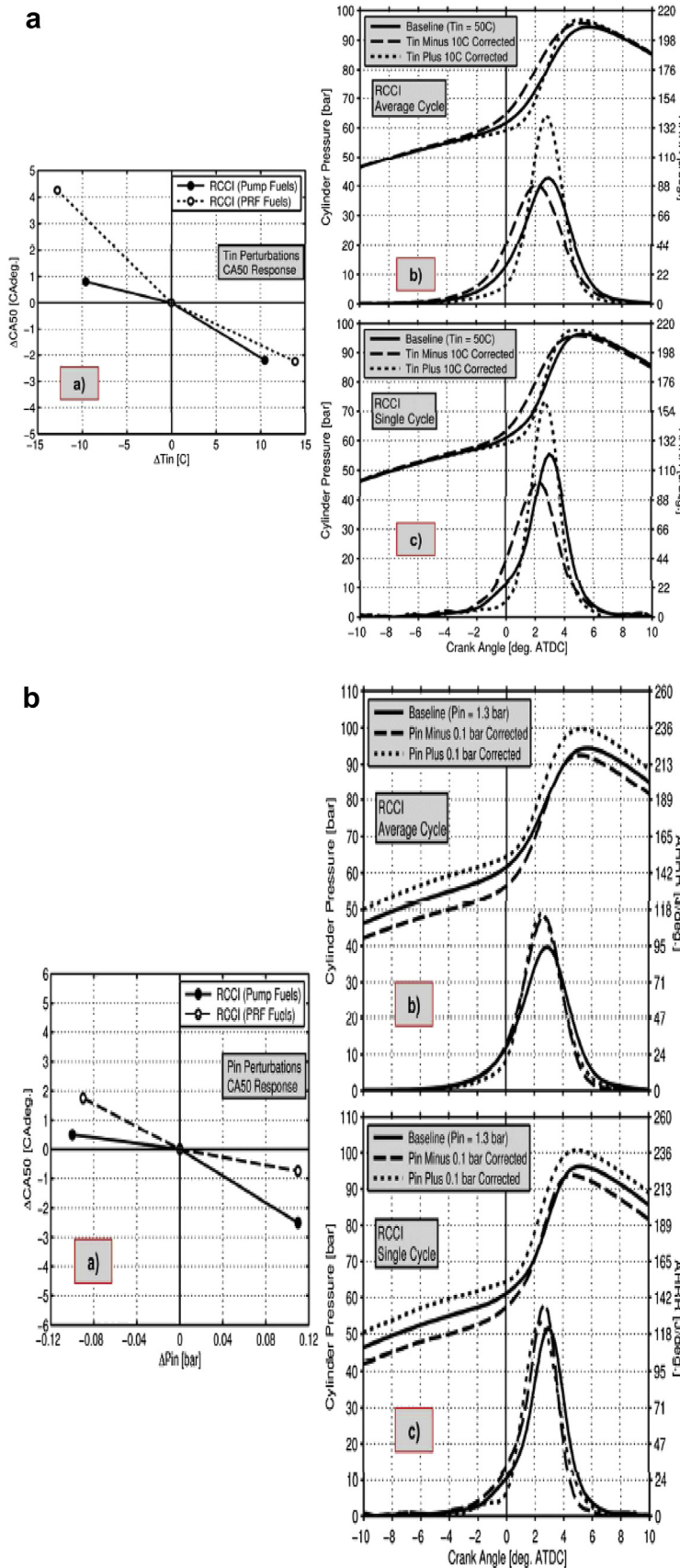


Fig. 18. a. Effect of intake temperature perturbations on dual fuel RCCI with pump fuels [5]. b. Effect of intake pressure perturbations on dual fuel RCCI with pump fuels [5].

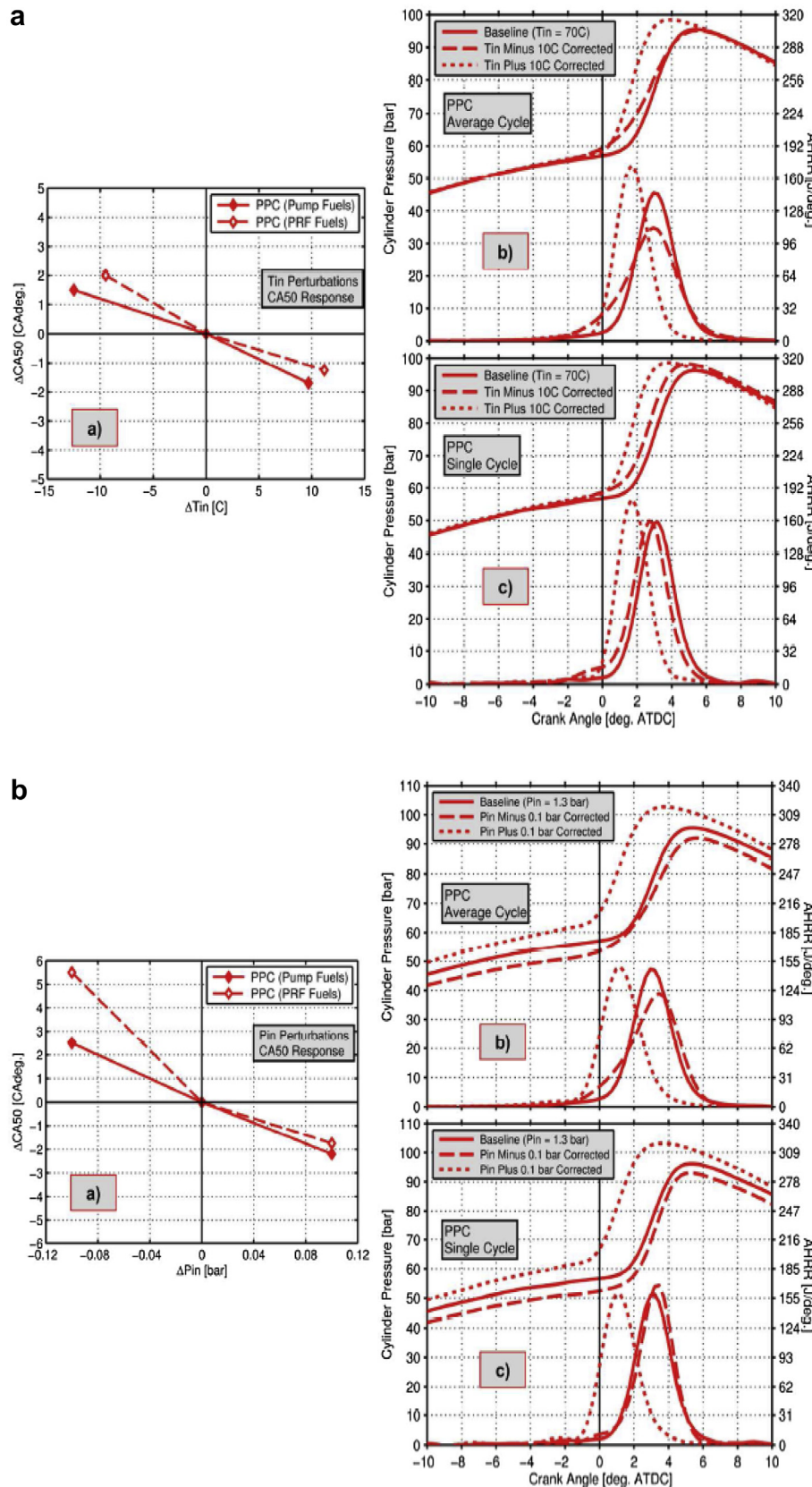


Fig. 19. a. Effect of intake temperature perturbations on Single fuel PPC with pump fuels [5]. b. Effect of intake pressure perturbations on Single fuel PPC with pump fuels [5].

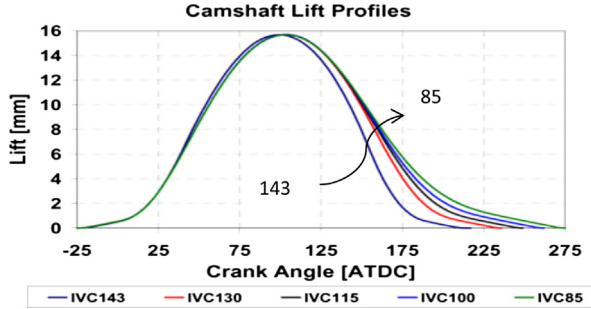


Fig. 20. Intake valve lift profiles for custom camshafts [34].

percentage. Further optimization of the global fuel reactivity was performed at an IVC timing of -143° aTDC through a gasoline percentage sweep. For each study the IVC pressure was adjusted with the -143° and -115° cams to match the peak motored

pressure of the -85° cam and to deliver the same trapped air mass of 5 g/cycle.

Fig. 24(a) shows the measured cylinder pressure and heat release results for a constant combustion phasing using three different IVC timings and the resulting gasoline percentages. For the different IVC timings, CA50 was kept constant by varying the gasoline percentage. The increased TDC temperatures from the earlier IVC timings of -143 and -115° aTDC demanded higher amounts of gasoline to maintain the combustion phasing over the -85° aTDC IVC timing case. Also interesting to note, is the difference in the shape of the heat release, as shown in the expanded plot of Fig. 24(b). As the amount of gasoline injection was increased, the magnitudes of the high temperature heat release (HTHR) increases accordingly. Consequently, less diesel fuel was injected for the earlier IVC timings. This decreased amount of diesel fuel then released less energy, which reduced the low temperature heat release (LTHR), as seen at $\sim -12^\circ$ aTDC. As is well known, gasoline typically does not exhibit an LTHR.

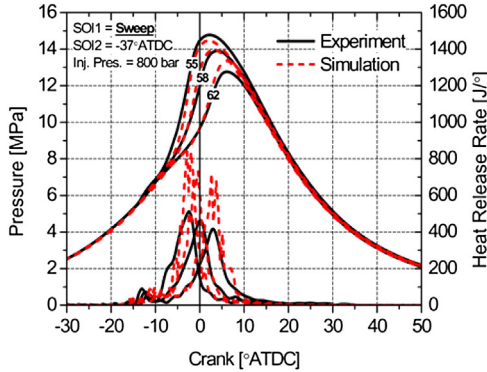


Fig. 21. Comparison of experimental and predicted pressure and AHRR between SOI-1&2 [34].

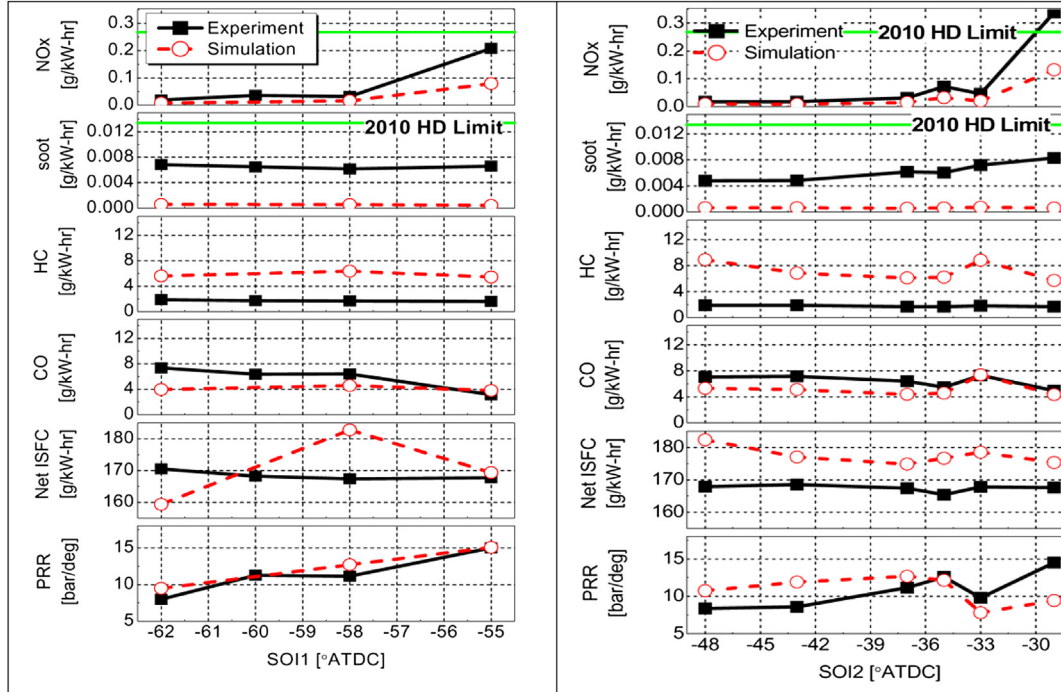
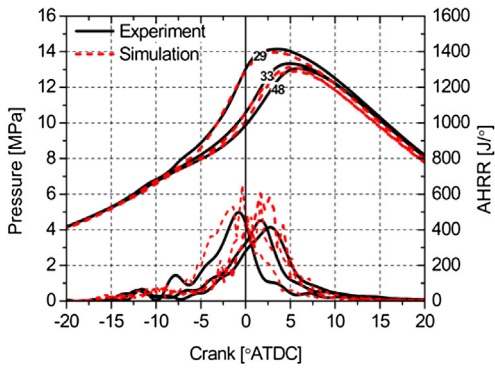


Fig. 22. Experimental and predicted performance and emissions between SOI-1 & 2 [34].

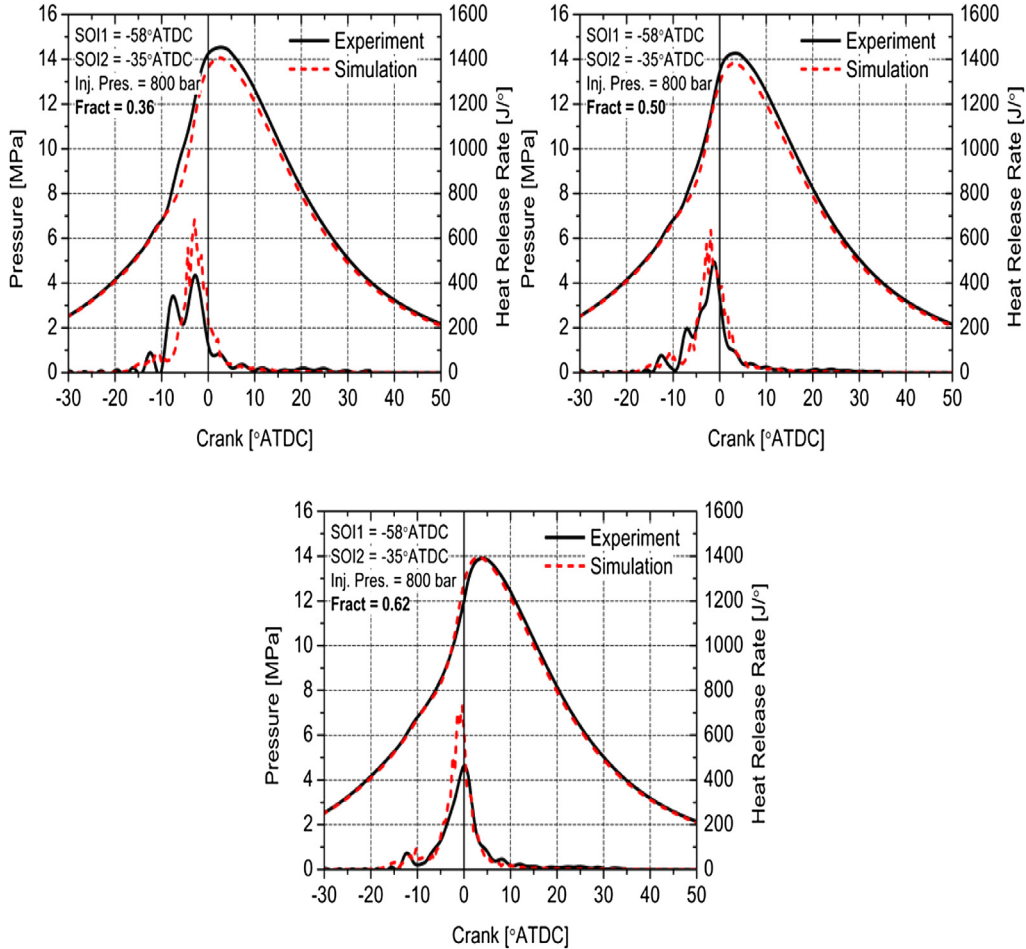


Fig. 23. Measured and computed pressures and heat release rates at SOI-1 fuel sweep [34].

Fig. 24(c) shows measured cylinder pressure and heat release data for gasoline percentages of 82, 86 and 89% at a constant IVC timing of -143° aTDC, which corresponds to the highest effective compression ratio case of 16:1. The additional gasoline percentage is seen to phase combustion later in the cycle by reducing the global fuel reactivity. This later phasing of combustion drops cylinder temperatures, which slows NO_x formation rates and lowers heat transfer [44]. HC and CO were seen to increase slightly due to the slower oxidation rates at these cooler temperatures.

Pressure rise rates were also decreased with the additional gasoline as the heat release rate reduced due to the increased combustion duration. The later combustion phasing also helped to decrease fuel consumption due to the lower rates of heat transfer from reduced injection-generated turbulence and reduced soot radiation. The combination of optimal combustion phasing, combustion duration and lower heat transfer achieved a net indicated thermal efficiency of 53% for the 89% gasoline and 11% diesel fuel case, while meeting US EPA 2010 on-highway NO_x and PM emissions in cylinder. It is noteworthy that the study used an inexpensive automotive-style port fuel injector and a low pressure (800 bar) large hole nozzle diesel injector, which is a very cost effective fuel injection system compared to current 2000 bar or higher common-rail-systems.

Ma et al. [45] also investigated the effects of diesel injection strategies on gasoline/diesel dual fuel combustion mode. They used single and double injection strategies (similar to the ERC experiments) to achieve the required charge distribution. The

experimental results confirmed that this type of combustion mode yields high efficiency with near zero NO_x and soot emissions at early injection timings and high gasoline ratios in the case of a single injection strategy. Operating parameters such as injection timing, diesel mass split between two injections and gasoline ratio were also optimized for a double injection strategy. Based on the optimized results, it was found that late second injection timing is an effective approach to expand the operational range to higher loads. However, the maximum load was limited by higher soot emissions. Ma et al. [45] expanded the operating range to a maximum IMEP of 13.9 bar by using a late second injection strategy with increased fuel mass, while still maintaining good emissions and MPRR within a given criteria (**Fig. 25**).

3.3.4. Mixing and auto-ignition processes in RCCI combustion

Understanding the mixing and auto-ignition process of RCCI combustion is very important in order to obtain the required fuel reactivity distribution in the cylinder. In this connection, recently, Benajes et al. [46] reported an experimental and numerical study to understand mixing and auto-ignition processes in RCCI combustion using diesel and gasoline as the high and low reactivity fuels, respectively. In their work a single-cylinder four stroke, compression ignition research engine representative of a commercial truck engine was used for studying RCCI combustion. The data obtained from the test engine were used as the input to an in-house 1-D spray model, DICOM [47–49]. The code was focused on clarifying the mixing process with respect to variations of the in-cylinder fuel

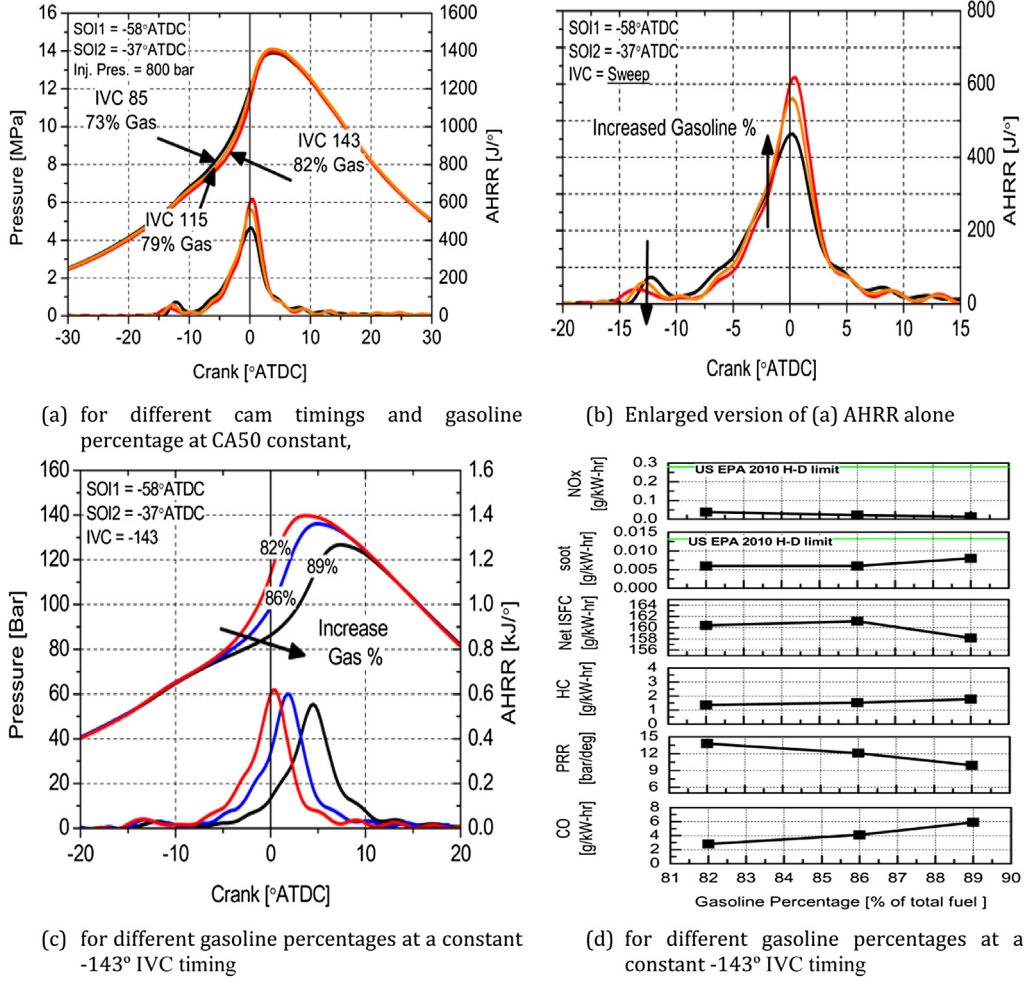


Fig. 24. Cylinder pressure, AHRR and emissions for gasoline percentage sweep at IVC timings [34].

blending ratio and injection timing. The numerical study revealed that combustion starts with the auto-ignition of the diesel fuel, followed by entrainment of gasoline. The subsequent increase in temperature and pressure was thought to initiate flame propagation across the lean diesel and gasoline regions of the combustion chamber. The energy release rate pattern obtained from the test

engine showed that the combustion behavior was changed when the diesel fuel was injected into a gasoline-air environment.

Once the effect of adding gasoline port injection to neat diesel combustion was understood, the study focused on varying the in-cylinder fuel blending ratio to understand the influence of global fuel reactivity on the combustion and engine-out emissions for staged RCCI combustion. The diesel fraction was reduced to 10% of the fuel mass and the fraction of gasoline was increased, while keeping the total amount of fuel supplied constant. The tests were conducted at a constant speed of 1200 rev/min with fixed diesel SOI of -24 CAD aTDC and EGR rate of 45%. An important change was noticed when the D/G ratio was reduced from 50/50% to 25/75%. The ignition delay increased, extending the mixing time and the first stage of combustion was lowered while the second was enhanced. Further tests with varying injection timing revealed that the advanced diesel SOI further increased the second stage combustion process.

3.4. RCCI combustion using fuel additives (single fuel strategy)

Splitter et al. [50] demonstrated a “single fuel” strategy (PFI fuel—gasoline, DI fuel – Gasoline doped with a small quantity of tertiary butyl peroxide (DTBP)) at a mid load condition on the HD diesel engine shown in Fig. 1. They found that a very small percentage of an appropriate additive could be used to establish a sufficient large reactivity gradient to match the performance of a

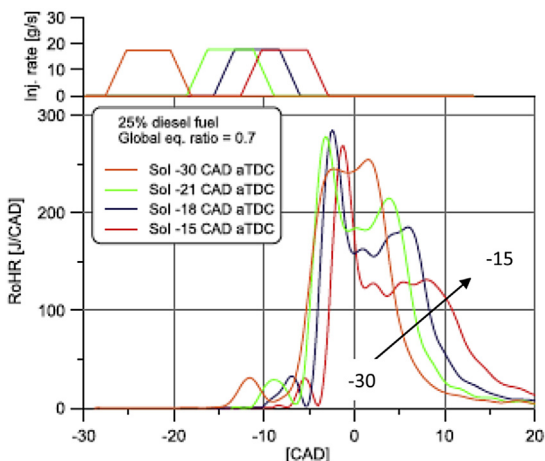


Fig. 25. Changes in combustion behavior in response to injection timing [46].

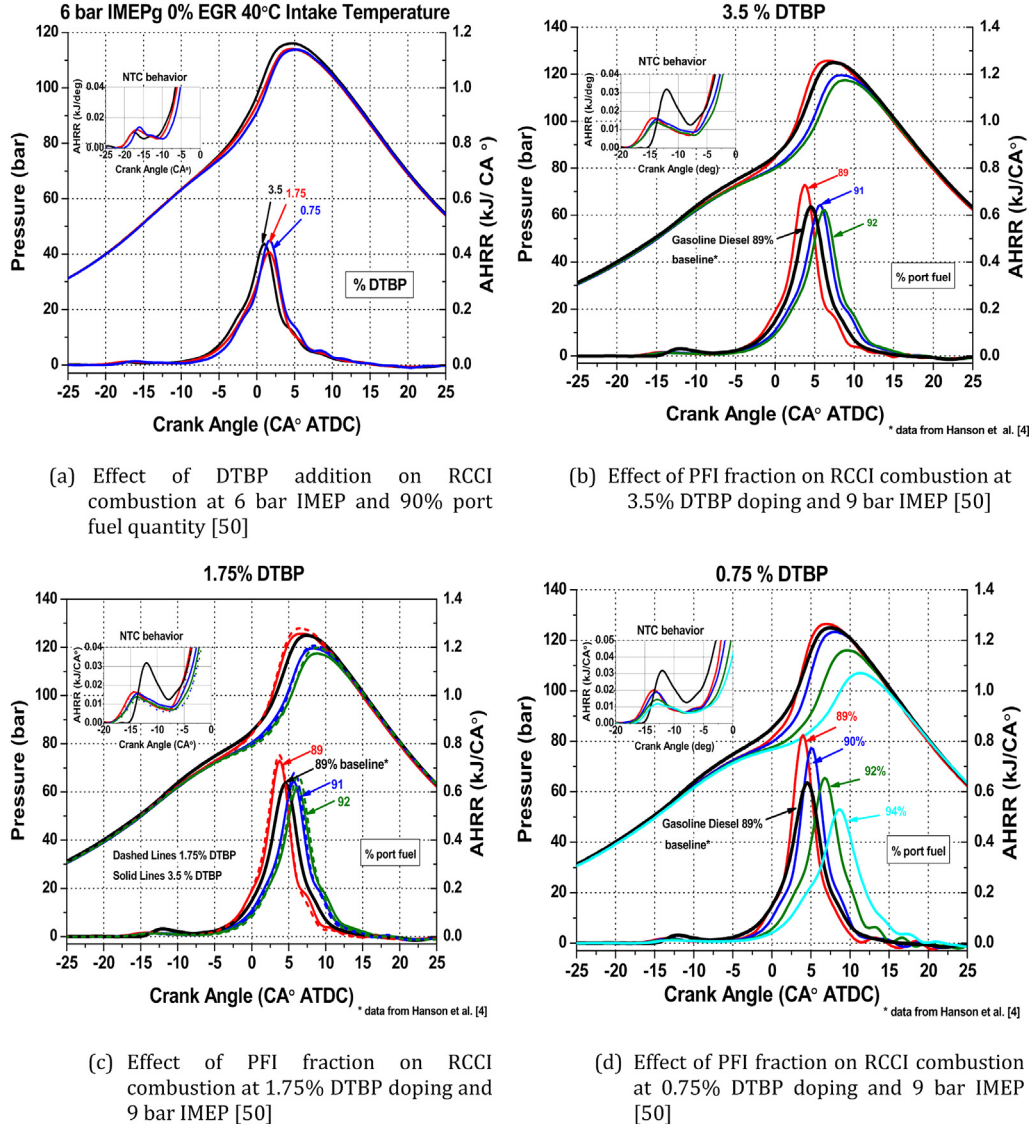


Fig. 26. Pressure and AHRR traces for single fuel strategy with DTBP doped gasoline at 6 and 9 bar IMEP loads and compared to the highest gross indicated thermal efficiency case of Hanson et al. [50].

dual fuel strategy when operated in the RCCI regime. They used DTBP as a cetane improver for the pump gasoline. The study focused on investigating the feasibility of using a single fuel as both the high and low reactivity fuels. The strategy involved PFI of gasoline and DI of gasoline doped with 0.75%, 1.75% and 3.5% DTBP by volume, which accounts approximately 0.2% of the total fueling. DTBP was selected based on research by Tanaka et al. [51]. In that

research, rapid compression machine experiments demonstrated that for gasoline-like fuels, 2% DTBP addition provided a greater effect in decreasing ignition delay than 2% addition of 2-EHN.

The single fuel results with DTBP were compared to previous high-thermal efficiency, low-emissions results with port injection of gasoline and direct injections of diesel. The comparison between the fueling strategies found that the higher volatility of gasoline enabled a reduction in the direct injection pressure from 800 (bar) with diesel to 400 (bar) with gasoline. At the tested conditions, the peak gross indicated based thermal efficiency was over 57%. The emissions trends and magnitudes of the single fuel strategy were also comparable to those of the diesel/gasoline dual-fuel strategy, and both engine-out NO_x and PM met EPA HD 2010 emissions [52] mandates without aftertreatment. Also, the decreased low temperature heat release with the single fuel strategy was found to lower compression work and increased the thermal efficiency by approximately 1% over the diesel/gasoline case.

In these experiments at 6 bar IMEP load and at 1300 rev/min operation, the intake temperature, PFI percentage, port injection pressure, port injection timing, direct injection pressure, direct injection timings were maintained as 40 °C, 90%, 4.14 bar, -320 °CA

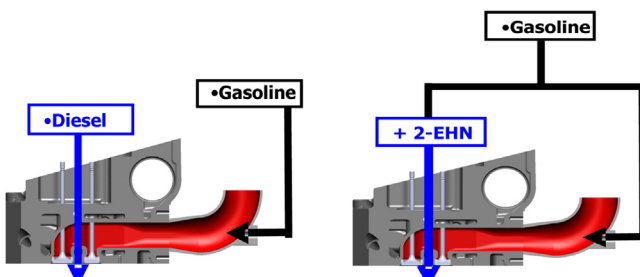


Fig. 27. Dual-fuel and single fuel injection strategies [55].

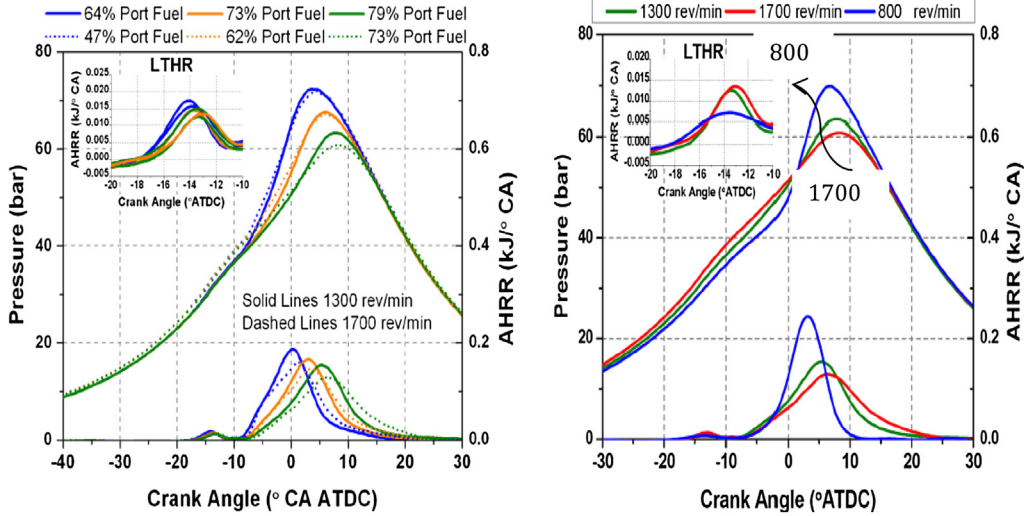


Fig. 28. PFI fraction and engine speed sweep at 4.5 bar IMEP [55].

aTDC, 400 bar, -55 and -36 °CA aTDC, respectively. From Fig. 26(a) it is noticed that the combustion is phased later in the cycle as the percentage of DTBP is decreased, and as the DTBP percentage decreases, the reactivity gradient of the in-cylinder blended fuel is decreased. This results in a globally and locally higher octane mixture, which resists combustion more than more reactive

mixtures. The combustion timing and patterns of the DTBP sweep in Fig. 26(a) were consistent with those of Eng et al. [53] who considered HCCI with cetane improvers.

Splitter et al. [50] also compared 9 bar IMEP doped single fuel strategy operation with 9 bar IMEP gasoline/diesel dual fuel work by Hanson et al. [54]. The operating conditions for this test were

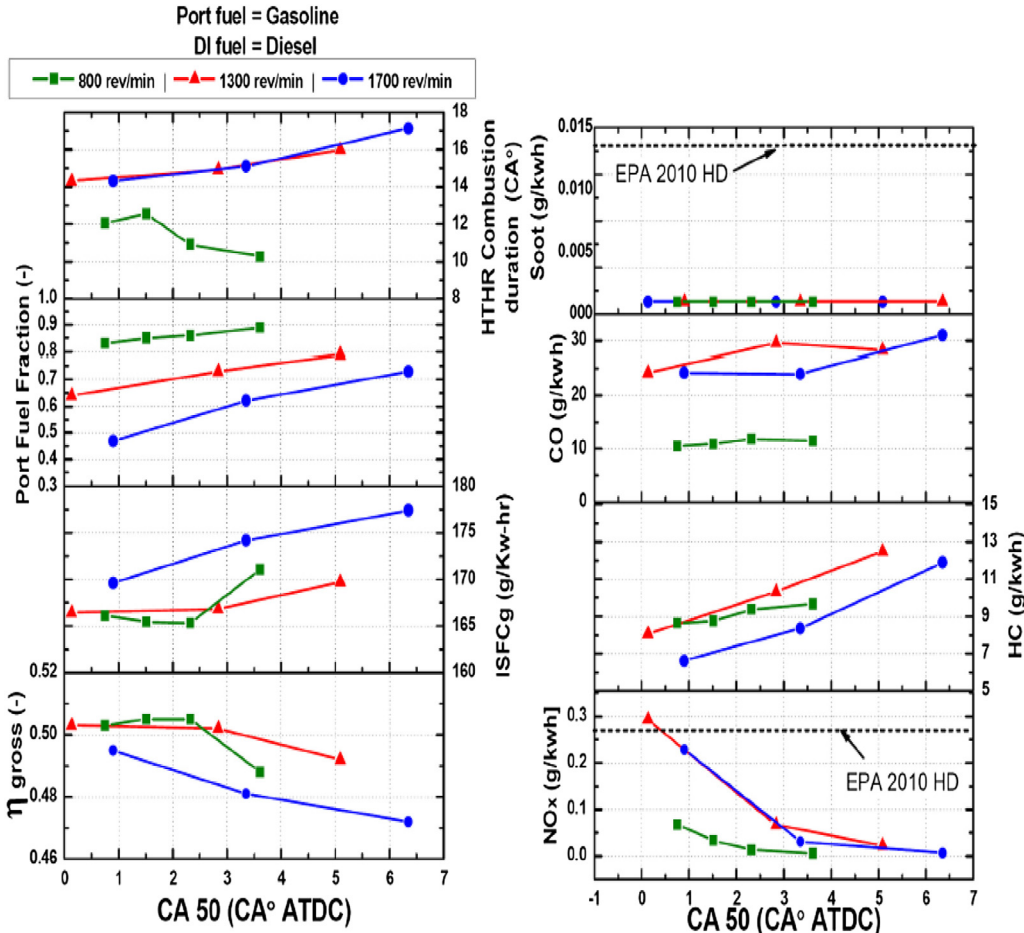


Fig. 29. RCCI combustion, performance and emission characteristics at 4.5 bar IMEP [55].

Table 15

Combustion duration, phasing and fuel consumption relative to DTBP doping percentage at 6 bar IMEP [50].

DTBP dosage (%)	Gross indicated thermal efficiency (%)	ISFC (g/kWh)	CA50 (degCA at TDC)	HTR durations (degCA)
0.75	54	154	0.5	7.8
1.75	55.2	150	0.9	8
3.50	54	152.5	0.25	8.5

Table 16

Comparison of Combustion duration, Phasing and Fuel Consumption Relative to DTBP Doping Percentage at 9 bar IMEP with 3.5% DTBP [50].

		Gross indicated thermal efficiency (%)		ISFC (g/kWh)		CA50 (degCA aTDC)		HTR durations (degCA)	
PFI fractions (%)	Ref.	[54]	[50]	[54]	[50]	[54]	[50]	[54]	[50]
82		55.5	57.0	151.0	143.0	1.5	2.0	6.0	7.0
86		54.0	56.5	152.5	145.0	1.0	4.0	6.5	8.0
89		55.0	56.0	150.0	147.5	4.0	5.0	7.1	8.0

maintained as those of Hanson et al. [54]. It is clear from Fig. 26(b) that 9 bar IMEP operation was possible with the single fuel strategy using DTBP dosing. Furthermore, when operated with identical conditions to those of the gasoline/diesel dual fuel strategy, the single fuel strategy exhibited similar high temperature combustion behavior and phasing. At the 9 bar IMEP condition, the PFI fraction was varied using 89% 91% and 92% for each dosing percentage and RCCI performance, emissions and combustion were analyzed.

In summary, the experiments performed by Splitter et al. [50] demonstrated that relatively small amounts of cetane improver could successfully be used to increase the fuel reactivity of the DI fuel fraction, thus enabling use of a single low reactivity fuel stock supplemented with a small quantity of additive.

3.5. Comparison of single and dual fuel strategies

Hanson et al. [55] conducted additional RCCI experiments on the heavy-duty 2.44 L Caterpillar 3401 of Fig. 1. The primary objective of the investigation was to study low load RCCI operation. The fueling strategy selected for low load RCCI operation included both dual-fuel and single fueling strategies. In-cylinder fuel blending for RCCI operation was achieved using port fuel injection (PFI) of gasoline and early cycle, DI of diesel fuel in the case of the dual-fuel injection strategy, and PFI of gasoline and DI of gasoline doped with 3.5% by volume of the cetane improver 2-ethylhexyl nitrate (2-EHN) in the case of the single fuel injection strategy. The selection of 2-EHN as the cetane improver was made based on the studies of Thomson et al. [56], and rapid compression machine (RCM) experiments with and without CN improved PRF90 (primary reference fuel) [57] and other studies [58–60].

Hanson et al. [55] investigated RCCI operation at loads 2 and 4.5 bar gIMEP at engine speeds between 800 and 1700 rev/min. This load range was selected to cover the low load operational

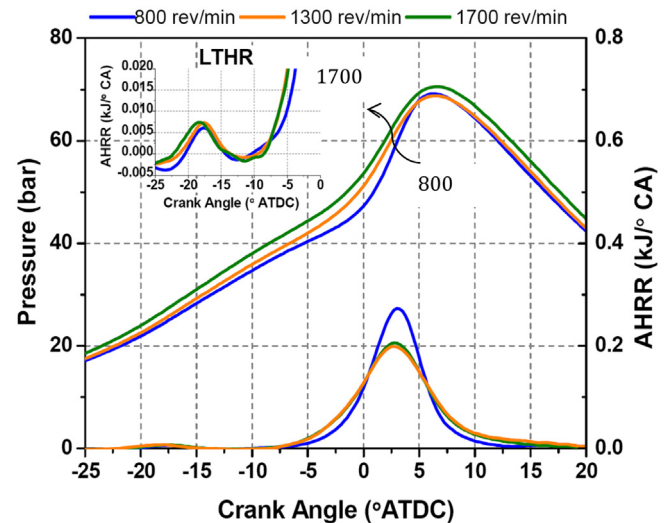


Fig. 30. Single fuel strategy engine speed sweep at 4.5 bar IMEP at CA50: 3.5 deg aTDC [55].

range. At these loads, the engine operating conditions such as inlet air temperature, port fuel amount and the engine speed were varied to investigate their effects on combustion. The DI injection strategy utilized one early injection to raise the reactivity of the fuel in the squish region near the cylinder liner, and a second injection closer to top dead center (TDC) to increase the reactivity in the center regions of the cylinder. The injection timings were fixed for all cases, with the squish conditioning pulse at -62° aTDC and the ignition pulse at -37° aTDC. Fig. 1 shows the experimental set up and Fig. 6 explains the injection timings, while Fig. 27 elucidates the injection strategies.

3.5.1. Dual fuel – gasoline/diesel light load operation

Hanson et al. [55] conducted the initial experiments at 4.5 bar IMEP with gasoline as the low reactivity fuel and diesel as the high reactivity fuel and investigated the effect of engine speed on combustion phasing, the ratio of the high reactivity to the low reactivity fuel (PFI fraction), thermal efficiency, as well as losses due to heat transfer, incomplete combustion, pumping, exhaust and emissions. Experiments with different PFI fractions at 1300 and 1700 rev/min showed that the AHRR and cylinder pressure decreased with increases in engine speed. Also, it was observed that the low temperature reaction (LTR) profiles for these speeds were similar, and the same characteristics were seen even at 800 rev/min. While the LTR profiles were similar at these speeds, it was observed that the high temperature reaction (HTR) became significantly shorter when engine speed was reduced from 1700 to 800 rev/min. Also, it was noticed that variation in the ratio of high reactivity to low reactivity fuel was required to maintain the desired combustion phasing (5 °CA aTDC). Another significant observation from the experiments was an evident decrease in thermal efficiency at higher engine speeds due to increased

Table 17

Emission characteristics at 9 bar IMEP with 3.5% DTBP dosage [50].

PFI Frac. (%)	NO _x , (g/kWh)		PRR bar/CAD		PM (g/kWh)		CO ₂ (g/kWh)		CO (g/kWh)		HC (g/kWh)		η_{comb} (%)	
	[54]	[50]	[54]	[50]	[54]	[50]	[54]	[50]	[54]	[50]	[54]	[50]	[54]	[50]
82	0.05	0.07	14	14	0.005	0.004	512	505	2.5	4.0	1.5	2.8	98.5	97.5
86	0.02	0.05	12	09	0.005	0.003	511	510	4.0	5.0	1.7	3	98.3	97.3
89	0.01	0.02	09	08	0.008	0.005	510	520	6.0	6.0	1.8	3.5	98	97.0

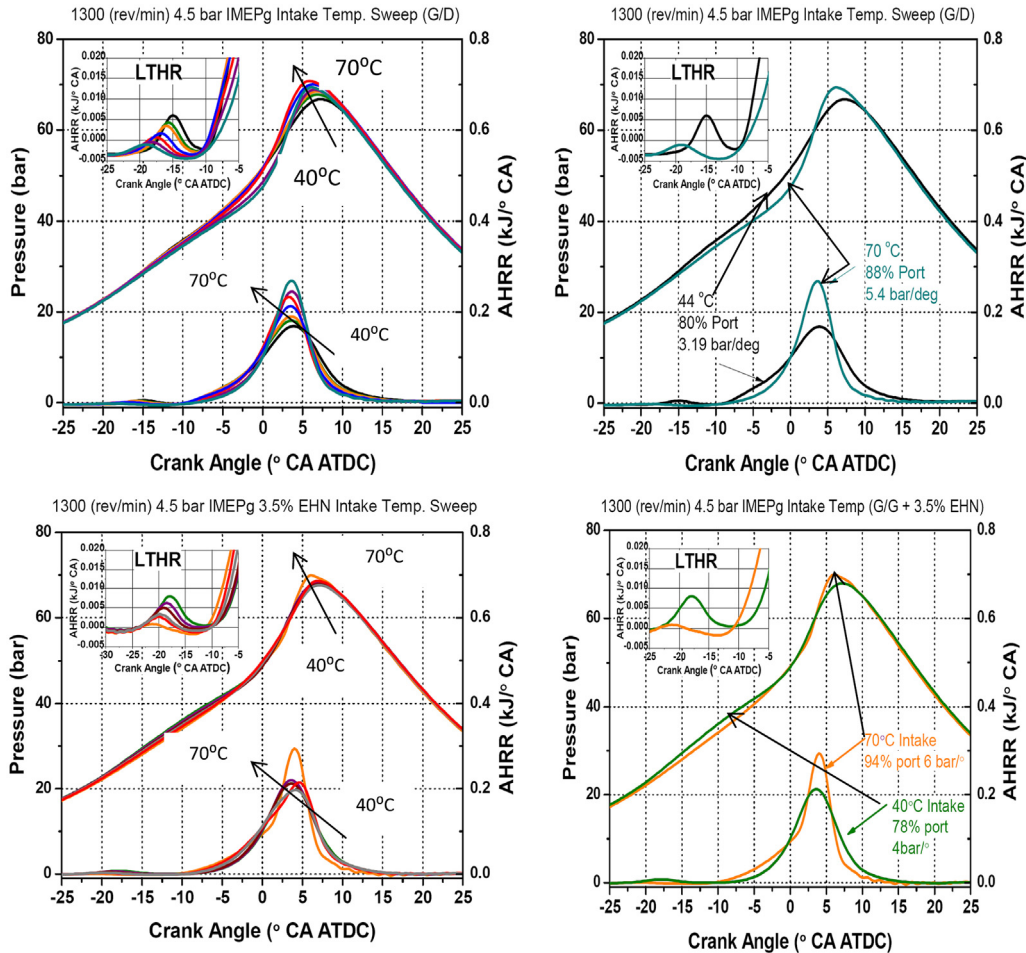


Fig. 31. Effect of intake temperature sweep on RCCI at 1300 rev/min and 4.5 bar IMEP [55].

combustion and pumping losses. The increased combustion losses were due to the fact that increased engine speed lowered the equivalence ratio (due to decreased volumetric efficiency), and the decreased equivalence ratio caused a larger decrease in combustion efficiency at higher speeds. However, NO_x and soot emissions were within the EPA limits (0.27 g/kWh and 0.013 g/kWh, respectively) at all speeds. The gross thermal efficiencies were near 50% for most

cases. The combustion phasing was well controlled and thus the results demonstrated successful light load gasoline/diesel RCCI operation. Figs. 28 and 29 show the results obtained at 4.5 bar IMEP at various speeds.

Table 20

Operating conditions for dual-fuel RCCI load sweep from 4.6 to 14.6 bar IMEP [60].

IMEP gross (bar)	4.6	5.9	9.3	11.6	14.6
Engine speed (rpm)	1300	1300	1300	1300	1300
Fuel flow rate (g/s)	0.57	0.71	1.02	1.36	1.74
Per cent gasoline (% by mass)	48	69	89	85	90
Air flow rate (kg/s)	0.026	0.029	0.03	0.026	0.026
DI SOI 1 (° ATDC)	-62	-63	-58	-67	-58
DI SOI 2 (° ATDC)	-37	-34	-37	-36	-37
DI duration 1 (° CA)	9.4	2.7	3.9	5.1	2.5
DI duration 2 (° CA)	5.1	5.9	2	2.3	4.3
Per cent of DI fuel in pulse 1 (% by mass)	65	32	67	68	37
DI injection pressure (bar)	400	600	800	800	800
Intake surge tank pressure (bar)	1.03	1.38	1.74	2	2.34
Exhaust surge tank pressure (bar)	1.1	1.45	1.84	2.13	2.52
Intake surge tank temperature (° C)	32	36	32	32	32
Air : fuel ratio (-)	45.4	40.9	29	19.1	15.1
EGR rate (%)	0	17	41	46	57
Fuel MEP (bar)	9.2	11.6	16.6	22.2	28.3
IVC (° ATDC)	-85	-85	-143	-85	-85
EVO (° ATDC)	130	130	130	130	130

Table 18

G/G+2-EHN (3.5%) @ 4.5 bar IMEP @ CA50 ~5°CA aTDC [55].

Engine speed, rev/min	NO _x , g/kWh	Soot, g/kWh	HC, g/kWh	CO, g/kWh
800	0.01	0.035	7.5	16
1300	0.02	0.040	9.0	22
1700	0.03	0.025	7.3	60

Table 19

G/G+2-EHN (3.5%) @ 4.5 bar IMEP @ 1300 rev/min [55].

G/D					G/G+2-EHN (3.5%)				
T _i intake (°C)	NO _x g/kWh	Soot g/kWh	HC g/kWh	CO g/kWh	NO _x g/kWh	Soot g/kWh	HC g/kWh	CO g/kWh	
48	0.20	0.001	8.7	14	0.10	0.001	8.0	12.5	
55	0.25	0.001	8.2	10	0.15	0.001	7.8	10.0	
62	0.10	0.001	8.0	8.8	0.21	0.003	7.8	8.8	
66	0.60	0.003	7.9	7.7	0.23	0.005	7.6	7.5	
72	0.45	0.006	8.0	7.6	0.20	0.004	7.5	7.4	

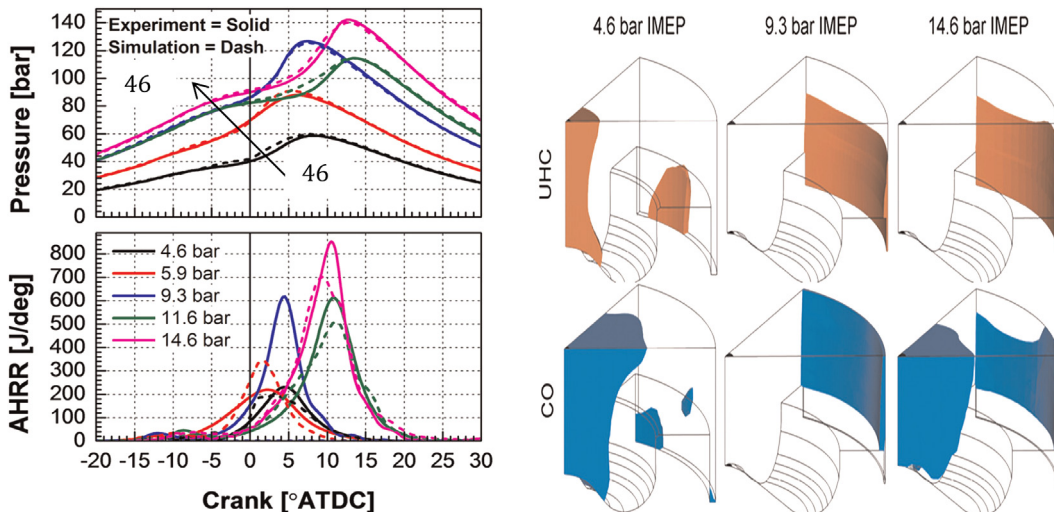


Fig. 32. Comparison of cylinder pressure, AHRR, UHC and CO (at EVO) over the load range from 4.6 bar to 14.6 bar IMEP [60].

3.5.2. Comparison of injection strategies

Hanson et al. [55] also compared “single fuel” strategy results with the dual-fuel strategy results. In that study, the cetane improver 2-EHN was used at a doping percentage of 3.5% by volume with the gasoline in the DI fuel stream, and un-doped gasoline in the port fuel stream (flow rate of 2-EHN was 0.4% of the total fueling rate). Identical experiments were performed with the single fuel strategy. Similar to the dual-fuel tests, the combustion phasing was found to be easily controlled by adjusting the ratio of the high reactivity to the low reactivity fuel. In this case, the HTR was faster than the dual-fuel strategy, and significant differences were noticed in the LTR too, due to the addition of 2-EHN with gasoline in DI stream. Since gasoline typically does not exhibit a two stage heat release, the LTR reactions occurred from the decomposition of the 2-EHN in the DI fuel stream (Tables 15–17).

Similar findings were also observed by Eng et al. [53] in HCCI experiments, and Splitter et al. [35] in RCCI experiments, where both studies concluded that the earlier and more gentle LTR of cetane-improved gasoline was primarily responsible for radical generation and heat generation. In the engine speed sweep, the single fuel strategy also showed similar trends in combustion and HTR duration at constant combustion phasing to that of the dual-fuel results. In the cylinder pressure history shown in Fig. 30 it is observed that the compression pressure was increased with increase in engine speed, even though the engine load and combustion timings were fixed for both strategies, which resulted from the change in equivalence ratio with engine speed.

The single-fuel strategy showed similar HC, CO and NO_x trade-offs as the dual-fuel tests. With both strategies, it was observed that as combustion was retarded, HC and CO increased, while NO_x decreased. It is interesting to note that although 2-EHN is an N-

containing compound, the measured engine-out NO_x emissions were still very low, with CA50 timings after 1° ATDC passing EPA 2010 mandates in-cylinder. Furthermore, PM emissions were very low for all cases, with all tested speeds and CA50 timings passing the EPA 2010 mandates in-cylinder. The thermal efficiency and indicated specific fuel consumption (ISFC) trend with combustion phasing showed higher efficiency at high speeds due to lower heat transfer to the cylinder walls. However, as expected the higher engine speed had higher pumping and heat losses to the exhaust, but these additional losses were less than the efficiency gains from the decreased heat transfer. Although 2010 US EPA HD PM and NO_x

Table 22
Flow of fuel energy over the load sweep [60].

IMEP	Combustion		Heat transfer		Gross indicated Work
	Loss	Loss	Loss	Loss	
4.6	8		22		50
5.9	5		20		51
9.3	3		11		56
11.6	2		16		52
14.6	3		13		51

Table 23
UHC and CO formation regions over the load sweep [60].

IMEP in bar	UHC regions	CO regions	Reasons
4.6	Both Centre line and Crevice regions	Centre line regions	Overly lean region which does not release enough energy and to completely oxidize the CO and UHC.
9.3	Crevice region	Near the cylinder liner	1. UHC is due to unreacted gasoline resulting from the premixed charge. 2. CO is due to relatively low temperatures due to HT from the gas to cylinder liner.
14.6	Crevice region	Near liner region and the centre line	1. Presence of CO near the liner is due to the combination of crevice out gasses and HT from the fluid resulting in low reaction rates. 2. Presence of CO near the centre line is not due to over lean region, but rather locally regions created by the DI event.

Table 21

Emissions and Performance of dual-fuel RCCI over range of loads [60].

IMEP	NO _x (g/kWh)		Soot (g/kWh)		Gross ind. thermal efficiency (%)		RI (MW/m ²)	
	EXP	SIM	EXP	SIM	EXP	SIM	EXP	SIM
4.6	0.02	0.19	0	0.01	49	48.5	0.4	0.5
5.9	0.05	0.02	0.015	0.01	51	52.5	0.4	2
9.3	0.02	0.01	0.012	0.01	56	54	3	4
11.6	0.01	0.01	0.008	0.012	52	54	1.8	1
14.6	0.01	0.01	0.015	0.25	52	53	2.5	2

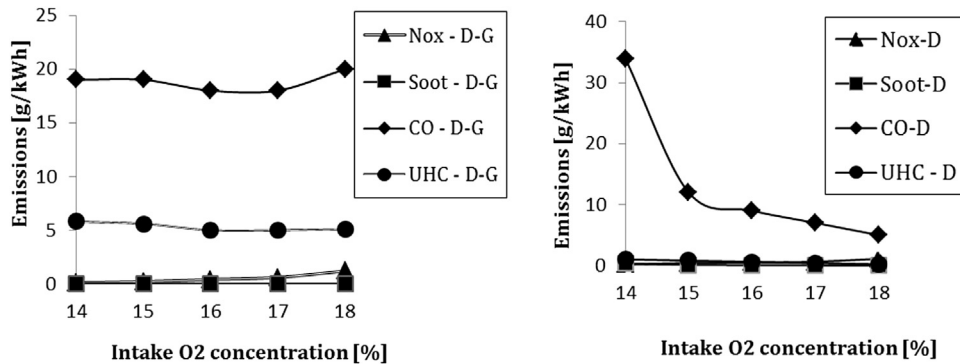


Fig. 33. Engine out emissions from the EGR sweep for Diesel and Diesel–Gasoline operation [60].

emissions standards were met in-cylinder, CO and HC were not, but could possibly be met with a suitable oxidation catalyst.

3.5.3. Intake temperature effects

Fig. 31 shows that a wide range of intake temperatures (40–70 °C) could be used with similar combustion phasings for both strategies. As the intake temperature was increased, the combustion tended to have a shorter duration, which was thought to be caused by the required higher ratio of PFI fuel (used to maintain constant combustion phasing), which tends to ignite more volumetrically. This can also be seen in Fig. 31, where combustion duration differences over the entire intake temperature sweep are seen for both fuel injection strategies. Specifically, the HTR event is more rapid with 2-EHN, displaying a slow ramp followed by a rapid HTR. The emissions and performance results of the intake temperature sweep for both the dual-fuel and single-fuel results can be seen in Tables 18 and 19. The HC and CO emissions from the single fuel case were lower than those of the dual-fuel case, resulting in increased thermal efficiencies across all intake temperatures. Here, the energy losses from heat transfer, pumping and exhaust were similar between the fueling strategies. Since the losses were similar, all of the thermal efficiency gains were due to improved combustion efficiency alone. The decreased combustion duration and increased port-fuel-fraction seen in the speed sweep was also seen in the temperature sweep. PM emissions between the two fuel injection strategies were also similar. The slight increase in PM was thought to be caused by increased PM formation rates from the increased intake temperatures and the results are summarized in Tables 18 and 19.

3.5.4. RCCI operation at idle

Additional tests were conducted at a very light load of 2 bar gross IMEP [55]. Here it can be seen that at both engine speeds the combustion phasing was easily adjustable, with low pressure rise rates and a low ringing intensity (pressure rise rate) of between 0.5 and 1 (MW/m²). The ringing intensity (RI) was obtained using the Eng et al. [53] correlation,

$$RI = \frac{1}{2\gamma} \left[\left(\frac{dp}{dt} \right)_{max} \right] \sqrt{\gamma RT_{max}}$$

Similar to the results at 4.5 bar gross IMEP, the combustion duration and PFI fuel fraction were seen to increase with engine speed and retarded combustion phasing. HC, CO and NO_x also followed a similar trade-off to that seen at 4.5 bar IMEP, with HC and CO increasing as combustion is retarded and NO_x tending to decrease with later phasing. The soot concentration was also weakly affected by phasing, but is still very low, even with a large

percentage of DI fuel. The differences in thermal efficiency between 1300 and 800 rev/min are likely due to the increased time for heat transfer from the slower engine speed.

Thus, RCCI operation was demonstrated successfully experimentally at loads as low as 2 bar gross IMEP. By keeping the global equivalence ratio above 0.3, HC and CO emissions were found to be similar to those at the 4.5 bar IMEP condition. From the results it was noticed that, for particular cases NO_x and PM could be below US 2010 EPA levels with thermal efficiencies of 44%.

3.6. RCCI- A pathway to controlled high efficiency and clean combustion

Kokjohn et al. [60] used the same HD engine shown in Fig. 1 and the only modification made for their work was that two of the cam shafts shown in Fig. 20 were used. As discussed above, the stock cam shaft of the HD test engine had an IVC timing of –143° aTDC and the modified camshaft with an IVC timing of –85° aTDC was also used. However, both the cams had the same IVO timing of –335° aTDC. Kokjohn et al. [60] demonstrated RCCI combustion over a range of loads from 4.6 bar IMEP to 14.6 bar IMEP.

Simulations were also performed using the computational grid shown in Fig. 5. Notice that the region above the top piston ring was resolved in this study; however, ring motion and flows past the compression rings were not included. From the CFD modeling, operation at 9 bar was selected for further analysis.

The injection strategy was same as shown in Fig. 3. The results focused on high efficiency cases from a number of experiments. Thus, the operating parameters and variables were not fixed over the load sweep, and the port fuel fractions and EGR combinations were selected based on chemical kinetic simulations of Kokjohn et al. [8]. The gross indicated efficiency was found to be 49% at the low load condition, and peaked at 56% at 9.3 bar IMEP, and then leveled out near 52% for the higher loads. The optimization was

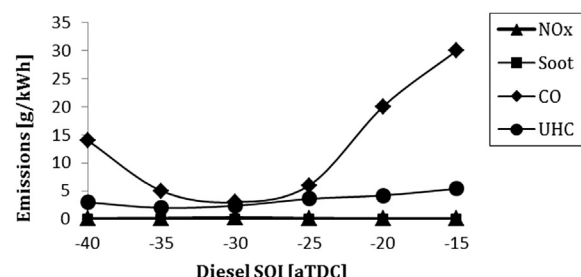


Fig. 34. Effect of diesel SOI on reduction in UHC and CO emission with low NO_x and Soot emissions [60].

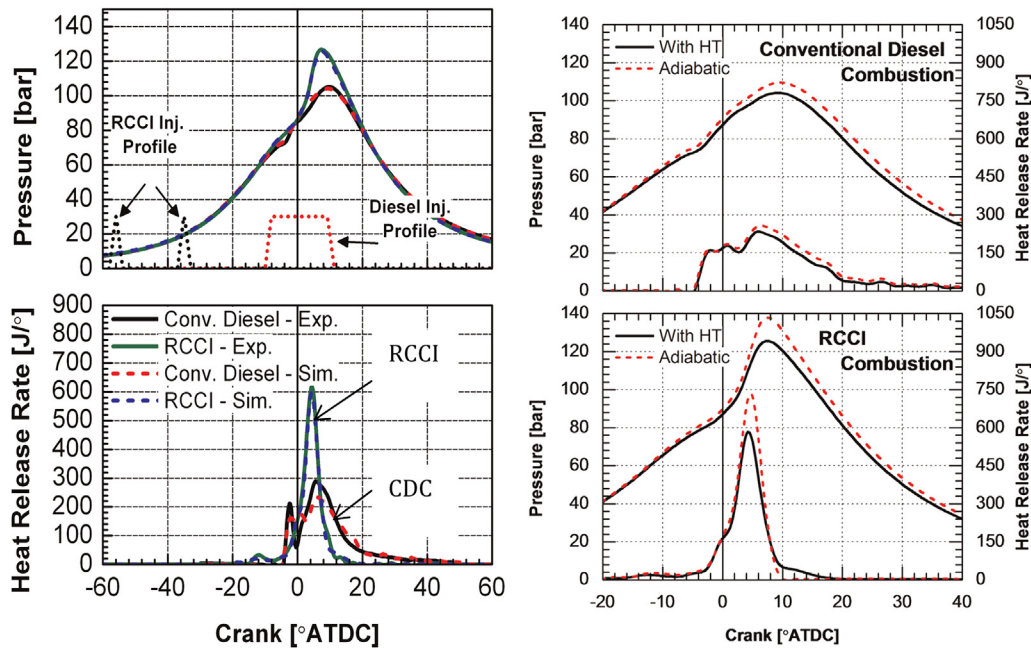


Fig. 35. Cylinder pressure and heat release rate for cases 9 bar, with HT and without HT for conventional diesel and RCCI combustion [60].

done at the 9.3 bar IMEP operating point. The operating conditions for the dual-fuel RCCI load sweep from 4.6 to 14.6 bar IMEP are given in Table 20.

Fig. 32 shows the measured and predicted cylinder pressures and AHRR over the load sweep. The simulations were able to accurately capture the combustion characteristics over the range of loads. Comparing the predicted and measured values in Fig. 32, it can be seen that the models do a reasonable job in capturing the emissions and engine performance over the load sweep. However, at the 4.6 bar IMEP condition NO_x was over predicted by the model, but for the remaining load sweep NO_x was predicted reasonably well (for these cases both the measured and predicted NO_x levels are very low; thus slight differences are not of significant concern). Comparing the measured and predicted soot emissions, it can be seen that the models did a reasonable job capturing the soot trends; however, soot was significantly over-predicted at the 14.6 bar IMEP operating point. It should be noted that the soot model constants were held fixed over the load sweep (i.e., no attempts were made to ‘tune’ the soot model to each specific operating condition). Recall that the 14.6 bar IMEP operation point is near stoichiometric and some portions of the combustion chamber could be expected to undergo slightly rich combustion. The over-prediction of soot as rich combustion is encountered may suggest that different soot model constants are required for rich and lean combustion. However, since the primary focus of the work was fuel consumption, adjustments to the soot model parameters were not explored. More importantly, it can be seen that both the trends and magnitudes of the gross indicated efficiencies were closely captured by the models. Furthermore, because PRR and combustion noise were major limiting factors for premixed operation, it is important to note that the simulations did an excellent job capturing both the trends and magnitudes of the RI (Tables 21 and 22).

Fig. 32 and Table 23 also explain the location and formation of UHCs over the load range from 4.6 bar to 14.6 bar IMEP. Considering Fig. 10, the trend in combustion efficiency and gross indicated efficiency is clear. At the lightest loads, operation borders on the lean limit for the premixed gasoline and complete oxidation of UHC and CO are difficult. At higher engine loads, as stoichiometric operation

is approached, the DI event must be carefully controlled to avoid rich regions and incomplete combustion due to insufficient oxygen. It is likely that at the highest engine loads the UHC and CO emissions could be reduced by increasing the boost pressure to eliminate the regions undergoing rich combustion. However, this was not been explored. Finally, the peak in gross indicated efficiency and combustion efficiency at 9.3 bar IMEP is evident as the result of operation that avoids both the lean and rich oxidation limits.

Although low temperature combustion of in-cylinder blends of diesel – gasoline offers low NO_x and soot emissions with improved engine efficiency and extendable load range, however this type of combustion can produce high unburned hydrocarbons (UHC) and carbon monoxide emissions. De Ojeda et al. [61] studied the chemical origins of the key hydrocarbon species detected in the engine exhaust under diesel-gasoline operation and further developed strategies to lower UHC emissions with low NO_x, low

Table 24
Operating conditions for the conventional diesel and RCCI operation [60].

	RCCI	Conventional diesel
IMEP gross (bar)	9.3	9.9
Engine speed (rpm)	1300	1208
Fuel flow rate (g/s)	1.02	1.19
Per cent gasoline (% by mass)	89	0
Air flow rate (kg/s)	0.03	0.042
DI SOI 1 (° ATDC)	-58	-10
DI SOI 2 (° ATDC)	-37	NA
DI duration 1 (° CA)	3.9	22
DI duration 2 (° CA)	2	NA
Per cent of DI fuel in pulse 1 (% by mass)	67	1
DI injection pressure (bar)	800	755
Intake surge tank pressure (bar)	1.74	1.72
Exhaust surge tank pressure (bar)	1.84	1.83
Intake surge tank temperature (°C)	32	36
Air: fuel ratio (-)	29	36
EGR rate (%)	41	0
Fuel MEP (bar)	16.6	20.5
IVC (°ATDC)	-143	-143
EVO (°ATDC)	130	130

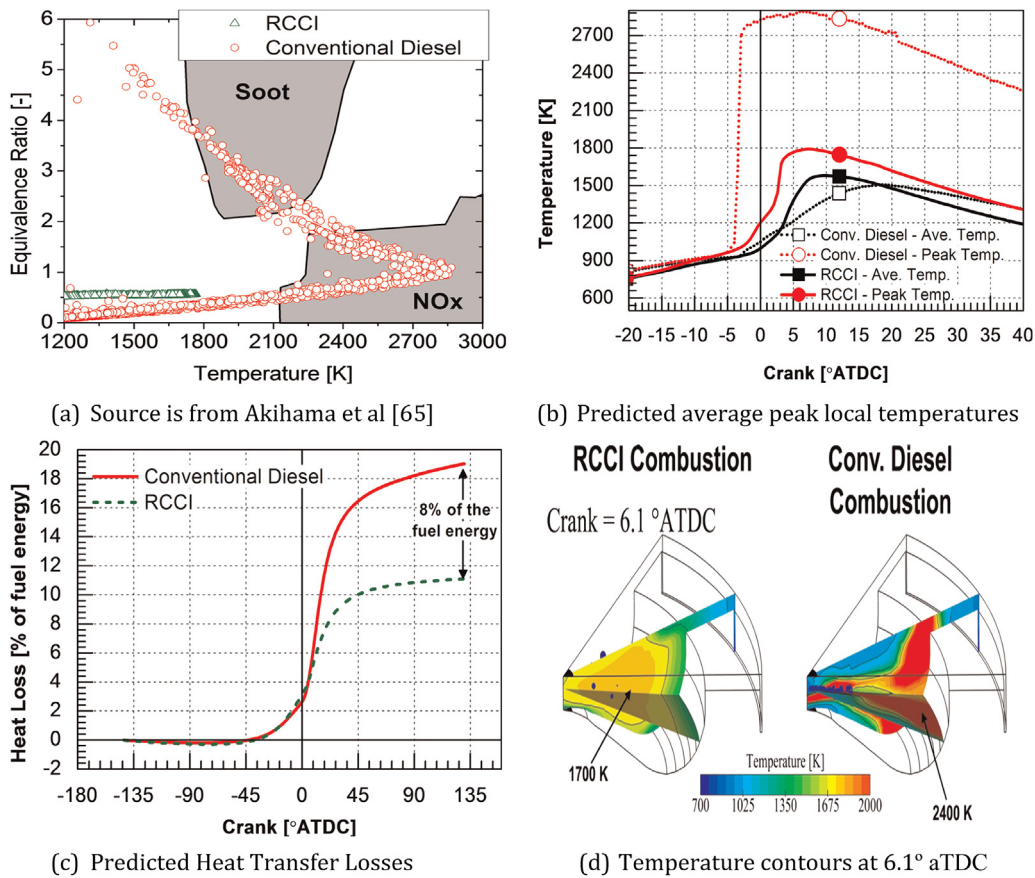


Fig. 36. Comparison of model predicted local temperature, Heat transfer losses and temperature contours for conventional diesel and RCCI operation [60].

soot, and efficiency benefits. The tests were conducted on a single cylinder research engine based on Navistar MAXFORCE 6L engine at a constant load of 10 bar nIMEP with a fixed engine speed of 1600 rev/min. The engine exhaust was analyzed with an FTIR analyzer for species investigation. In their investigation, HC species were categorized as (1) Non-oxygenated species: C₁–C₃ hydrocarbons (methane, ethylene, acetylene, and propylene), C₄–C₇ alkanes (butane, pentane and heptane), and mono-aromatics (toluene), and (2) Oxygenated species: aldehydes (formaldehyde, acetaldehyde, and benzaldehyde).

It was found that C₁–C₃ hydrocarbons were the dominant hydrocarbon species in the engine exhaust of diesel-only operation with EGR, whereas in diesel-gasoline operation UHC appeared as mono-aromatics and C₄–C₇ alkanes, which are mainly formed due to the partially oxidized gasoline constituents. These results helped to suggest suitable strategies for reducing hydrocarbon emissions

from diesel–gasoline operation. The results revealed that an increase in diesel fraction in diesel–gasoline operation reduced UHC emissions with an increase in soot emissions due to enhanced overall fuel reactivity. The results also indicated that advanced

Table 26
Piston properties [66].

Piston owl shape	Open crater	Bathtub	Pancake
r_c	16.1:1	14.9:1	18.7:1
Undercut blank	No	Yes	Yes
Combustion mode	CDC	RCCI	RCCI
Relative reduction in surface area vs. open crater (%)	N/A	4.25	5.1
Polished surface	No	No	Yes

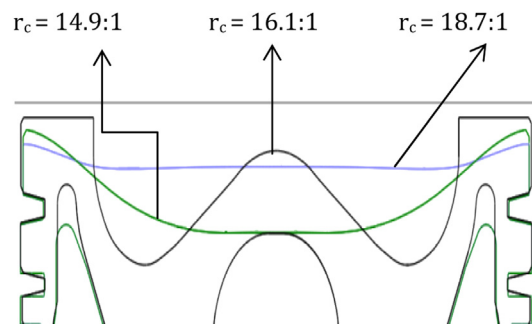


Fig. 37. Piston profile schematic [66].

Table 25

Emissions and performance of RCCI and conventional diesel combustion [60].

	RCCI		Conventional diesel	
	Experiment	Simulation	Experiment	Simulation
ISNOx (g/kW-h)	0.011	0.006	10	9.2
ISsoot (g/kW-h)	0.012	0.019	0.076	0.133
RI (MW/m ²)	3.3	3.8	0.9	1
Maximum PRR (bar/deg)	9.7	10.3	4.9	5.2
Gross indicated efficiency (%)	56.1	54.3	48.2	47.6
Combustion losses (%)	2	1.3	0.1	0.3
HT (%)	11.4	10.9	NA	19.1
Exhaust energy (%)	30.5	33.4	NA	33

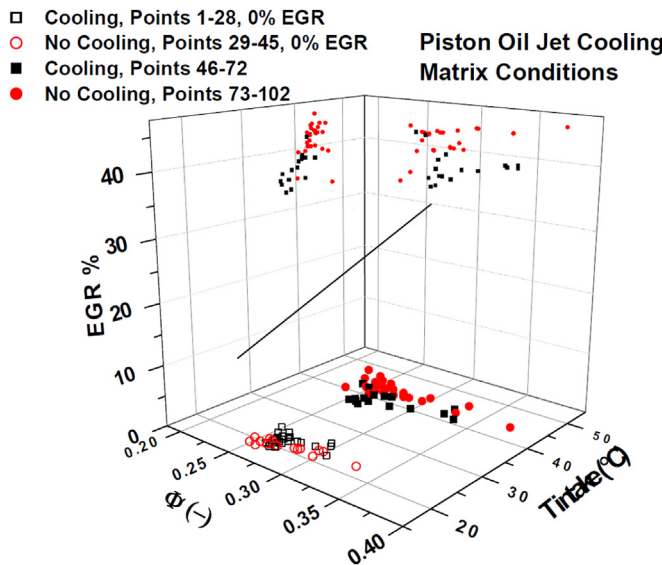


Fig. 38. Piston oil gallery cooling test conditions [66].

diesel SOI also significantly reduced the UHC emissions without compromising the simultaneous low reduction in NO_x and soot emissions. Since one of the reasons for the higher UHC emissions in diesel–gasoline operation is due to the presence of partially oxidized gasoline constituents, the advanced diesel SOI overcomes this by enhancing the reactivity homogeneity of the in-cylinder charge, which in turn minimizes low reactivity regions in the engine, and thereby the UHC emissions were significantly reduced. The overall UHC reduction observed was 65% with an 8% improvement in engine cycle efficiency (Figs. 33 and 34).

3.6.1. Dual direct injection RCCI combustion to control UHC and CO emissions

Prior work on RCCI used port injection of the low reactivity fuel and direct injection of the high reactivity fuel. In an effort to decrease UHC and CO emissions while retaining the benefits of RCCI, Wissink et al. [62] explored the direct, separate injections of both the low and high reactivity fuels. With port fuel injection the reactivity gradient in the cylinder is directly proportional to the equivalence ratio gradient. By direct injecting both fuels these gradients become decoupled and independent stratification of reactivity and equivalence ratio becomes possible. By direct injecting both fuels, a more controlled distribution is possible through spray targeting, potentially reducing the

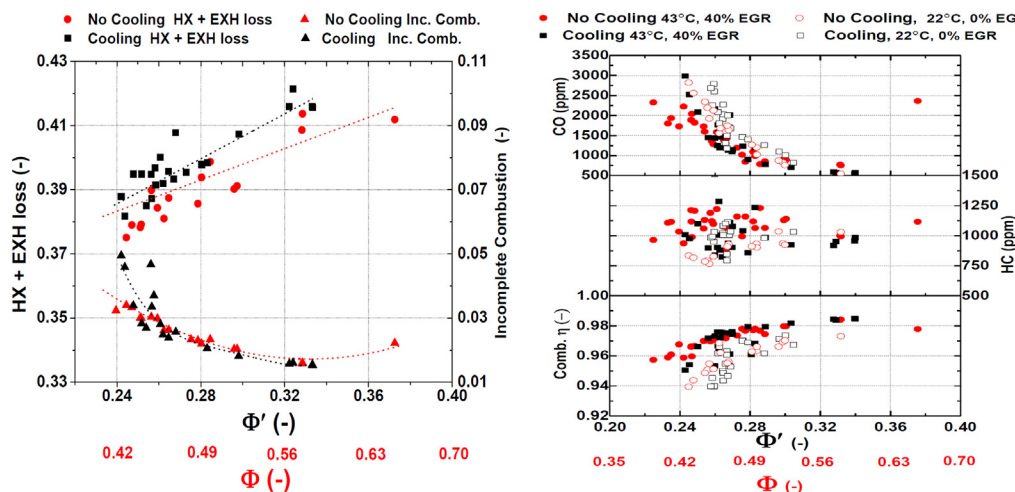


Fig. 39. Loss trends for cooled (open) and uncooled operation (closed) and incomplete combustion emissions concentrations and corresponding fuel energy loss [66].

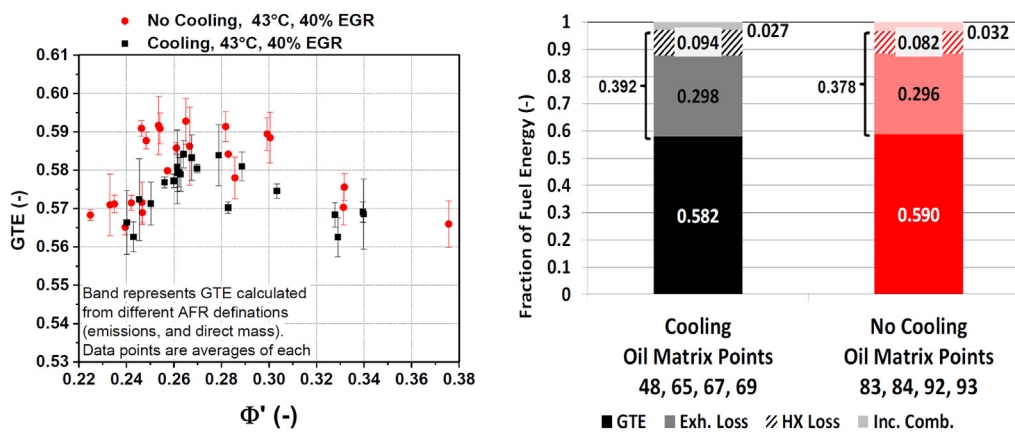


Fig. 40. GTE results with 40% EGR and 43 °C intake temperature at CA 50 of 0.5 °CA ATDC, 6.45 bar IMEP and energy budget at maximum GTE operation with (black) and without (red) piston oil gallery cooling [66]. (For interpretation of the references to color in this figure legend, the reader is referred to the web version of this article.)

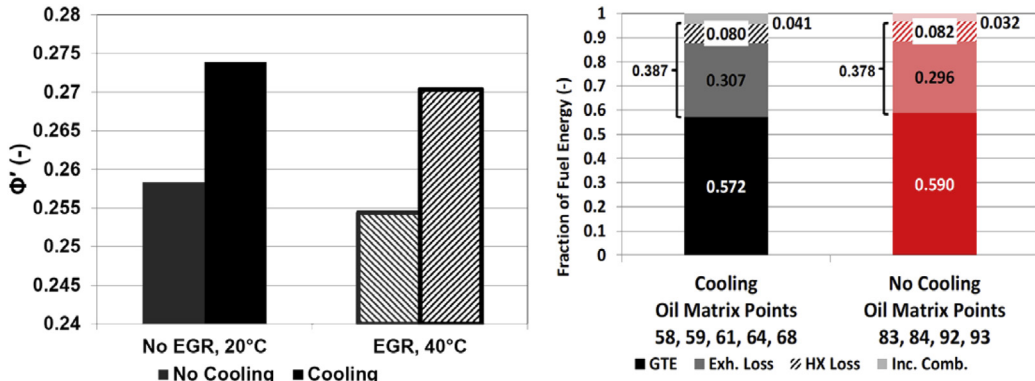


Fig. 41. Φ' at maximum efficiency operation with cooling (black) and without cooling (red). Hashed bars are with 40 °C intake temperature 40% EGR operation, solid bars are with 20 °C intake 0% EGR operation and Matched Φ' operation with (black) and without (red) piston oil gallery cooling [66]. (For interpretation of the references to color in this figure legend, the reader is referred to the web version of this article.)

Table 27
Piston oil gallery cooling test conditions [66].

Matrix data points	1–28	29–45	46–72	73–102
Piston cooling	Yes	No	Yes	No
EGR (%)	0	0	40	40
Intake Temp. (°C)	20	20	40	40
Range of Φ	0.234, 0.304	0.246, 0.329	0.332, 0.542	0.333, 0.684
Range of Φ'	0.234, 0.304	0.246, 0.329	0.239, 0.333	0.223, 0.373

amount of unburned fuel in crevice regions. The experimental results showed that direct injection of both fuels provides performance at least as good as the standard port-fuel strategy, but with significantly less NO_x and similar HC and CO. The direct injection of diesel through use of a low pressure the GDI injector rather than the common rail system also resulted in significant PM reduction. This clearly indicates that the injector hardware requirements for RCCI may be substantially different from those of CDC, and that further investigation into optimum diesel injector design for RCCI will be worthwhile. Also, from computational studies it understood that piston-liner crevice flows are the primary source of UHC and that proper spray targeting can reduce UHC and CO [60].

Due to the scale of the variable space, further optimization of this strategy will require a continued collaboration between experimental and computational studies. Important variables include the nozzle included angle, the quantity, timing and number of the gasoline and diesel injections, the ratio of gasoline to diesel, the temperature and pressure boundary conditions and EGR levels.

The modeling study of Lim and Reitz [63] investigated these parameters with use of dual direct injectors for combustion phasing control of high load RCCI combustion. This work demonstrated that 21 bar gross IMEP RCCI was achievable using dual direct injections. The study used an NSGA II algorithm for finding optimum injection strategies. The goal of the optimization was to find injection timings and mass splits among the multiple injections that simultaneously minimized six objectives, including such as soot, NO_x, CO, UHC, ISFC and RI. The simulations were performed for a 2.44L HD engine with 15:1 compression ratio at a speed of 1800 rev/min. Two iso-octane injections were used with one targeting the squish region and the other targeting the bowl. The single *n*-heptane injection was the ignition source for the entire charge. The results indicated that the *n*-heptane injection mass and timing was most effective for combustion control. The optimum injection strategy resulted in a reasonable 158 bar maximum in-cylinder pressure, 12.6 bar/deg peak pressure rise rate, and 48.7% gross thermal

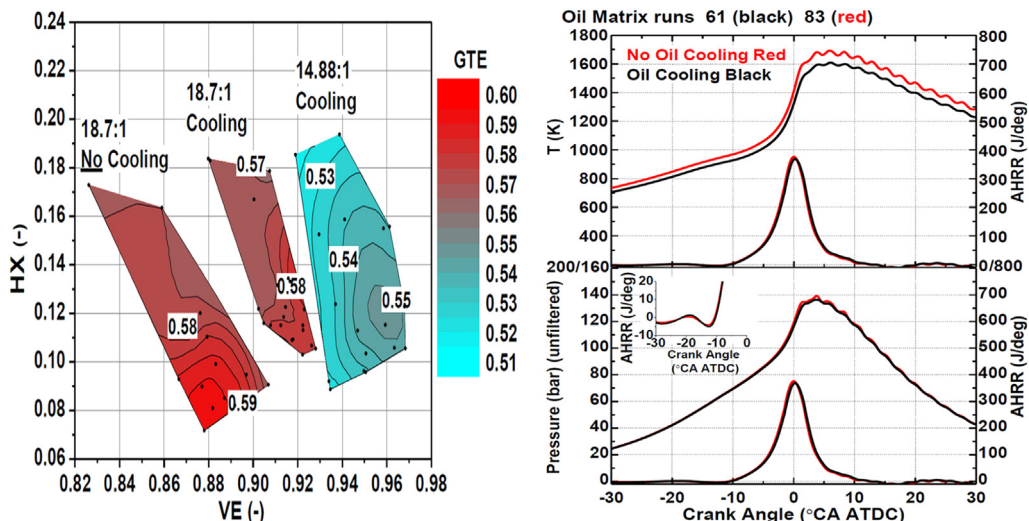


Fig. 42. GTE plotted in volumetric efficiency (VE) and heat transfer space and cylinder pressure and bulk gas temperature for operation with (black) and without (red) piston oil gallery cooling, data are unfiltered [66]. (For interpretation of the references to color in this figure legend, the reader is referred to the web version of this article.)

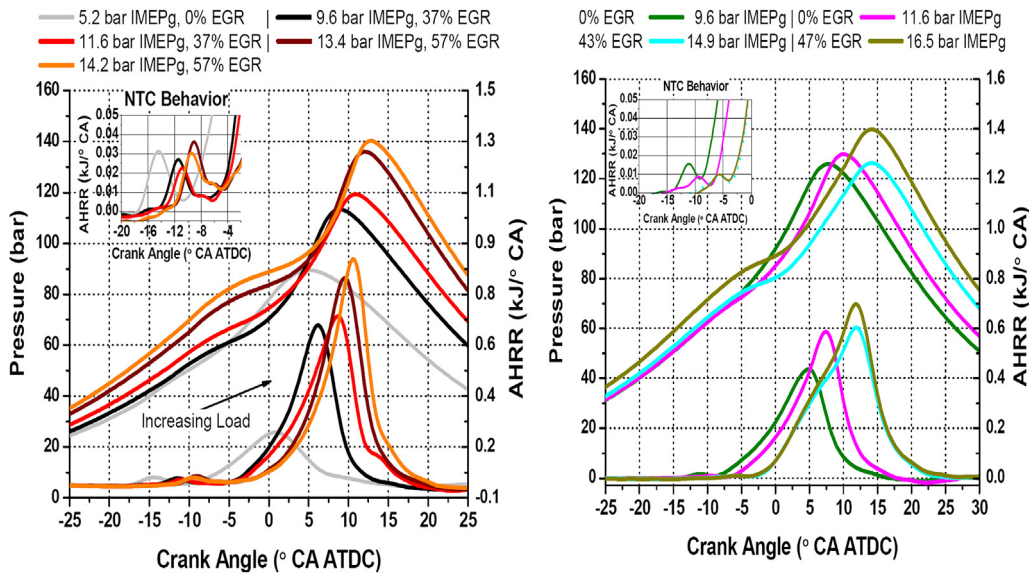


Fig. 43. Cylinder pressure and AHRR traces for G/D and E85/Diesel with load sweep [78].

Table 28
Engine operating condition and preparation strategy [78].

Port fueling %	Varied with load
Engine speed (rpm)	1300
PFI pressure (bar)	4.14
DI pressure (bar)	800 (D)/400 (G + DTBP)
DI – SOI-1 (%)	-60
Timing ($^{\circ}$ aTDC)	-55
DI – SOI-2 (%)	-40
Timing ($^{\circ}$ aTDC)	-36
PFI timing ($^{\circ}$ aTDC)	-360

efficiency. The predicted NO_x, CO and soot emissions were very low. The study concluded that understanding the effect of increased squish land length on the combustion control is of future interest due to the increased heat transfer in that region local surface to volume ratio.

3.6.2. Comparison of conventional diesel and RCCI combustion

Direct comparisons were made by Kokjohn et al. [60] between conventional diesel operation and RCCI operation at the 9 bar IMEP operating point (see Fig. 35). The conventional diesel case was taken from Ref. [64]. There were small differences in the operating conditions (see Table 24) between the RCCI and conventional diesel. The speed differed by less than 100 rev/min, and it was thought that these would not influence the findings of the RCCI

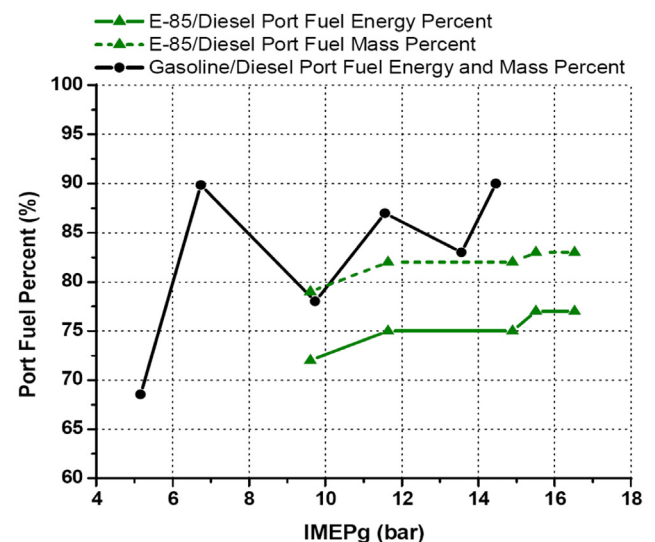


Fig. 44. Port fuel mass and energy % for G/D and E85/D operation [78].

investigation. Compared to conventional diesel combustion, RCCI demonstrated three orders of magnitude lower NO_x, a factor of six lower soot levels, and 16.4% higher gross indicated efficiency. However, RCCI showed increased PRR, RI and combustion losses.

Table 29
Gasoline–Diesel and E85–Diesel load operating conditions [78].

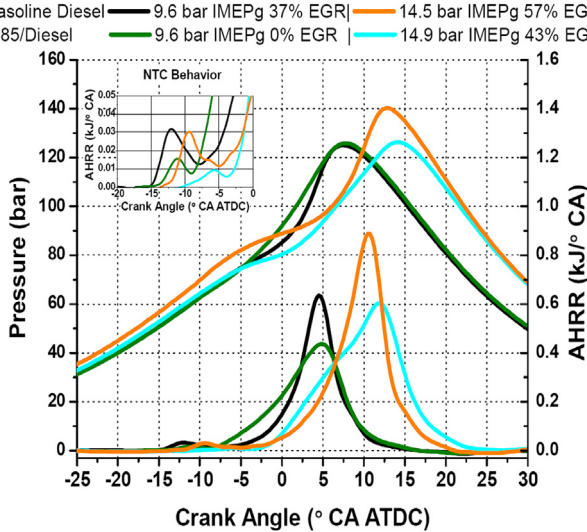


Fig. 45. G/D and E85/D comparison at 9.6 and ~14 bar IMEP_g engine load [78].

But the ringing intensity was still within the limit (5 MW/m^2) suggested by Dec and Yang [13].

Fig. 35 shows comparisons of cylinder pressure and AHRR for cases with and without heat transfer (HT) included in the simulations. In the adiabatic cases, the IVC temperatures were adjusted slightly to provide the same combustion phasing as the cases considering HT. For the RCCI case, in the model the IVC temperature was reduced by 7 K and for the conventional diesel case the initial temperature was reduced by 5 K. Notice that, since the HT is eliminated, the peak AHRR for the RCCI case increases significantly. However, since the rate of heat release for conventional diesel combustion is controlled by transport (i.e., the transport of reactive material to the reaction zone) the combustion rate for the conventional diesel case is relatively insensitive to the elimination of HT. However, the RCCI case shows that, aside from an increase in the peak heat release rate, the end of combustion is much more

rapid. This is due to the elimination of cool regions near the cylinder liner where reaction rates are relatively low and combustion struggles to reach completion.

From the combined effort of the experiments and CFD modeling, it was understood that the observed NO_x and soot reductions are due to the avoidance of high equivalence ratio and high temperature regions in the combustion chamber, as shown in Fig. 36(a). Two factors were found to explain the improved thermal efficiency. First, RCCI combustion avoids the high temperature regions that are located near the piston bowl surface, as observed in the comparisons with the conventional diesel combustion case shown in Fig. 36(d). Thus, the HT losses are reduced by nearly a factor of two. Second, RCCI combustion shows improved control over the start-and end-of-combustion. This improved combustion control allows the combustion timing and duration to be optimized for minimum compression work and maximum expansion work (i.e., maximum indicated efficiency). The improved control over the start- and end-of-combustion was highlighted by exploring adiabatic operation with the CFD modeling. It was found that when consideration of HT is removed, the RCCI combustion process converted 14% more of the recovered HT energy into useful work than conventional diesel operation (Table 25).

3.7. RCCI operation toward 60% thermal efficiency

Splitter et al. [66] explored methods to obtain the maximum practical cycle efficiency with RCCI. The study used both zero-dimensional computational cycle simulations and engine experiments. The experiments were conducted using the single-cylinder heavy-duty research diesel engine shown in Fig. 1 adapted for dual fuel operation, with and without piston oil gallery cooling. In previous studies, RCCI combustion with in-cylinder fuel blending using port-fuel-injection of a low reactivity fuel and optimized direct-injections of higher reactivity fuels was demonstrated to permit near-zero levels of NO_x and PM emissions in-cylinder, while simultaneously realizing gross indicated thermal efficiencies in excess of 56%. The present study considered RCCI operation at a fixed load condition of 6.5 bar IMEP at an engine speed of 1300 rev/

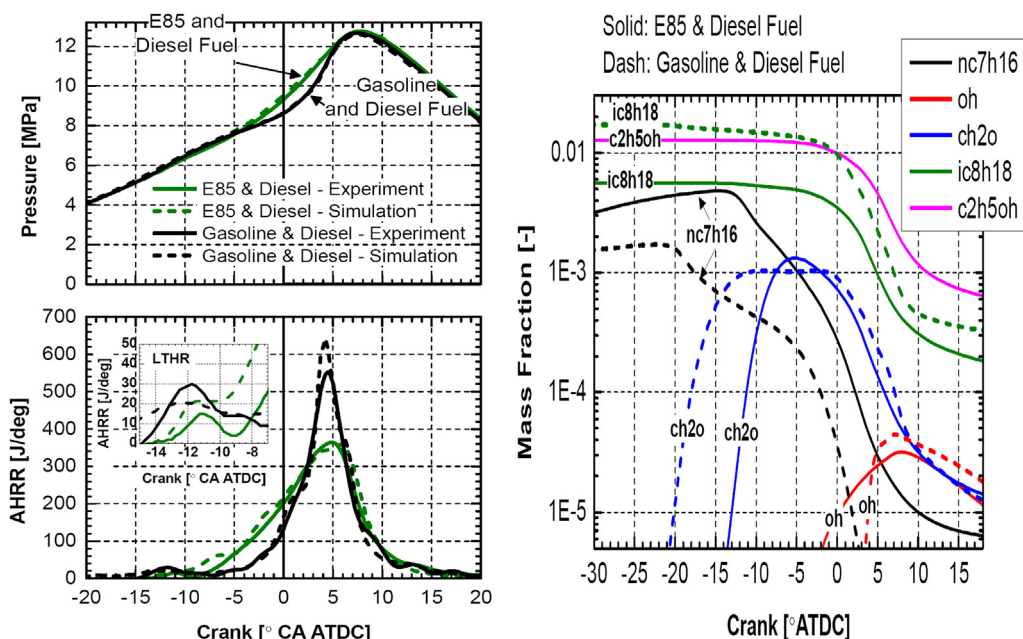


Fig. 46. Comparison of cylinder pressure, AHRR and mass fractions between G/D & E85/D at 9 bar IMEP and 1300 rev/min [78].

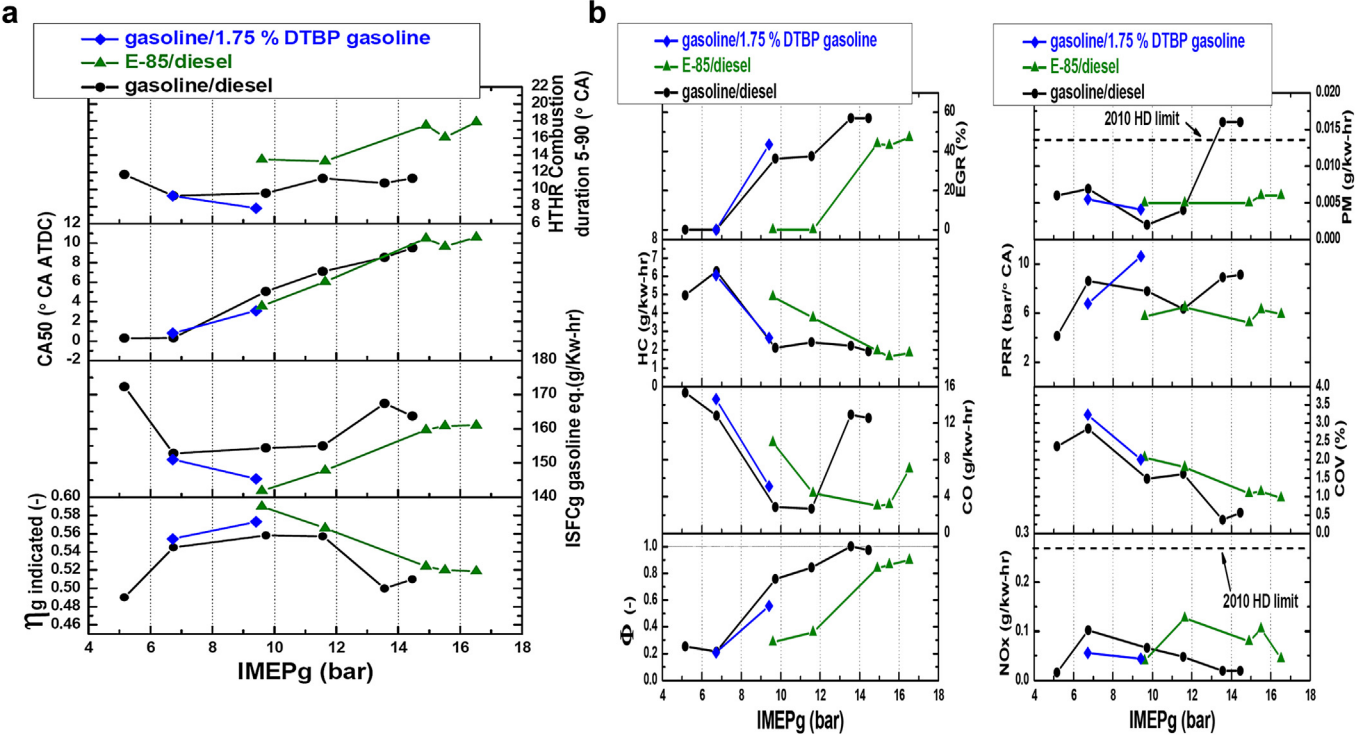


Fig. 47. a. Comparison of combustion and emission characteristics for all tested loads and fuels [78]. b. Comparison of combustion and emission characteristics for all tested loads and fuels [78].

min. The experiments used a piston with a flat profile with 18.7:1 compression ratio and its properties and profile are shown in Table 26 and Fig. 37, respectively.

The results demonstrated that the indicated gross thermal efficiency could be increased by not cooling the piston, by using high dilution, and by optimizing in-cylinder fuel stratification with the two fuel technique using large reactivity differences. The best results achieved gross thermal efficiencies (GTE) near 60%. By further analyzing the results with zero-dimensional engine cycle simulations, the limits of cycle efficiency were investigated. The simulations demonstrated that RCCI operation without piston oil cooling rejected less heat, and that ~94% of the maximum cycle efficiency could be achieved while simultaneously obtaining ultra-low NO_x and PM emissions.

HCCI relies on the autoignition of a fully premixed air-fuel charge, affording operation with very lean mixtures ($\Phi < 0.3$). As noted by Foster [67], the lean charge reduces combustion gas

temperatures, reducing the driving potential for heat transfer, and increasing the expansion γ , both increasing work potential. However, to capitalize on these advantages the combustion event must be knock-free, as it is well known that combustion knock increases engine heat transfer. For example, Grandin et al. [68] using in-cylinder Coherent Anti-Stokes Raman Spectroscopy (CARS) laser diagnostics coupled with in-cylinder thermocouples demonstrated that during knocking conditions the thermal boundary layer thins, and heat losses increase.

A different stratification approach [69–72] is partial fuel stratification. This technique introduces controlled equivalence ratio (Φ) stratification into the chamber. Results in Refs. [73,74]

Table 30

Comparison of Zhang et al. [83] with Splitter et al. [78] Heavy Duty engine dual fuel combustion.

Zhang et al. [83] Constraints:	MPRR 15 bar/deg, NO _x < 0.2 g/bhp-h	Splitter et al. [78] Constraints:	MPRR 10 bar/deg, CO < 5000 ppm, HC < 4000 ppm
--------------------------------	--	-----------------------------------	---

Parameters	G/D		E85/D		Parameters	G/D		E85/D	
	CM1	CM2							
BMEP, bar	10.3	9.9	11	gIMEP, bar		13.6 bar	14.9 bar		
SOI, °bTDC	12	58	12.5	SOI 1 & 2, °bTDC		55 and 36	55 and 36		
EGR, %	46	47	42	EGR, %		57	44		
PFI, %	84	93	75	PFI, %		83	75		
NO _x , g/kWh	0.068	0.041	0.1361	NO _x , g/kWh		0.05	0.13		
Smoke, FSN	0.32	0.18	0.11	PM, g/kWh		0.015	0.006		
BTE, %	42.2	42.1	42.5	Gross ITE, %		53	57		
Speed, rev/min	1200	1200	1200	Speed, rev/min		1300	1300		

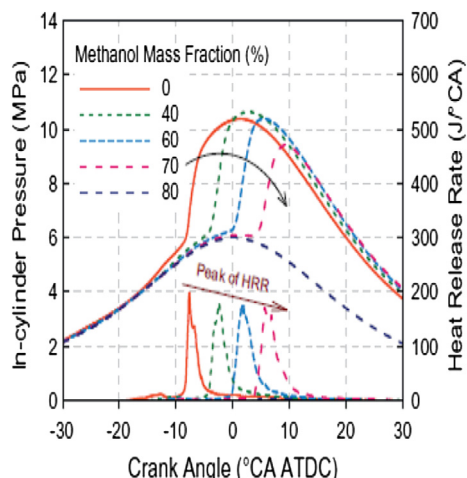


Fig. 48. Effect of premixed combustion over mixing controlled combustion [85].

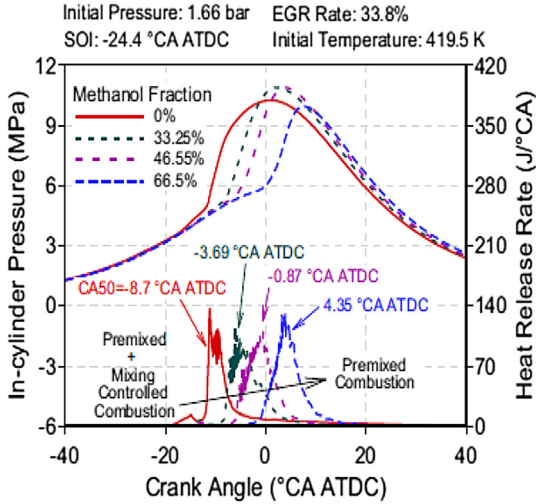


Fig. 49. Effect of methanol fraction on pressure, HRR and CA50 [86].

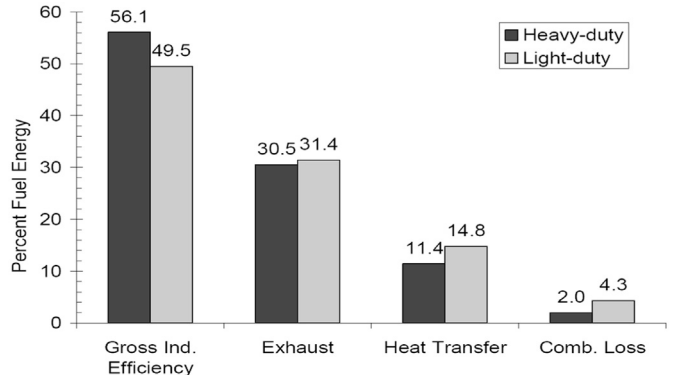


Fig. 51. Energy balances for the LD and HD engines [88].

show that partial fuel stratification can increase engine efficiency at high loads by reducing engine knocking and enabling more efficient combustion phasing. Alternatively, fuel stratification can be compounded by introducing simultaneous reactivity and ϕ stratification through the use of dual-fueling. Modeling results by Kokjohn and Reitz [75] have shown that ϕ plus reactivity stratification further enhances the ignition gradient within the charge, enabling knock-free autoignition combustion phasings near TDC at mid-high load operation. In-cylinder planar laser induced fluorescence (PLIF) measurements by Kokjohn et al. [76] supported earlier emissions spectroscopy work by Splitter et al. [77], which demonstrated that this dual-fuel combustion event is controlled by zones of reactivity sequentially igniting from the most to least reactive.

In Splitter et al. [66] the fuels used were splash blended on site. The low reactivity fuel used was E85, determined through blending a measured volume of 85% ethanol with a separate measured volume of 15% gasoline, and the blend comprised the port injected fuel. The high reactivity fuel was cetane improved gasoline. 3% by volume of 2-Ethylhexyl-Nitrate (EHN) was added to gasoline, and

Table 31
Operating conditions for HD and LD engine [88].

Parameters	Heavy duty	Light duty
Engine	CAT	GM 1.9 L
IMEP (bar)	9	
Engine speed (rev/min)	1300	1900
Mean piston speed (m/s)	7.2	5.7
Total fuel mass (mg)	94	20.2
EGR (%)	41	
Premixed gasoline (%)	82 to 89	81 to 84
Diesel SOI 1 (°aTDC)	-58	-56
Diesel SOI 2 (°aTDC)	-37	-35
Diesel injection pressure (bar)	800	500
Intake pressure (bar)	1.74	0.86
Intake runner temperature (°C)	32	39
Air flow rate (kg/min)	1.75	0.46
Abs. exhaust back pressure (bar)	1.84	1.98
Ave. Exhaust Temperature (°C)	271	319
Equivalence ratio	0.52	0.62
Port injected fuel	Gasoline Fuel	
Direct injected fuel	Diesel Fuel	

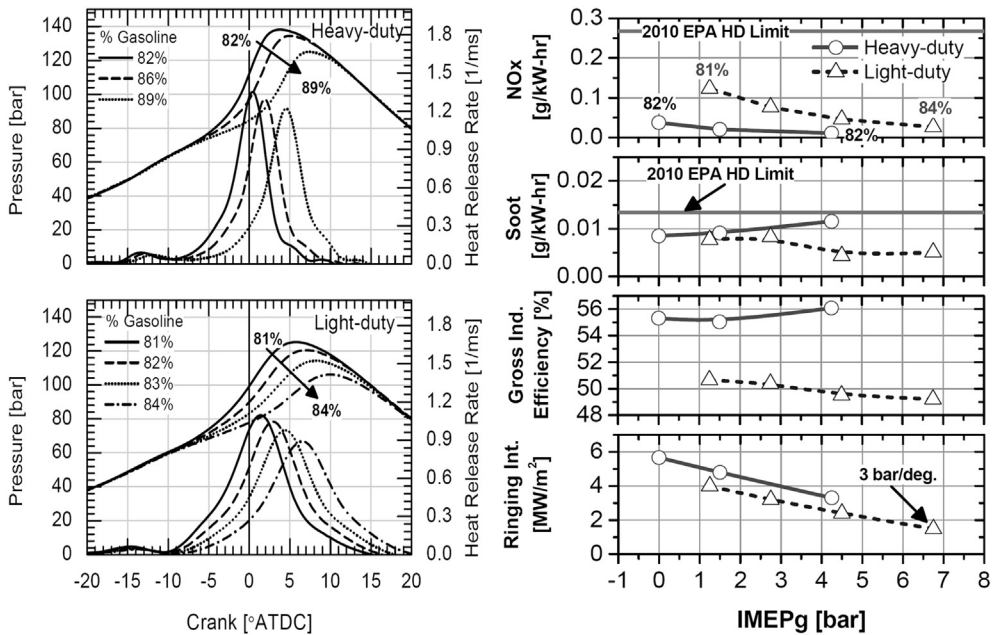


Fig. 50. Comparison of combustion, performance and emission characteristics of the LD and HD engines over a gasoline percentage sweep [88].

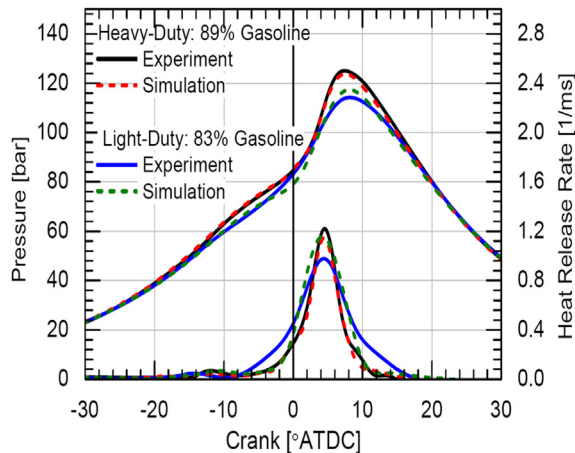


Fig. 52. Comparison of simulated and experimental values at 9 bar IMEP and fixed CA50 4°aTDC [88].

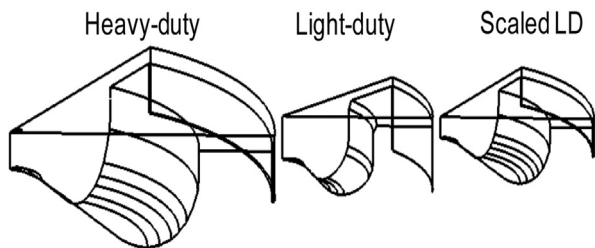


Fig. 53. Comparison of combustion chamber [88].

Table 32

Engine parameters comparing HD, base line LD and scaled LD engine [88].

Engine	HD	LD	Scaled LD
Displacement (L)	2.44	0.48	0.48
Bore (cm)	13.72	8.2	8.0
Stroke (cm)	16.51	9.04	9.64
CR	16.1	15.2	16.1
IVC (°aTDC)	-143	-132	-132
EVO (°aTDC)	130	112	112
Injector type	Common rail		
Nozzle holes	6	8	6
Hole size (μm)	250	128	146
Included angle (°)	145	130	145
TDC surface area to volume ratio (1/cm)	2.7	5.6	4.7

this was the direct injected fuel. Experiments with and without piston oil gallery cooling were conducted to assess if reduction losses and increase in GTE were possible. The tested conditions can be seen in Table 26 with all 102 data points graphically shown in Fig. 38.

The results of Fig. 39 show that for low heat transfer and exhaust losses, lean operation is required. This competes with incomplete combustion losses, which were less at intermediate Φ' ($\Phi' = \Phi$

Table 33

Levels of swirl, speed and geometry [88].

Factor	High	Low
Swirl	2.2	0.7
Speed (rev/min)	2239	1900
Geometry	Scaled LD	Base LD

Table 34
Results of heat transfer reduction investigation [88].

Case	Swirl ratio	Speed (rev/min)	Engine geometry	Premixed fuel PRF	Heat loss (% of fuel energy)
1	2.2	1900	LD	96	14.9
A	0.7	1900	LD	96	14.0
B	2.2	2239	LD	88	15.2
C	2.2	1900	HD	100	14.2
AB	0.7	2239	LD	88	14.0
AC	0.7	1900	HD	100	13.3
BC	2.2	2239	HD	94	14.1
ABC	0.7	2239	HD	94	13.0

(1 – EGR)) operation. However, without piston oil cooling (red markers) the tradeoff in these losses is reduced, enabling good combustion efficiency at leaner operation, thus compounding increases efficiency. The results of Fig. 40 clearly demonstrate that without piston oil gallery cooling, RCCI can exhibit an improved maximum efficiency of approximately 1% point higher. The reasons for this are surprisingly not from improved combustion efficiency, as there is actually a 0.5% point decrease without cooling, but are from reduced heat transfer and exhaust losses of over 1% point. Also, it is clearly demonstrated that without piston oil gallery cooling GTE can be increased, however it was not demonstrated if the increases were from leaner operation, or the change in piston cooling. Therefore, to explore these relations, further analysis was performed. Fig. 41 displays the Φ' associated with maximum efficiency for the four conditions presented in Table 27.

The results illustrated that without piston oil cooling efficiency was maximized at leaner conditions. Therefore, the reductions in heat transfer in Fig. 40 are likely partially dependent on reduced in-cylinder temperatures associated with leaner operation. Thus, to better isolate the trapped mass effects on losses, matched Φ' operation was compared. The results are presented in Fig. 41. However, as seen in Fig. 42, without piston oil gallery cooling the volumetric efficiency of the engine was reduced. This has an indirect impact on gross efficiency. With piston oil gallery cooling, the highest GTE coincides with high volumetric efficiency and low heat transfer (HX). That is, improved engine breathing and thus trapped mass improve GTE.

Conversely, without piston oil gallery cooling, the highest GTE values coincided with the lowest HX and intermediate volumetric efficiency. This suggests that decreased engine breathing may enable improved GTE and reduced HX. However, the relations between breathing and net efficiency were strongly linked, and thus careful and well-engineered air handling systems are required. Additionally, the effect of reduced volumetric efficiency was found to be strongly linked to piston cooling and not to differences in the fueling (PFI/DI ratio), suggesting that piston cooling is primarily responsible for the reduced volumetric efficiency. To understand the reasons for this volumetric efficiency and HX trend reversal, select cooled and uncooled cases were compared. Fig. 42 also

Table 35

Predicted emissions and performance of the HD, baseline LD and LD engine with swirl ratio of 0.7, speed 2239 rev/min and the scaled HD piston bowl geometry [88].

	Heavy-duty	Light-duty	LD improve
ISNOx (g/kWh)	0.01	0.04	0.03
ISsoot (g/kWh)	0.01	0.01	0.01
Ringing intensity (MW/m ²)	2.7	3.7	4.8
Gross indicated Eff. (%)	54.3	46.8	53.2
Heat loss (%)	10.9	13.8	11.6

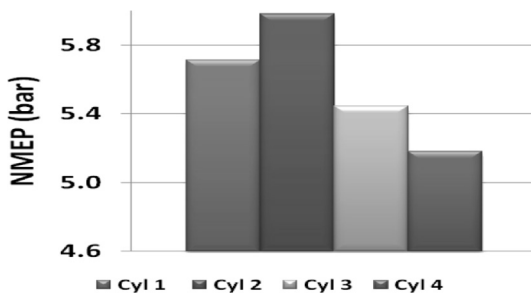


Fig. 54. NMEP for each cylinder in CDC [90].

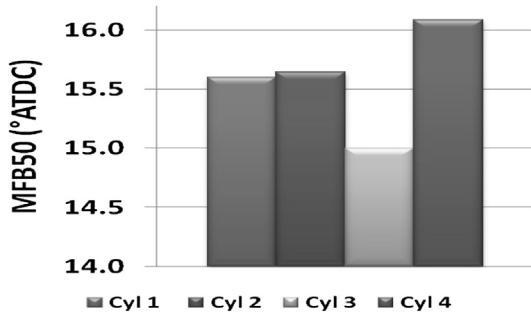


Fig. 55. MFB50 for each cylinder in CDC [90].

illustrates the trends in bulk gas in-cylinder temperature at matched conditions.

Based on the experimental results, 0-D GT-Power simulations were used to help analyze the experimental findings and to determine cycle efficiency limits. The simulations were conducted using the experimental inputs for the initial conditions, and were used to assess pathways for achieving 50% BTE or greater in an HD engine. The simulations suggested that gross thermal efficiencies upwards of 60% would be required, with simultaneous low pumping and frictional losses. The results show that with optimized combustion management and thermodynamic conditions, 60% gross engine efficiencies are possible with RCCI, thus providing a pathway to meet the DOE Super Truck 50% BTE engine efficiency goal, as well as a pathway for reaching 55% BTE. However, the results have also shown that improvements to boosting system efficiencies for low exhaust temperatures and overall reductions in friction are required to best capitalize on the high gross efficiencies.

Table 36

Conventional diesel combustion (CDC) condition for 2300 rpm and 5.5 bar NMEP [90].

BTE (%)	ITE _{net} (%)	NO _x (g/kgf)	CO (g/kgf)	HC (g/kgf)	FSN	Boost (bar)	Intake temp (°C)	Swirl angle (°)	EGR (%vol)
32.10	39.42	3.65	1.67	4.15	1.78	1.18	90.1	35.8	33

3.8. RCCI operation with conventional and alternative fuels (mid and high loads)

Splitter et al. [78] investigated the effect of fuel properties on RCCI combustion by considering gasoline-diesel dual-fuel operation, ethanol (E85)-diesel dual fuel operation, and a “single fuel” gasoline–gasoline + DTBP. Remarkably high gross indicated thermal efficiencies were achieved, reaching 59%, 56%, and 57% for E85-diesel, gasoline-diesel, and gasoline–gasoline + DTBP, respectively. Splitter et al. performed the engine experiments using conditions based on CFD simulations for the heavy duty engine shown in Fig. 1 and modeling was further used to explain the experimentally observed trends. To examine the differences between the three fueling strategies, the results of the E85-diesel and gasoline-diesel dual-fuel results were compared to the single fuel gasoline–gasoline + DTBP results at 9.6 bar IMEP_g load. Compared to gasoline–diesel, significantly higher quantities of diesel fuel were required to maintain optimal combustion phasing with the E85-diesel fuel blends. This is because of the combination of lower reactivity and higher enthalpy of vaporization of ethanol (compared to gasoline) and combustion chemistry effects of ethanol–diesel blends. Secondly, the single fuel gasoline–gasoline + DTBP yielded near identical emissions and ISFC results to gasoline–diesel operation. Although the emissions and ISFC of all three strategies were similar, the LTHR were different with all three fuels, and the HTHR was different with the E85-diesel blends. Fuel chemistry effects for all three fuels were investigated and their effect on the reactivity gradient was found to be responsible for the combustion differences, as discussed next.

3.8.1. Reactivity reduction and enhancement strategies

Splitter et al. [78] adopted ethanol as the fuel reactivity reducing agent for several reasons. First, ethanol has a very high resistance to auto-ignition [79]. Second, ethanol is commercially available in blends with gasoline in ratios as high as 85% by volume. Third, research by Hashimoto [80] has demonstrated that ethanol/n-heptane mixtures exhibit significantly different low temperature chemistry. To explore the effect of a greater reactivity gradient, port-fuel-injection of E85 was used instead of gasoline port fuel injection.

The RCCI experiments are summarized in Fig. 43. The only difference between gasoline-diesel, E85-diesel dual fuel operation and single fuel operation is that the DI pressure was reduced from 800 bar to 400 bar. The reduction in injection pressure was done to account for the volatility differences of gasoline and diesel fuel. Because gasoline vaporizes much faster than diesel fuel, a lower injection pressure was used to produce larger, less easily vaporized droplets, as discussed by Shi et al. [81].

Srinivas et al. [82] investigated the effect of ethanol energy fraction and diesel injection timing on engine efficiency and emissions. Their study was conducted on a single cylinder common-rail diesel engine which was modified to adopt dual fueling technology. In the investigation ethanol was introduced into the intake manifold using a port fuel injector, while diesel was injected directly into the cylinder. Srinivas et al. found that with increased ethanol energy fraction at fixed diesel injection timing

Table 37

Experimental and modeling of dual-fuel conditions [90].

Description	NMEP	Speed	Total fuel mass	Gasoline	Diesel SOI timing	Diesel injection pressure	Intake pressure	Intake temp	RH
Units	(bar)	(rpm)	(g/s)	(% mass)	(°aTDC)	(bar)	(bar)	(°C)	(%)
Modeling	5.5	2300	1.16	65 to 85	-20 to -60	500	1.3	40	14
Experiment	5.5	2300	1.25	65 to 85	-30 to -70	500	1.3	38–43	58

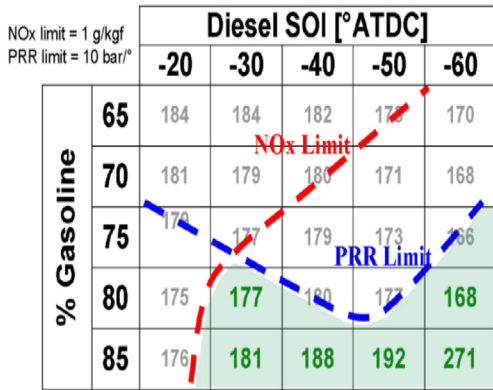


Fig. 56. ISFC operating regime map [90].

the engine efficiency increased until the engine operation became limited by misfire due to over-retarded combustion phasing. Also it was noticed that energy share up to 60% of diesel by ethanol achieved a 10% efficiency gain compared to diesel-only operation. The results indicated that the decreased burn duration was the primary cause for the efficiency gain. The engine emissions shows that HC, CO and NO_x emissions were increased with increase in ethanol fraction, which raises a question on the advantages of utilizing ethanol in a diesel engine. Moreover, negligible smoke emissions were measured at ethanol energy ratios of 20% or higher, suggesting that optimization of these emissions would be much easier compared with conventional diesel combustion.

3.8.2. Engine operating condition and charge preparation strategies

During the ethanol–diesel engine tests of Splitter et al. [78] the total fueling was progressively increased to increase engine load, and the thermodynamic conditions and fuel reactivity were altered to maintain operation under the operator-imposed cylinder pressure and PRR limits. For all these tests and fuels the engine was operated with the injection strategy described in Table 28.

3.8.3. Gasoline–diesel (G/D) and E85–diesel (E85/D) strategies

Table 29 shows the tested loads, where at each operating condition exhaust emissions were sampled, and indicated cylinder pressure measurement were acquired. While changing load the 50% mass fraction burned combustion timing (CA 50) was allowed to adjust as needed to retain the PRR below the imposed 10 bar/°CA and 150 bar peak cylinder pressure limits. Select indicated cylinder

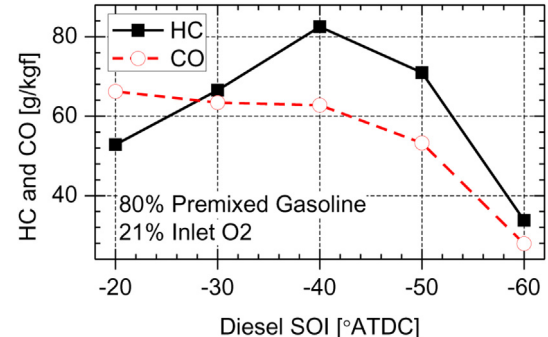


Fig. 58. Predicted HC and CO emissions [90].

pressure and apparent heat release rate (AHRR) traces of this load sweep can be seen in Fig. 43.

It is important to note that for E85-diesel testing a similar port fueling mass was used as with the previously demonstrated gasoline–diesel testing, but due to the reduced lower heating value of ethanol, the distribution of energy between the port and direct injection streams was not the same. Fig. 44 demonstrates the relation between mass and energy between the two port fuels. The E85-diesel operation was performed at engine loads between 9.6 and 16.5 bar IMEP_g, and cylinder pressure and AHRR are shown in Fig. 43.

The increase in port fuel percentage and EGR rate were such as to phase combustion later and to allow low pressure rise rate operation at high loads. Furthermore, the combustion duration of E85-diesel displayed extended HRR compared to gasoline–diesel operation.

3.8.4. Mid load G/D and E85/D comparisons

Fig. 45 compares E85-diesel to gasoline–diesel operation at the lowest and highest comparable loads, where the extended combustion duration of E85-diesel at both engine loads is more apparent. Fig. 46 shows a comparison of the measured and simulated cylinder pressure and apparent heat release rates for operation at the nominal 9 bar IMEP_g and 1300 rev/min using both E85-diesel and gasoline–diesel fuel blends.

It can be seen that the simulations do an excellent job in capturing the combustion characteristics for both blends. More specifically, notice that the change in combustion characteristics between gasoline–diesel and E85-diesel is captured well by the simulations. For instance, dual-fuel PCCI combustion using a blend of E85 and diesel fuel shows a nearly “triangular shaped” HTHR profile and a very broad combustion duration, quite different from the more symmetric Gaussian-like gasoline–diesel result. Also the magnitude of the LTHR is significantly reduced in the E85-diesel

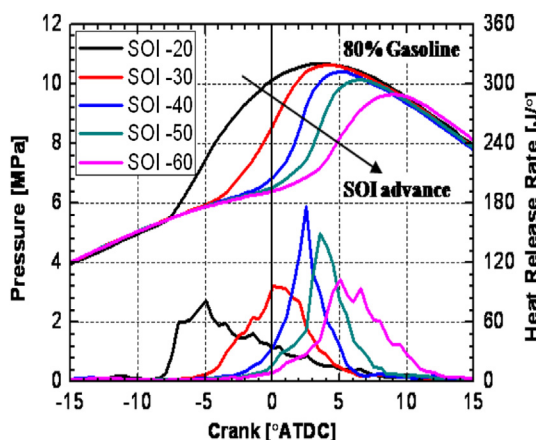
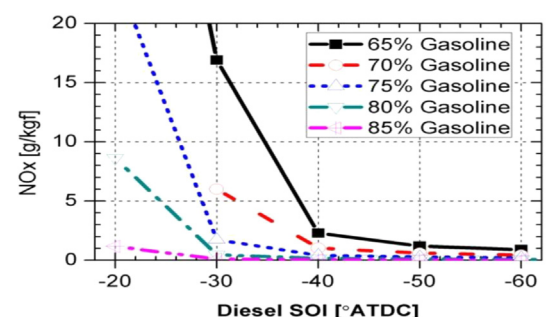


Fig. 57. Predicted cylinder pressure and HRR [90].

Fig. 59. Predicted NO_x emissions for G/D [90].

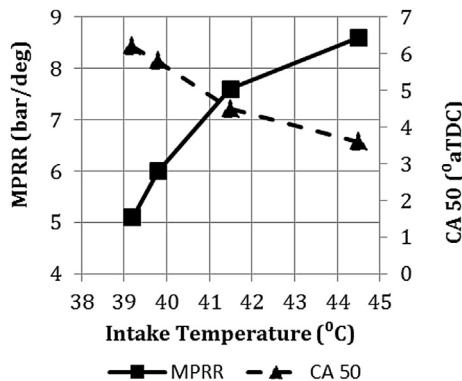


Fig. 60. Effect of intake temperature [90].

case, as compared to the gasoline-diesel case. This is somewhat counterintuitive considering that the LTHR is dominated by the diesel fuel, and the mass fraction of diesel fuel with E85-diesel operation is nearly twice that with gasoline-diesel operation (11% vs. 21%). These results differ from those by both [34] and [25], where increased reactive fuel fraction corresponded to an increase in LTHR magnitude.

To understand the noted differences in the LTHR and HTHR combustion characteristics between E85-diesel fuel blends and gasoline-diesel fuel blends, CFD simulations were used. Fig. 46 shows the CFD-predicted evolutions of several key species for both fueling strategies. It can be seen that, in general, the combustion processes between gasoline-diesel fuel and E85-diesel fuel blends are very similar. Reactivity enhancement results were also discussed in Section 3.2.2 [50].

3.8.5. Combustion and emission comparisons

Quantitative comparisons of combustion and emissions trends for each fueling strategy are plotted as a function of load in Fig. 47. Although there are many similarities in the combustion trends between the fuels, there are differences, specifically in the HTHR combustion duration, which with E85-diesel operation is approximately 50% longer. As previously discussed, when operating with E85-diesel both the LTHR and HTHR events were quite different, and the lengthened HTHR is thought to occur from the greater RON stratification and the ethanol inhibitor effect. Since the combustion

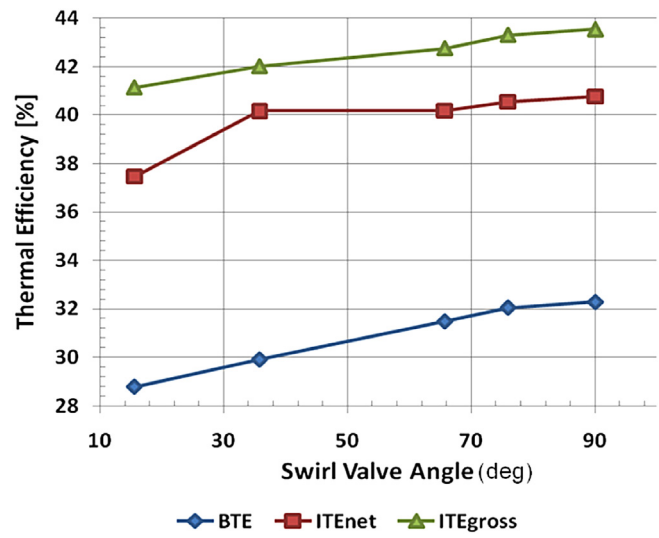


Fig. 62. Effect of swirl on efficiency [90].

phasing of all fuels is similar for a given load, fuel chemistry effects should be better isolated between the fuels. However, there is a benefit in thermal efficiency and thus gasoline equivalent ISFC when operating with E85-diesel. This is primarily thought to be an effect of both the fast transition from the LTHR to HTHR and the improved expansion gamma caused by the EGR-free or reduced EGR requirements of E85-diesel as compared to the other fuels.

Furthermore, with all the tested fuels the indicated specific fuel consumption trends demonstrated a local minimum, of approximately 150 g/kWh (gross), at the 6–12 bar IMEPg operating conditions. The low fuel consumption at these loads is believed to be due to the more extensive optimization that was performed at these loads. Further optimization of the higher load operation points could possibly yield further fuel consumption gains, for instance by lowering the CO emissions at the high equivalence ratios through leaner operation (Fig. 47a and b demonstrates stoichiometric operation at the higher loads). Another operating condition that was not optimized for performance was the lowest load operating condition of 5.2 bar IMEPg.

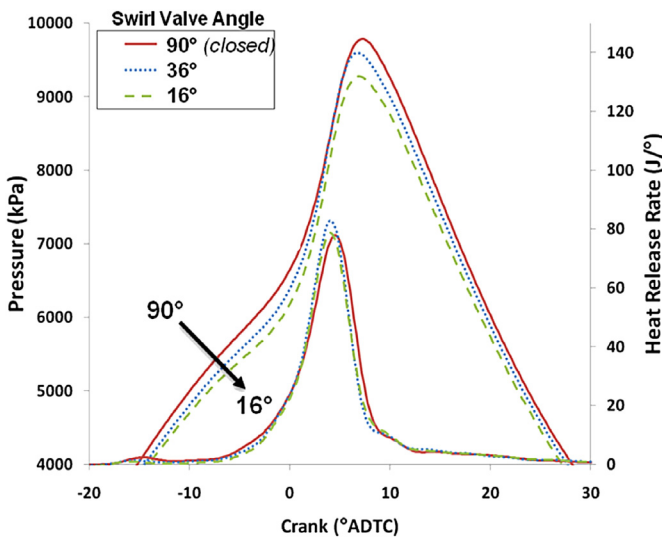


Fig. 61. Effect of swirl on pressure and HRR [90].

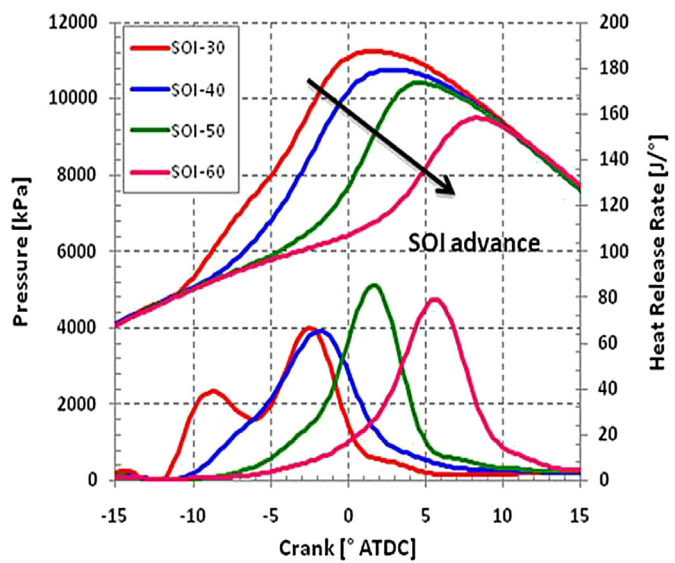


Fig. 63. Effect of SOI on pressure and HRR [90].

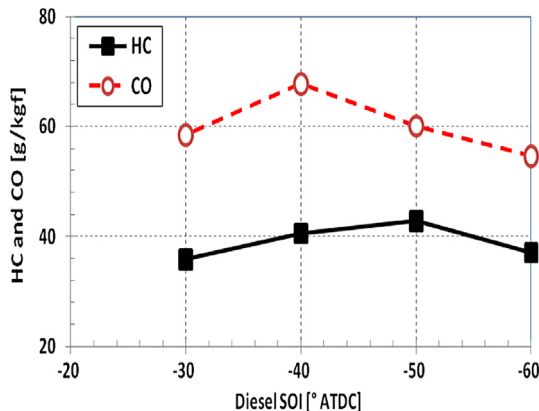


Fig. 64. Effect of SOI on HC and CO [90].

This operating condition was also explored in Ref. [50], where optical tests of the combustion process were conducted. In that research optics were installed into a modified cylinder head that was limited to low PRR (~4 bar/°) and peak cylinder pressure for structural considerations. In that case the combustion timing was adjusted from the optimal efficiency timing to maintain the PRR. More recent results by Hanson et al. [55] have demonstrated improved operation with low pressure rise rates at the lighter loads, with a gross based ISFC of 155 g/kWh and corresponding gross thermal efficiency of 54%. This study demonstrated that with an injection strategy optimized for mid-load, good results are possible at both low and high load operation. It has also been demonstrated that fuel effects and the resulting reactivity gradients are responsible for controlling the combustion event.

Model-based dual fuel combustion optimization was performed by Zhang et al. [83] on a Navistar 12.4 L HD truck engine at 11 bar BMEP and 1531 rev/min. Design of Experiments (DOE) was used to explore various engine operating parameters such as compression ratio, A/F ratio, EGR rate, G/D ratio, single and double diesel injections, split ratio between two diesel injections and injection timings. The optimization recommended suitable diesel injection strategies and air system targets that were required for stable engine operation. The KIVA-3V release 2 code coupled with CHEMKIN II was used for the combustion optimization. In the study iso-octane and *n*-heptane was used as gasoline and diesel surrogates. A reduced PRF mechanism that consists of 45 species and 142 reactions was used to simulate the gasoline and diesel fuel chemistry. The combustion optimization was done from compression ratio

(CR) of 16 to a lower compression ratio of 14. It was found that compared to a compression ratio of 16, a compression ratio of 14 required lower G/D ratio and provided improved fuel consumption. At the CR of 14 suitable air system targets were identified first through simulations and subsequently further optimization of fueling strategies was performed. The air system targets were identified based on NO_x and soot targets. Additional simulations were performed at EGR rates of 40%, 45% and 50% with single and double injection strategies. The required EGR rate was optimized by observing NO_x and MPRR targets. In both injection strategies EGR rates of 45 and 50% met the NO_x and MPRR targets, but a 50% EGR rate is an aggressive target for a practical air system to deliver in HD engines. Therefore, an EGR rate of 45% was identified as a reasonable air-system target. The subsequent simulation results indicated that at a CR of 14 the fuel consumption was improved by 11–13% over baseline diesel combustion for both single and double injections and 85% PFI was appeared to be optimal at the speed of 1531 rev/min. The study also demonstrated that the computational tools can be successfully used to develop viable dual fuel strategies for HD engine applications.

In continuation of the work, Zhang et al. [84] at the Argonne National Laboratory performed a low temperature combustion experimental study of in-cylinder blending of fuels on a Navistar MaxxForce 13 heavy – duty compression ignition engine. The modified heavy-duty engine had a geometric compression ratio of 14 and used sequential, multi-port-injection of low reactivity fuels (Gasoline and E85) with in-cylinder direct injection of diesel. The tests were conducted at 1200 rev/min and varying loads from 5.5 bar BMEP to 19 bar BMEP. The engine operation was optimized within the constraints of NO_x < 0.2 g/bhp-h and pressure rise rate <15 bar/deg, (similar to the constraints used by the ERC group for optimizing RCCI operation) by adjusting the diesel injection strategy, fraction of port fuel supplied, and air intake conditions (Table 30). The tests were conducted in two modes, namely CM1, CM2 where the primary difference between the modes was the diesel injection strategy. The CM1 mode was extended up to 11.6 bar BMEP when compared to the 9.9 bar BMEP of CM2, because of the more robust combustion control provided by its near TDC diesel injection timing, which provided a more stratified reactivity distribution. CM2 used early diesel injection and a lower diesel injection pressure compared to CM1 operation due to the sufficient time available for the air and fuel to mix. The maximum PFI percentage recorded for CM2 operation was 93% compared to 82% for CM1 operation for stable engine operation. Two major factors limited the extension of load with CM1 beyond 11.6 bar BMEP; (1) excessively high pressure rise rates and (2) deteriorated combustion stability. The best BTE recorded for CM2 was 42.1% at 9.9 bar BMEP while it was 43.6% for CM1 at 11.6 bar BMEP. The study also tested E85/diesel dual operation and demonstrated maximum load operation of 19 bar BMEP. The reduced reactivity of E85 was effective in extending the load range and required less EGR, lower PFI fractions compared to gasoline/diesel combustion. The best BTE of E85/diesel combustion was 45.1% and the maximum PRR reached was 14 bar/deg at 19 bar BMEP.

3.8.6. Methanol/diesel reactivity controlled compression ignition (RCCI) engine

Methanol/diesel reactivity controlled compression ignition engine combustion and its emission characteristics were investigated by Li et al. [85]. In this study the effect of the mass fraction of methanol, SOI and intake temperature was investigated. The results show that both the amount of premixed methanol and SOI have a significant impact on the reactivity distribution. It was also noticed that, when the methanol mass fraction was increased from 0 to 80% the peak pressure and heat release rates were retarded, i.e.,

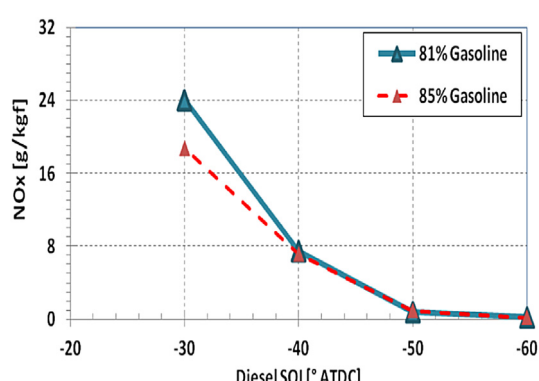


Fig. 65. Effect of SOI on NO_x emission [90].

Table 38

Operating conditions and GA parameters and allowed limits [91].

Operating condition	Low load	Mid-load			High-load		Design Parameter	Min.	Max.
Gross IMEP (bar)	4	9	11	13.5	16	23	Premixed methane	0%	100%
Engine speed (rev/min)	800	1300	1370	1460	1500	1800	DI Diesel SOI 1 (°aTDC)	-100	-50
Intake pressure (bar)	1	1.45	1.94	2.16	2.37	3	DI Diesel SOI 2 (°aTDC)	-40	20
Intake temperature (°C)	60	60	60	60	60	60	Diesel Frac. in First injection	0%	100%
							Diesel inj. pressure (bar)	300	1500
							EGR	0%	60%

combustion was phased closer to TDC due to improved charge homogeneity and reactivity distribution (see Fig. 48). It was observed that while increasing methanol fraction, the high CN diesel fuel ignited first followed by the low CN methanol which shortened the combustion duration compared to premixed combustion of methanol instead of mixing controlled combustion of diesel. Addition of methanol was also beneficial in terms of HC and CO emissions, especially at less than 60% PFI fraction. Li et al. [85] inferred that compared to a PCCI strategy with diesel, methanol/diesel RCCI combustion with higher intake temperatures provides a beneficial path for fuel efficiency and emission reductions. Overall, it was demonstrated that methanol/diesel combustion is capable of reducing emissions and improving fuel efficiency.

As a follow up study, Li et al. [86] performed an optimization of an RCCI engine fueled with methanol and diesel using a non-dominated sorting genetic algorithm II (NSGA-II) modeling approach. Parameters included the mass fraction of methanol, EGR rate, IVC pressure, IVC temperature and SOI. The sensitivity of fuel efficiency, emissions, ignition timing and RI these parameters was analyzed. The investigation confirms that IVC temperature and EGR rate were the most significant operating parameters for overall engine performance and emissions due to their influence on the in-cylinder gas temperature. Also, it was noticed that higher energy fractions of methanol, namely more than 70% (refer to Fig. 49) with advanced SOI provided higher fuel efficiency and lower emissions. The study also revealed that adjusting the methanol–diesel ratio is the only feasible solution to control the ignition timing and to have acceptable levels of RI and CA50.

3.8.7. Hydrogen addition to DME/CH₄ dual fuel RCCI engine

The effect of hydrogen addition to a DME/CH₄ dual-fuel RCCI engine was investigated by Liu et al. [87] using three dimensional calculations coupled with chemical kinetics. Their study also proposed a new reduced DME (Dimethyl Ether) oxidation mechanism. Addition of hydrogen was seen to advance the ignition timing and increase the peak cylinder pressure. The simulations showed that hydrogen addition has a greater effect on the early stages of combustion, which resulted in low CH₄ and CO emissions. Addition of hydrogen increased the NO emissions, but this trend depended on the injection strategy and quantity of pilot fuel used. From the simulations it was inferred that by optimizing these two parameters the NO_x emissions could be controlled.

3.9. Extension of RCCI to LD engines

Based on the results from the ERC heavy-duty (HD) engine RCCI studies, Kokjohn et al. [88] applied the RCCI concept to a light-duty (LD) engine, and comparisons were made between the LD and HD engine platforms. The light-duty engine was the single cylinder version of the GM 1.9 L diesel and is typical of an automotive application. The light-duty engine displacement volume is ~5 times smaller than the heavy-duty engine and its specifications were given in Table 2.

3.9.1. Comparisons of RCCI combustion between HD and LD engines

As discussed earlier, most of the optimization work in the HD engine was performed at 9.3 bar IMEP. Hence, 9.3 bar IMEP operation was also the focus of comparisons between the LD and HD engines in Ref. [89].

The operating conditions for the two engines are presented in Table 31. If the sizes of the engines were perfectly scaled [88], the LD engine would need to be operated at around 3800 instead of 1300 rev/min to scale the heat transfer losses. To make a compromise between the kinetics (which should be same) and heat transfer timescales, an intermediate speed of 1900 rev/min was selected. The premixed gasoline fraction was used to control the combustion phasing and to account for the differences in the speeds between the two engines. The quantity of premixed gasoline in the HD engine was swept from 82 to 89% by mass and the quantity of the premixed gasoline in the LD engine was swept from 81 to 84% by mass. Note that the range of the premixed gasoline fraction sweeps for the LD and HD engines are different due to several factors. First, since the engine speed of the light-duty engine is higher than that of the HD engine, and the LD engine has less time available for ignition, and for a given fuel blend, the LD engine will ignite later than that of the heavy-duty engine. Furthermore, the heat transfer differences between the two engines may result in differences in the thermal conditions.

Fig. 50 shows cylinder pressure and apparent heat release rates for the light-and heavy-duty engines over the premixed gasoline percentage sweeps. Note that to facilitate comparisons between the two engines operating at different speeds, the heat release rates are normalized by the fuel energy and shown as time derivatives (i.e., 1/ms), rather than crank angle derivatives. It can be seen that in both engines the combustion phasing is easily controlled by adjusting the premixed gasoline percentage. That is, increasing the gasoline mass percentage in the fuel results in a very predictable delay in the combustion phasing.

The predictable dependence of combustion phasing on the premixed gasoline percentage has several implications for practical application of the RCCI combustion concept. First, an engine operating in the RCCI combustion mode must have accurate control over the fuel quantity delivered in each of the two fuel streams. Second, the RCCI combustion process regains the coupling between the injection and the combustion events that is lost with traditional HCCI or early injection PCCI combustion. Notice that the dependence of combustion phasing on the premixed gasoline percentage is different for the two engines; however, recall that the two engines were operated at different speeds. For the LD engine a percent increase in the premixed gasoline and corresponding decrease in the direct injected diesel quantity resulted in a retard in combustion phasing of 2° CA at 1900 rev/min or 175 μs, while for the HD engine a percent increase in the premixed gasoline percentage resulted in a retard in combustion phasing of 0.6 °CA at 1300 rev/min or 78 μs. The increase for the LD engine is likely due to the increased expansion rate due to the higher engine speed. Thus, it appears that at higher engine speeds the combustion phasing becomes more sensitive to changes in the premixed gasoline percentage.

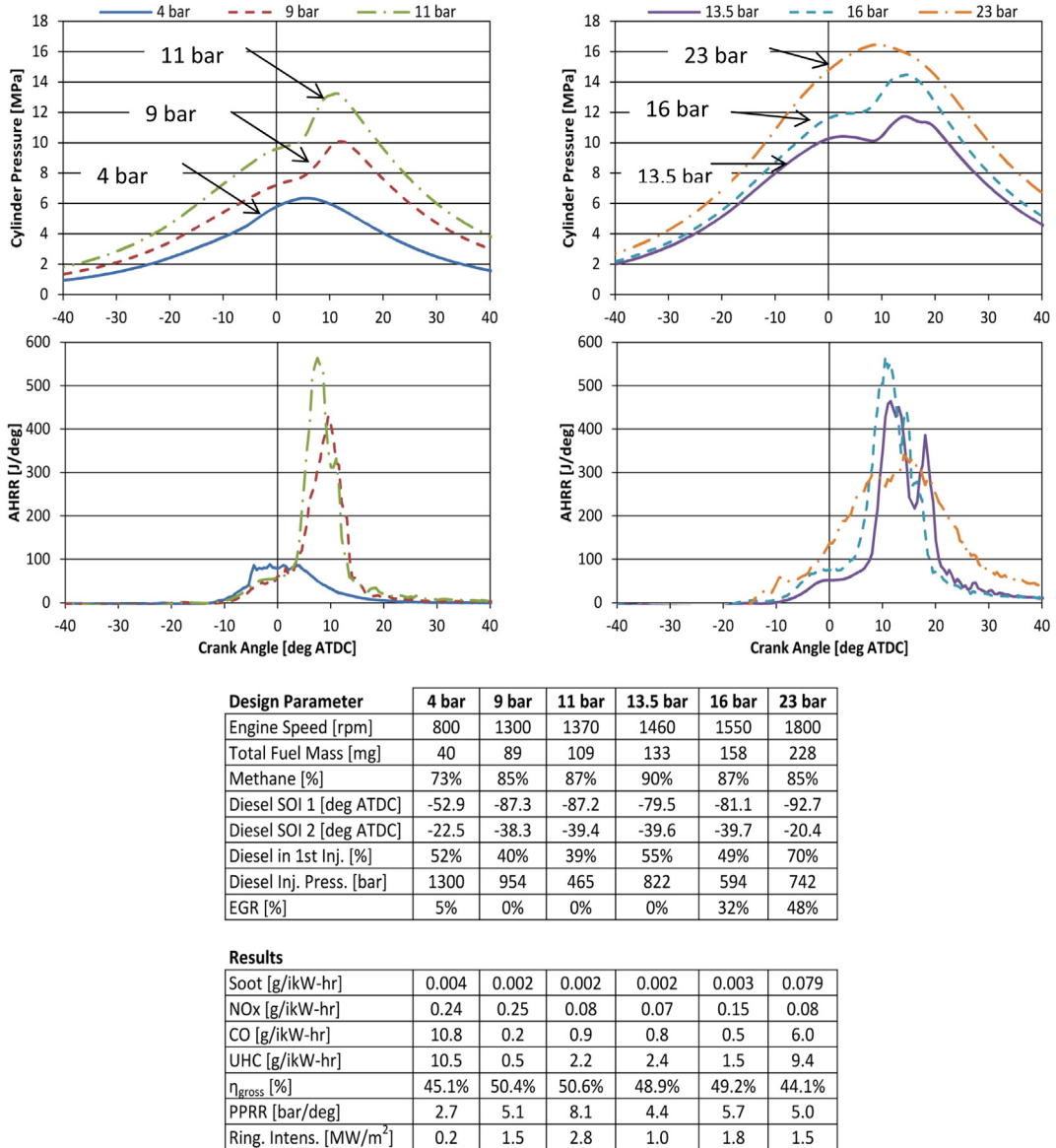


Fig. 66. Pressure and AHRR traces, as well as the optimum strategies for heavy-duty methane/diesel RCCI combustion. Low-to-mid load traces are on the left, while mid-to high-load traces are on the right [91].

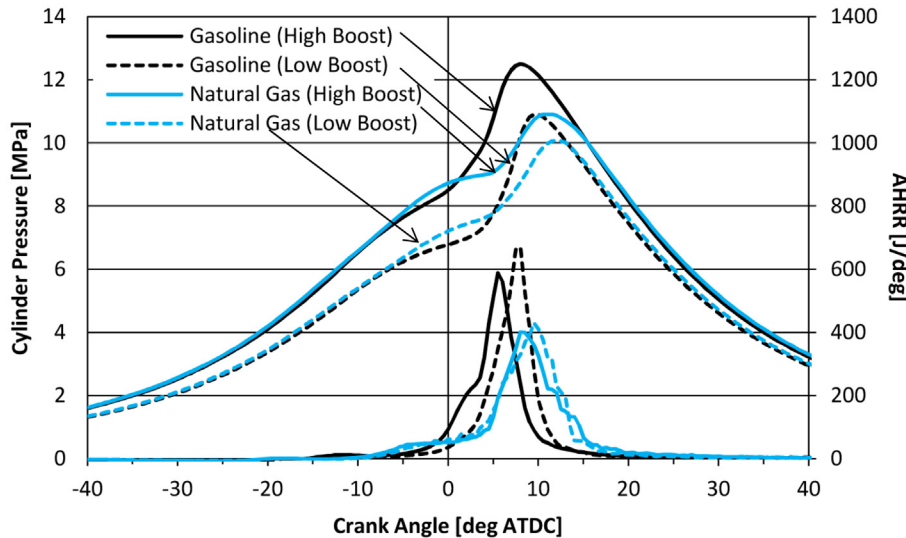
From Fig. 50 it is noticed that the NO_x levels are significantly below the 2010 HD limits. However, it can be seen that for similar combustion phasing the NO_x emission for the LD engine is slightly higher than the limits. NO_x decreased significantly as the combustion phasing was retarded further. Soot emissions were nearly identical for the two engines and, similar to the NO_x both engines had soot levels below the 2010 HD limit. In addition, both engines had acceptable ringing intensities (RI). More importantly the engines show significant control over the RI via changes in the pre-mixed gasoline percentage. Comparing gross indicated efficiencies it can be seen that the HD engine showed ~7% higher indicated efficiency than the LD engine. This difference in gross indicated efficiencies (see Figs. 51 and 52) was found to be due to increased combustion losses, i.e., higher HC and CO and increased heat transfer.

3.9.2. Methods to reduce heat transfer losses in LD engines

From Fig. 53 it was observed that the heat transfer losses are higher for the LD engine. This could be due to several reasons. First,

the swirl ratio of the LD engine was more than three times higher than that of the HD engine. Next, the LD engine operates at a lower mean piston speed than the HD engine. Finally, the two engines have different combustion chamber and injector geometries. The combustion chamber geometry influences heat transfer losses directly through the amount of wall surface area. In this case the surface-to-volume ratio of the LD engine was more than two-times higher than that of the HD engine. Furthermore, the combination of combustion chamber and injector geometry can also play a role in heat transfer losses via the fuel distribution.

In a comparison between heat transfer losses in RCCI and conventional diesel combustion, Kokjohn et al. [60] showed that heat transfer losses were reduced for RCCI combustion not only through reductions in the peak temperature, but also by keeping high temperature regions away from the piston surface. Thus, it is of interest to apply the combustion chamber and injector geometry of the heavy-duty engine to the light-duty engine. Accordingly, the heavy-duty engine geometry was scaled down to the light-duty displacement by applying a scaling factor defined as the cube



Design Parameter	Natural Gas/Diesel		Gasoline/Diesel	
	Low Boost	High Boost	Low Boost	High Boost
Intake Pressure [bar abs.]	1.45	1.75	1.45	1.75
Intake Temperature [°C]	60	60	32	32
Total Fuel Mass [mg]	89	89	94	94
Low-Reactivity Fuel (Premixed) [%]	85%	85%	89%	89%
Premixed Fuel Equiv. Ratio [-]	0.35	0.29	0.42	0.35
Diesel SOI 1 [deg ATDC]	-87.3	-87.3	-58.0	-58.0
Diesel SOI 2 [deg ATDC]	-38.3	-38.3	-37.0	-37.0
Diesel in 1st Inj. [%]	40%	40%	60%	60%
EGR [%]	0%	0%	43%	43%

Results

Soot [g/ikW-hr]	0.002	0.003	0.007	0.014
NOx [g/ikW-hr]	0.25	0.02	0.02	0.01
CO [g/ikW-hr]	0.2	1.8	1.2	3.6
UHC [g/ikW-hr]	0.5	2.5	2.7	4.0
η_{gross} [%]	50.4%	50.4%	52.1%	52.2%
PPRR [bar/deg]	5.1	4.8	10.6	9.9
Ring. Intens. [MW/m ²]	1.5	1.2	5.1	3.7

Fig. 67. Comparison of gasoline/diesel and natural gas/diesel strategies at 9 bar IMEP [91].

root of the ratio of the light-duty to heavy-duty TDC volumes. The specifications of the heavy-duty engine, baseline light-duty engine, and scaled geometry light-duty engine are shown in Table 32 and a comparison of the three combustion chamber geometries is shown in Fig. 53.

Table 33 shows the high and low levels of swirl ratio, engine speed and combustion chamber geometry that were investigated to study their effects. The range of swirl ratios investigated was bounded by the swirl ratios of the LD and HD engines, respectively. The engine speed increase was considered by increasing the speed to give the scaled geometry of the LD engine the same mean piston speed as that of the heavy-duty engine (note that this is a relatively small increase in engine speed). Finally, the effect of combustion chamber geometry was investigated by considering the piston geometries of both the HD and LD engines, as

previously discussed. Note that the scaled light-duty combustion chamber has a geometric compression ratio of 16.1:1. In this study meticulous steps were taken to isolate the influences of the varied parameters and combustion phasing. The combustion phasing (CA50 = 2°CA aTDC) was selected in such a way that the cases with low engine speed and high compression ratio operated with premixed iso-octane (PRF 100). Tables 34 and 35 show the results of the heat transfer reduction investigation at a constant CA50 of 2°CA aTDC (Fig. 54).

A final comparison was made between the LD and HD engines and it was found that with the improved parameters the LD engine was able to achieve 53% gross indicated efficiency, while maintaining near zero NO_x and soot and an acceptable ringing intensity, which is comparable to the performance of the HD engine, as shown in Table 35.

4. RCCI For improved efficiency and low emissions on a multi-cylinder LD diesel engine

Curran et al. [90] investigated in-cylinder blending of gasoline with diesel fuel on a multi-cylinder LD diesel engine as a strategy to control in-cylinder fuel reactivity for improved efficiency and the lowest possible emissions. The objective of their study was to develop better understanding of the potential and challenges of RCCI on a multi-cylinder engine. More specifically, the effect of cylinder-to-cylinder imbalances and in-cylinder charge motion as well as the potential limitations imposed by real world turbochargers were investigated on a 1.9 L four-cylinder engine that is similar to the ERC LD engine. The investigation focused on one engine operating condition 2300 rev/min, 5.5 bar net mean effective pressure (NMEP).

Parameter sweeps in the investigation included variations of the gasoline-to-diesel fuel ratio, intake charge mixture temperature, in-cylinder swirl level and diesel start-of-injection timings. In addition, engine parameters were trimmed for each cylinder to balance the combustion process for maximum efficiency and lowest emissions. An important observation was the strong influence of the intake charge temperature on the cylinder pressure rise rate. The work was guided by the dual fuel modeling and experiments of Refs. [8,34]. The operating point mentioned was chosen such that no EGR would have to be used to allow simplified cylinder-to-cylinder balancing and to avoid thermal management of the EGR cooler. To further simplify the multi-cylinder engine experiments, a single direct injection of diesel fuel was used instead of a split injection strategy. The engine operating parameters were based on the multi-dimensional CFD modeling and single cylinder experiments performed by Kokjohn and Reitz [88]. The test engine

specifications are given in Table 2, and a schematic diagram of the test engine was shown in Fig. 2.

The goal of the work was to provide a roadmap of how to achieve improved efficiency with the lowest possible emissions with dual-fuel RCCI in a multi-cylinder LD diesel engine. To this end, the dual-fuel RCCI performance and emissions were compared against conventional diesel combustion at the 2300 rev/min, 5.5 bar NMEP modal point. Diesel SOI timing sweeps were performed to compare multi-cylinder dual-fuel performance against the model predictions. No manual cylinder balancing was done for the conventional diesel combustion mode and the natural cylinder-to-cylinder imbalances are obvious in the graphs of NMEP and MFB50 for each cylinder in Figs. 54 and 55. These imbalances clearly show the need for control over each cylinder in the RCCI combustion mode. The performance and emission data for the CDC condition are shown in Table 36.

4.1. Dual fuel modeling and experiments

The experimental and modeling study of dual fuel RCCI is summarized in Table 37 [90]. Predicted ISFC maps over the diesel fuel SOI timing sweep, NO_x, HC, CO, cylinder pressure and heat release rates are shown in Figs. 56–59 [90].

4.1.1. RCCI multi-cylinder experiments

The effects of intake charge temperature, swirl and diesel SOI timing are presented in Figs. 60–65 [90]. The effect of intake charge temperatures on cylinder pressure rise rate and combustion phasing is shown in Fig. 60. It can be seen that, at a fixed gasoline and diesel fuel ratio, as the intake temperature was varied from 39° to 44 °C, CA 50 advanced by 2° CA. The advanced CA 50 resulted in

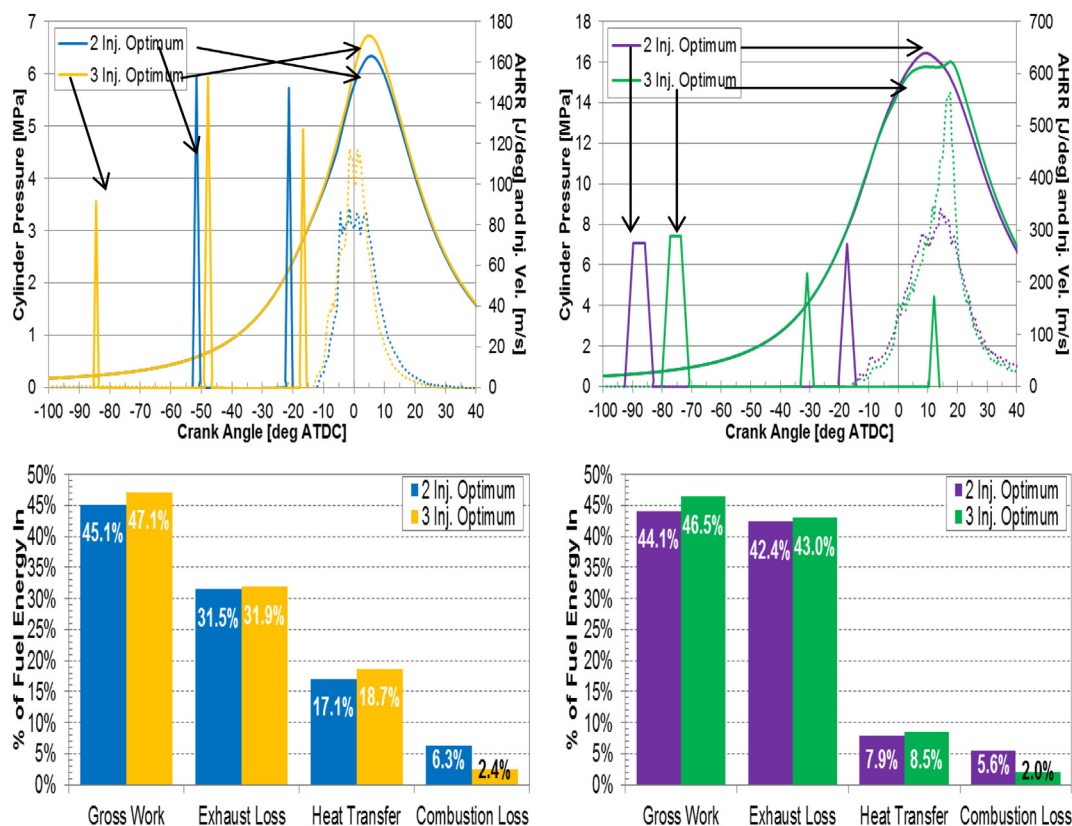


Fig. 68. Comparison of double with triple injection at 4 bar IMEP (left) and 23 bar IMEP (right) [91].

Table 39

Performance and emission results of double and triple injection [91].

4 bar IMEP			23 bar IMEP		
Results	2 inj. optimum	3 inj. optimum	Results	2 inj. optimum	3 inj. optimum
Soot [g/kW h]	0.004	0.004	Soot [g/kW h]	0.079	0.014
NO _x [g/kW h]	0.24	0.10	NO _x [g/kW h]	0.08	0.17
CO [g/kW h]	10.8	7.3	CO [g/kW h]	6.0	1.7
UHC [g/kW h]	10.5	3.8	UHC [g/kW h]	9.4	3.3
η_{gross} [%]	45.1%	47.1%	η_{gross} [%]	44.1%	46.5%

an increase in MPRR by nearly a factor of two. These results show the importance of controlling the combustion phasing to control the MPRR and the need for precise control for intake charge variations. Like intake temperature, during the course of the experiments it was found that adjusting the swirl ratio had a significant effect on both thermal efficiency and emissions for dual-fuel RCCI operation, as shown in Fig. 62. Fig. 61 shows a representative pressure and heat release rate plot from the 81% gasoline case for various swirl ratios, demonstrating that, as the swirl level increases, the heat release rate is reduced while the peak cylinder pressure and the area under the pressure curve increase. To find the optimum swirl ratio for each ratio of gasoline-to-diesel fuel tested, a sweep of swirl valve position (i.e., swirl ratio) was performed for the 77%, 81% and 85% gasoline cases at a diesel SOI timing of -60° ATDC (swirl valve angles of 0° and 90° correspond to the lowest and highest swirl ratios, respectively).

Fig. 62 shows the effect of swirl ratio on BTE and net and gross ITE for the 77% gasoline case. It was found that thermal efficiency is strongly affected by changing the swirl ratio. The thermal efficiency was found to increase with a more open swirl valve, indicating that better in-cylinder mixing is needed to realize the maximum thermal efficiency with the current multi-cylinder configuration (i.e., single diesel injection, injector technology, compression ratio).

Fig. 63 shows cylinder pressure and heat release rates for the diesel fuel SOI timing sweep from -30° to -60° ATDC at a swirl valve angle of 65.7° . When the diesel SOI timing was advanced to -70° ATDC, combustion was found to be unstable. The trends of pressure and heat release from the multi-cylinder engine experiment agreed well with the modeling predictions, as shown in Fig. 63. The two peaks for the case with a diesel SOI timing of -30° seem to indicate two-mode combustion. These trends also held for

different swirl ratios and for the 85% gasoline case, as explained in the dual-fuel RCCI work of Hanson et al. [34]. The HC and CO emissions trends for the diesel SOI sweeps are shown in Fig. 64, and the NO_x trends for 81% and 85% gasoline are shown in Fig. 65.

This work successfully demonstrated the application of dual-fuel RCCI operation on a multi-cylinder LD engine and the model results were valuable in directing the experiments. The work also showed the relationship between intake and temperature and gasoline-to-diesel fuel ratio during dual-fuel operation. The need for increased understanding of the performance of turbomachinery for low temperature combustion also became apparent due to the observed importance of boost pressure.

4.2. Effect of alternative fuels on RCCI performance and emissions

4.2.1. Heavy-duty engine natural gas – diesel RCCI operation

To operate at moderate to high loads with gasoline/diesel dual fuel, high amounts of EGR or an ultra-low compression ratio had been found to be required. Considering that both of these approaches inherently lower thermodynamic efficiency, Nieman et al. [91] replaced the gasoline with natural gas as the low reactivity fuel and examined the sensitivity of RCCI combustion at high load to injection system parameters. Due to the lower reactivity of natural gas compared to gasoline, it was proposed to be a better fuel for RCCI combustion to control the maximum pressure rise rate by using the large reactivity gradient that exists between these two fuels.

A nondominated sorting genetic algorithm (NSGA-II) along with the CFD code described in 2.1.3 was used to perform optimization for a wide range of engine operating conditions. Engine design parameters that were controlled by the genetic algorithm included the fraction of total fuel that was premixed (methane), the timing of the two diesel injections, the amount of diesel in each injection, the diesel fuel injection pressure, and the EGR percentage. The objective of the optimization was to simultaneously minimize soot, NO_x, CO, and UHC emissions, as well as ISFC and ringing intensity. Typical heavy-duty engine load/speed combinations at six operating points from 4 to 23 bar IMEP and 800–1800 rev/min were investigated on the test engine shown in Fig. 1 and optimized. The results emphasized that precise injection control was needed for combustion control. The load speed combinations, which ranged from low-load/low-speed to high-load/high-speed, proposed by Dempsey et al. [21] were selected for the optimization of natural gas/diesel operation [91]. At each operating condition, the engine

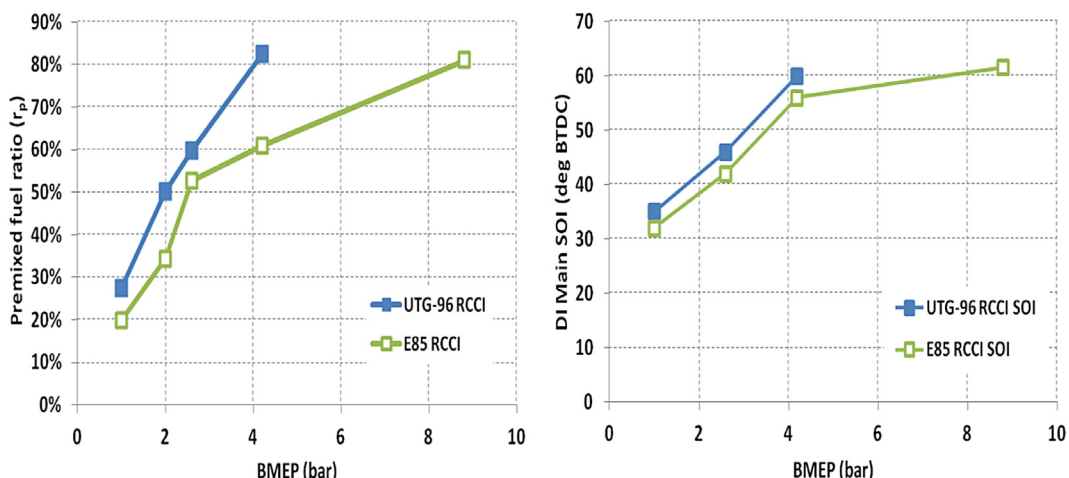


Fig. 69. Variation of premixed fuel ratio and DI main SOI timing with BMEP [93].

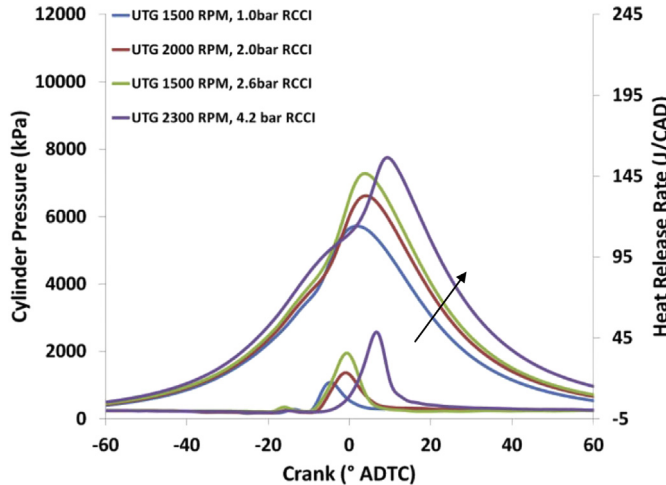


Fig. 70. Pressure and HRR for gasoline [93].

speed, fuel energy introduced into the cylinder, and intake pressure were fixed throughout the optimization. The conditions, the corresponding IMEP values, and variable design parameters are listed in Table 38.

As indicated in Fig. 66, efficient combustion strategies were achieved over the entire load/speed range. NO_x and soot emissions regulations were met across the entire range with the exception of soot at high load. However, high EGR levels at the 23 bar IMEP condition reduced combustion efficiency, and at the 4 bar IMEP condition, the ultra-low reactivity of methane caused the combustion efficiency to be relatively poor. However, the low load and high load case employed a later second injection, which occurred at approximately -20° aTDC and acted as a strong ignition source. The 13.5 bar IMEP case required the least amount of diesel fuel (on percent basis) and it was noticed that the diesel fraction decreased as load was increased, because the background equivalence ratio of methane was increased, thus increasing its reactivity and less diesel fuel was needed to ignite the mixture. This trend continued until 16 bar IMEP.

A comparison between the optimum 9 bar IMEP gasoline/diesel HD RCCI strategy developed by Kokjohn et al. [8,26,34,33] and the 9 bar IMEP natural gas/diesel strategy described in Fig. 66 is seen in

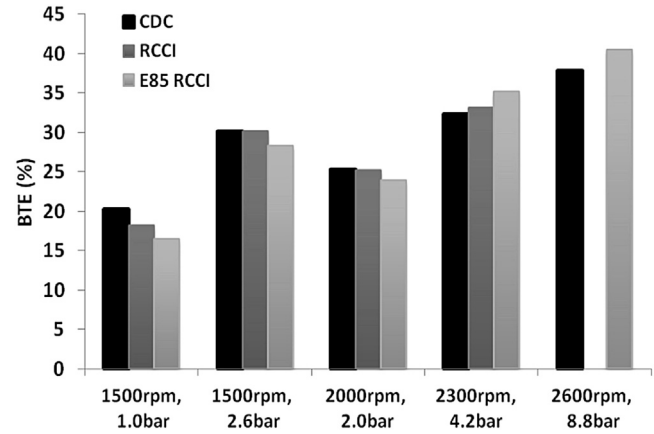


Fig. 72. BTE for G & E85 compared to CDC [93].

Fig. 67. The gasoline/diesel strategy was optimized at a relatively high intake pressure of 1.75 bar absolute, while the natural gas/diesel strategy utilized 1.45 bar intake pressure. The combustion event of the gasoline/diesel strategy was retarded with lower intake pressure, whereas the natural gas/diesel strategy was unaffected by the changed intake pressure.

The use of natural gas as the low-reactivity fuel in the RCCI combustion strategy is seen to be able to yield clean, quiet and efficient combustion throughout the entire tested load/speed range. Additional work by Nieman [92] has shown that the use of triple injections is effective to further reduce NO_x and PM at high and low loads, as shown in Fig. 68 and Table 39.

4.2.2. Use of E85-diesel in a light-duty multi-cylinder engine

The effect of alternative fuels, i.e., E85 on load expansion and Federal Test Procedure (FTP) modal point emissions indices under RCCI operation has been investigated by Curran et al. [93]. The GM 1.9L four-cylinder engine shown in Fig. 2 was modified to allow port fuel injection and operated with E85. The effect of E85 on the Ad-hoc FTP modal points was explored, along with the effect of load expansion throughout the LD diesel engine's speed range. Previous results [90] with gasoline-diesel dual-fuel operation showed that with the stock hardware, the 2600 rev/min, 8.8 bar BMEP modal point was not obtainable due to an excessive cylinder pressure rise rate and unstable combustion both with and without

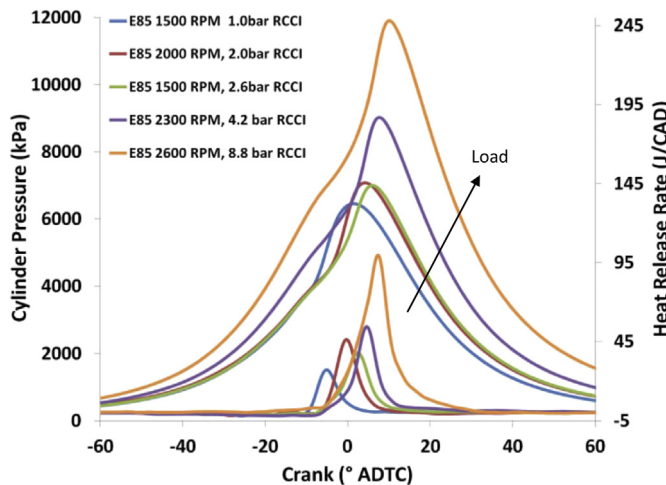
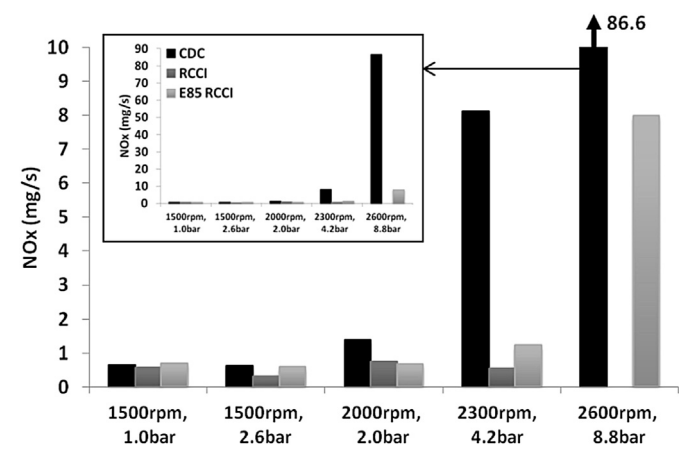


Fig. 71. Cylinder pressure and HRR for E85 [93].

Fig. 73. NO_x emission extended scale [93].

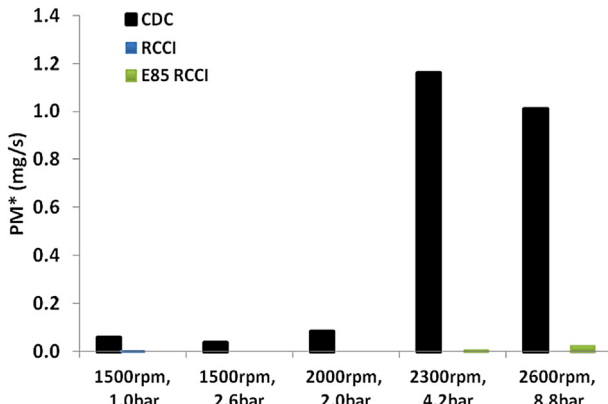


Fig. 74. Estimated PM emissions [93].

EGR. In this experiment the performance and emissions of RCCI operation with E85 and diesel was explored and compared against CDC and RCCI operation with gasoline and diesel. The use of renewable fuels such as E85 not only has the potential for expanding the operating load of RCCI, but also is effective for decreasing petroleum energy use through a combination of direct petroleum displacement and increased efficiency, as well as a reduction in life-cycle emissions.

Formaldehyde emissions were not examined by Curran et al. [93], but a previous study [94] revealed increased HCHO production compared to CDC and PCCI with RCCI operation. It was concluded that a diesel oxidation catalyst could be effective in controlling the tailpipe emissions. RCCI operation with E85 was achieved through early DI (single or double pulse) of diesel fuel (between 30 and 70° bTDC) and port fueling of E85 onto a closed intake valve. The fuel rail pressure was decreased to 500 bar as the diesel fuel start of injection was advanced to avoid spray impingement on the cylinder walls. For RCCI operation with the stock piston geometry and stock DI diesel injectors, it was found that increased swirl intensity is needed to create a well-mixed cylinder charge [93] for the highest BTE and lowest possible emissions, and the mass ratio of premixed fuel to direct injected fuel varied depending on engine speed and load. As the load increased, the premixed fuel ratio was required to increase and SOI was advanced toward 60° bTDC for both gasoline and E85, as shown in Fig. 69.

Previous studies [90] have shown that the maximum BTE was obtained with a minimum amount of pre-mixed fuel, but enough to control the pressure rise rate. The same holds true with keeping the diesel SOI as retarded as possible since, as the diesel SOI becomes more advanced, the mixture is more premixed and less stable, and more HCCI-like combustion occurs. The combined effect of higher

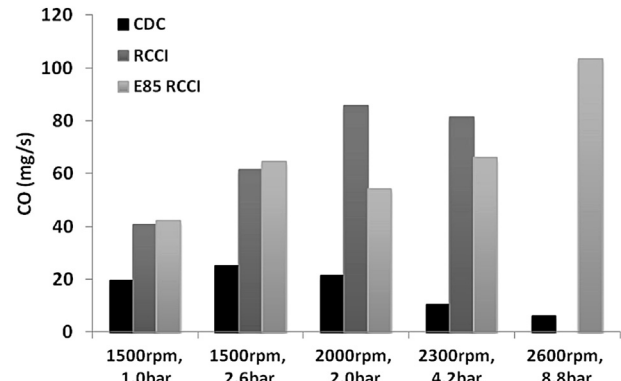


Fig. 76. CO emissions [93].

octane and intake cooling effects made higher load operation difficult with E85, namely, the stability of combustion was reduced.

The effect can almost be described as self-extinguishing. Higher boost pressures were needed, but the stock VGT was not suited for supplying the requisite boost pressure with the low exhaust temperatures associated with RCCI operation. To combat this effect, a split injection technique was used for the 2600 rev/min, 8.8 bar BMEP operating point. This point was not reachable with RCCI operation using gasoline even with EGR. The sensitivity of higher-load RCCI operation to intake temperature makes the use of high-pressure EGR difficult in terms of cooling the EGR sufficiently without condensing HC in the EGR cooler. In order to reach the 2600 rev/min, 8.8 bar BMEP operating point with E85 RCCI, the intake temperature had to be lowered to approximately 40 °C in order to keep the cylinder pressure rise rate under the self-imposed limit of 10 bar/deg. However, the use of E85 in RCCI operation allowed the amount of DI diesel fuel to be increased. The cylinder pressure and heat release rate traces for RCCI operation over the speed and load range of the Ad-hoc modal points is shown for gasoline and E85 in Figs. 70 and 71, respectively. The peak cylinder pressure for higher load RCCI operation was increased and there was a slight increase in NO_x emissions, as discussed next. It is also apparent from the heat release traces that combustion phasing is generally advanced with E85.

From Fig. 72 it can be seen that the BTE of CDC is higher than gasoline-diesel RCCI operation and E85-diesel operation at 1 bar and 2.6 bar BMEP (at 1500 rev/min) and 2 bar BMEP (at 2000 rev/min). But, at 4.2 bar BMEP, 2300 rev/min and 8.8 bar BMEP, 2600 rev/min the efficiency of E85-diesel RCCI is more than gasoline-diesel RCCI and CDC operation. It is clearly seen that E85-diesel RCCI operation provides better BTE at higher loads than at lower loads, and the improvements in BTE of E85/D with CDC at 4.2 bar BMEP and 8.8 bar BMEP are 8.8% and 6.9% respectively. The higher BTE at the higher loads with RCCI operation with E85 is attributed to the lower premixed fuel amount allowed by the use of E85.

The NO_x emissions of RCCI operation with E85 are marginally higher than for RCCI operation with gasoline at almost all loads and speed, but lower compared to CDC operation at all load and speeds. The lower premixed fuel-to-diesel ratio with E85 leads to slightly higher NO_x mass emissions at the lowest loads since much more diesel fuel is required to maintain stable operation. The NO_x emission trends for CDC, G/D RCCI and E85/D RCCI operation are depicted in Fig. 73 [93].

PM emissions estimated from the soot concentration correlation from the filter smoke number (FSN) are shown in Fig. 74. The results indicated that engine-out PM emissions from RCCI operation were

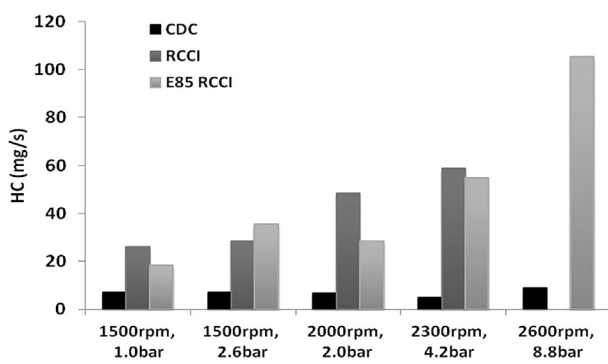


Fig. 75. HC emissions [93].

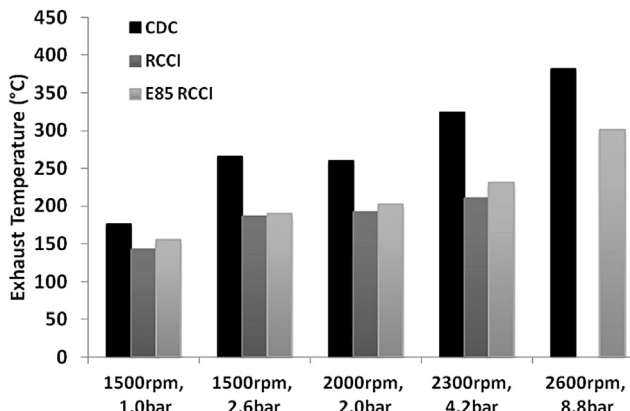


Fig. 77. Exhaust temperatures [93].

nearly zero. Though these PM emissions are nearly zero, previous work has shown that the apparent mass of RCCI PM as collected on filter paper can be higher than CDC or PCCI due to the amount of soluble organic fraction (SOF) present. The FSN for RCCI operation with both E85 and gasoline averaged at 0.01, which indicates very little opacity in the exhaust. The FSN for CDC operation varied from as low as 0.23 for the 2300 rev/min, 4.2 bar BMEP case to as high as 1.66 for the 1500 rev/min, 2.6 bar BMEP case.

The hydrocarbon emissions for G/D RCCI and E85/D RCCI were higher than for CDC operation (see Fig. 75). RCCI with E85 provided decreased HC emissions compared to RCCI with gasoline and this decrease in HC was observed with increases in load and speed. The reason for the reduction in HC emissions for E85 RCCI was arranged to be due to the decreased premixed fuel ratio, which is enabled by the higher octane, as well as due to the intake cooling effect of E85. Brake specific HC emissions were found to decrease with increasing load for both PFI fuels. Brake specific hydrocarbons varied from as low as 10 g/kWh for E85 RCCI to as high as 48 g/kWh with RCCI with gasoline for the 2000 rev/min, 2.0 bar BMEP case. RCCI HC emissions averaged around 2600 ppm for E85 RCCI and 3200 ppm for RCCI with gasoline.

The CO emissions followed the same trends as seen for the HC emissions, as shown in Fig. 76. At lower load, CO emissions for RCCI with E85 were higher than RCCI with gasoline and vice versa at the higher load, but at all the loads and speed CO emissions of RCCI

with both the PFI fuels were higher than with CDC operation. The brake specific CO emissions ranged from 10 to 63 g/kWh for RCCI operation compared to 0.55–25 g/kWh for CDC operation. The CO emissions averaged around 3800 ppm for RCCI with gasoline and 3300 ppm for RCCI with E85. At the 2300 rev/min, 4.2 bar point, E85 RCCI CO emissions were below 1500 ppm.

The exhaust temperatures as measured at the turbocharger outlet are shown in Fig. 77. The exhaust temperatures for RCCI operation range from 22% to 35% lower than that of CDC operation. This correlates to around a 20 °C difference at the lower loads and up to a 112 °C difference at the higher loads. The exhaust temperatures for E85 RCCI are slightly higher than RCCI with gasoline by an average of approximately 6%.

Curran et al. [93] concluded that, despite successful RCCI with the stock engine configuration, hardware challenges still exist, especially in the turbo machinery and the HP EGR system. In the case of the stock VGT, the higher load operation demanded more boost, which was not possible with the exhaust temperatures that existed in RCCI operation. Similarly, at lower loads increased boost levels are required to improve BTE. In addition, due to the limitation of the VGT to drive the EGR and due to condensation of the hydrocarbons in the EGR cooler with low intake temperatures, it is difficult for HP EGR to provide the high dilution levels demanded by higher load RCCI operation. Thus, it was suggested that future study should focus on using mixed LP and HP EGR systems.

4.2.3. Effect of DI fuel (diesel & 3% 2-EHN doped gasoline) properties on engine gross thermal efficiency

The effect of dual fuel and single fuel strategies on gross thermal efficiency of RCCI engines has been studied by various groups. Splitter et al. [95] studied the effect of direct-injected fuel properties on gross thermal efficiency with respect to intake pressure and temperature, and equivalence ratio as function of engine operating parameters, such as fuel reactivity, CA50 and load. In Splitter et al. the gross thermal efficiency of the engine was maximized at approximately 67% of premixed fuel and 33% of DI fuel. In this investigation two fuels namely, #2 ULS and 3% 2-ethylhexyl nitrate doped gasoline were used as the DI fuel to study fuel property effects on RCCI efficiency. The experiments were conducted in the heavy-duty single-cylinder engine shown in Fig. 1 at constant net IMEP of 8.45 bar, 1300 rev/min engine speed, with 0% EGR, and a CA50 combustion phasing of 0.5 °CA ATDC. The engine was port-fueled with E85 for the low reactivity fuel and direct-injected

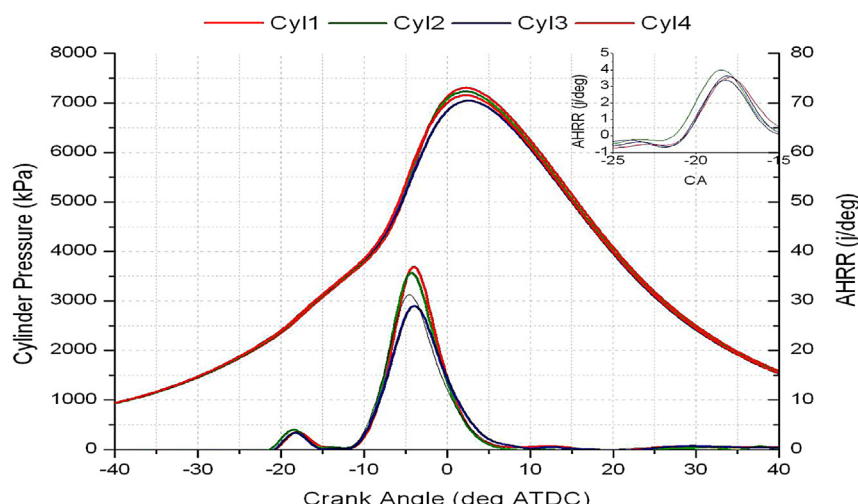


Fig. 78. Balanced combustion phasing and load over all four cylinders [96].

Table 40

KIVA CFD simulation parameters [96].

Engine speed (rev/min)	1900
Compression ratio	16.1
IMEP (bar)	9
Intake pressure (bar)	1.86
EGR	0.41
Intake temperature (°C)	40
Bowl radius (cm)	2–4
Compression ratio	15.25–18.1

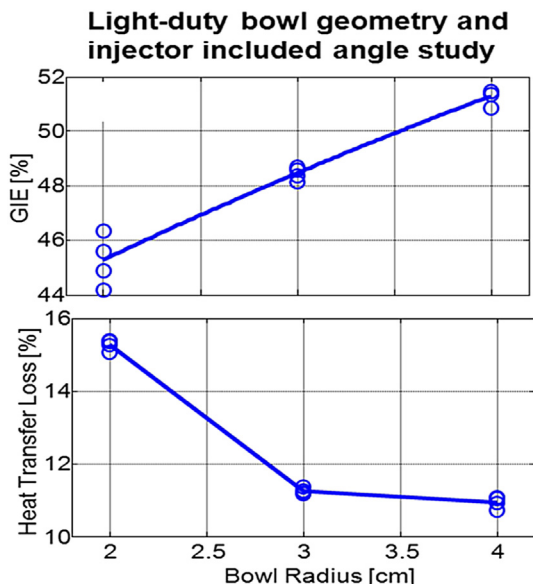


Fig. 79. Simulated RCCI piston bowl radius vs. gross indicated efficiency (GIE) [96].

with either #2 ULSD or 3% 2-ethylhexyl nitrate doped into gasoline for the high reactivity fuel. The experimental results showed that fuel reactivity differences affect engine efficiency magnitudes, and also the findings demonstrated that losses could be minimized through proper balancing of the intake pressure and temperature, as a function of the fuel reactivity differences. In their study the intake pressure and temperature were swept independently of each other while combustion phasing and load were maintained by adjusting the global fuel reactivity and DI fuel timing as required. Particularly with the EHN + Gas/E85 strategy, at reduced high and low reactivity fuel differences, it was noticed that combustion was

more abrupt due to reduced effectiveness of the DI fuel. The results demonstrated that through proper optimization of both engine conditions, and the fuels, further increases in engine efficiency were possible with RCCI.

4.3. Piston bowl optimization for RCCI combustion in a LD multi-cylinder engine

Based on the above RCCI studies, in order to reduce unburned fuel emissions and the piston bowl surface area (to reduce heat losses), improved pistons were designed by Hanson et al. [96] with assistance of the KIVA 3V CFD code and genetic algorithm optimization. The piston bowl profile was optimized for dedicated RCCI operation and it was tested in the test engine shown in Fig. 2 at three operating points. These operating points were chosen to cover the range of conditions seen in the US EPA LD FTP tests. The operating points were those chosen by an Ad Hoc working group to simulate operation in the FTP test [97,98]. Hanson et al. [96] found that the thermal efficiency of the optimized engine was improved, while maintaining low NO_x and PM emissions. The results showed that with the new piston bowl profile and an optimized injection schedule, RCCI brake thermal efficiency was increased from 37% with the stock EURO IV configuration to 40% at the 2600 rev/min, 6.9 bar BMEP condition, and NO_x and PM emissions targets were met without the need for exhaust after treatment.

4.3.1. Cylinder balancing with RCCI

In a multi-cylinder engine there are significant variations in the initial conditions, i.e., cylinder temperature, EGR, trapped mass, fuel rail pressure, etc., from cylinder-to-cylinder. These imbalances can lead to decreased performance due to overly advanced or delayed combustion in each cylinder in a kinetically controlled combustion strategy like RCCI. Exhaust emissions can also vary significantly from each cylinder with corresponding variations in combustion phasing. To adjust for these variations, the total fueling and ratio of gasoline-to-diesel for each cylinder can be varied to match the IMEP and combustion phasing over all 4 cylinders (see Fig. 78).

The balancing was accomplished by Hanson et al. [96] using the Driven code by applying an “adjustment factor” multiplier to the PFI and DI duration commands for each cylinder. First, for each cylinder, the DI and PFI adjustment factors were tuned to vary the ratio of gasoline-to-diesel fuel to match CA50 over all 4 cylinders. Next, once the combustion phasing was balanced, the PFI and DI adjustment factors were then raised or lowered in equal amounts to match the IMEP over all 4 cylinders. Typically, the PFI and DI

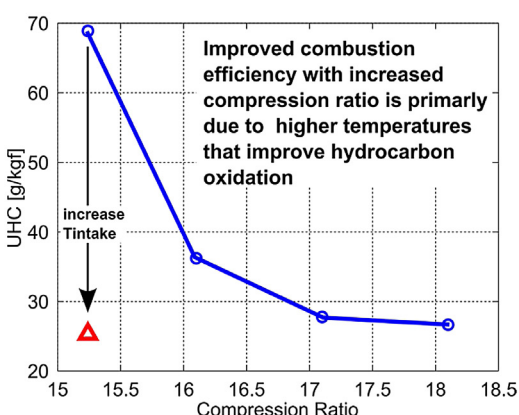
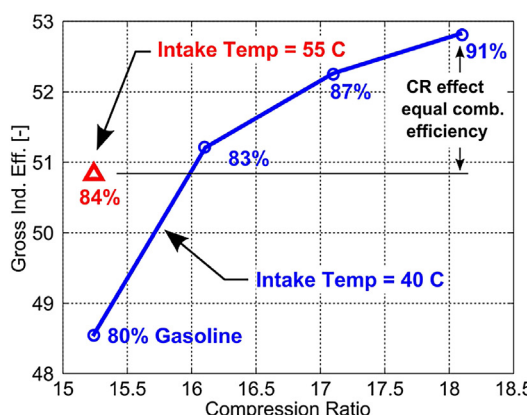


Fig. 80. Comparison of GIE, UHC with Compression ratio [96].

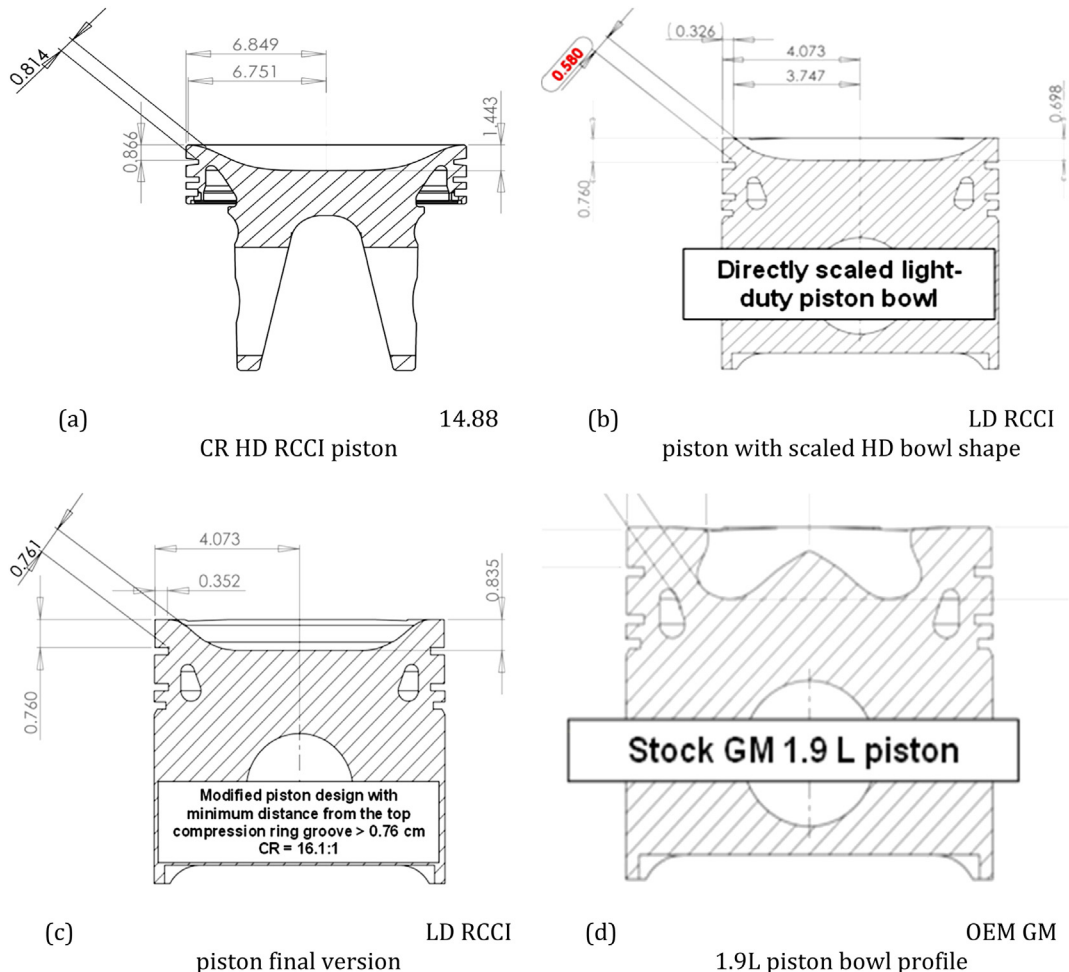


Fig. 81. Comparison of piston bowl geometries [96].

adjustment factors needed to be varied by $\pm 10\%$ from cylinder-to-cylinder. Sample results of the cylinder balancing for a typical operating condition are shown in Fig. 78.

4.3.2. RCCI piston design

Conventional diesel engines are designed for non-premixed fuel burning in a mixing-controlled combustion mode. This type of combustion uses the piston geometry to assist fuel/air mixing and ensure complete combustion. Additional mixing from piston-bowl-generated flows is not required in RCCI combustion due to the early fuel injections, which allow additional time for sufficient mixing before combustion. Therefore, a dedicated RCCI engine requires a bowl shape that is optimized for RCCI operation to fully realize the benefits of this premixed combustion strategy. An optimized RCCI piston was used in the multi-cylinder engine and the LD RCCI piston design was based on Refs. [99,100]. CFD engine simulations using the KIVA code were used to examine bowl shape parameters to increase thermal efficiency and reduce emissions of RCCI operation in the LD engine.

The two parameters varied in the piston design were the bowl diameter and compression ratio in order to determine the limits of the design parameters through modeling. The bore radius was varied from a narrow, diesel type bowl to nearly flat piston (48–98% of the piston radius). The specific conditions for the CFD simulations were chosen from previously tested RCCI cases (see Table 40). From the CFD simulations it was found that, when bowl

radius was varied from 2 to 4 cm, the gross indicated thermal efficiency increases with increase in bowl radius, as seen in Fig. 78. Based on this result, the bowl radius was fixed close to 4 cm. This resulted in a wider bowl that covered most of the piston. Next, the compression ratio selection was made through further CFD simulations at a constant radius of 4 cm and constant combustion phasing, as discussed in Refs. [8,17,26,76] with increase in compression ratio from 15.25 to 18.1 (Fig. 79).

As expected, the higher compression ratio led to higher gross indicated thermal efficiency and a decrease in HC emissions, as shown in Fig. 80. HC emissions could also be decreased at lower compression ratios by increasing the intake temperature from 40 to 55 °C. The combustion efficiency improvements can make up about half of the efficiency gain from increasing the compression ratio alone. Based on these results, a compression ratio of 16.1:1 was selected to allow for improved low load operation with acceptable high load operation, keeping in mind that the LD vehicle would operate more exclusively at light loads. Based on the selected compression ratio (16.1:1) and bowl radius (4 cm) the HD RCCI piston (CR = 14.88:1) was directly scaled to fit the LD piston blank, but due to structural concerns over the bowl-to-ring land clearance; the bowl radius was reduced to 3.721 cm. Finally, it must be noted that, while the piston was designed to be 16.1:1 compression ratio, the compression ratio of the final machined RCCI piston was measured in the engine to be ~15.1:1. (This difference was thought to be caused by machining errors to the piston

Table 41

Operating conditions for RCCI, RCCI OEM and CDC OEM pistons [96].

Speed	Piston	BMEP (bar)	ϕ	P_{intake} (kPa abs)	P_{exhaust} (kPa abs)	T_{intake} ($^{\circ}\text{C}$)	EGR (%)	CA50 ($^{\circ}\text{aTDC}$)	DI Pr (bar)	DI SOI1 ($^{\circ}\text{bTDC}$)	DI SOI2 ($^{\circ}\text{bTDC}$)	%DI in SOI1	PFI fraction (%)
1500 ^a rev/min	RCCI piston	2.6	0.28	102	107	61	0	-0.74	500	58	43	60	0.52
	RCCI OEM	2.53	0.28	104	118	57	0	-0.60	500	—	43	60	0.52
	CDC OEM	2.61	0.51	104	125	60	39	20.0	400	8	0	3	0
2300 ^a rev/min	RCCI piston	4.24	0.34	118	129	51	0	2.5	500	63	46	3	0.76
	RCCI OEM	4.2	0.33	128	143	41	0	2.65	500	—	60	0	0.81
	CDC OEM	4.21	0.31	128	143	62	0	13.5	750	14	3.7	60	0
2600 rev/min	RCCI piston	6.92	0.40	140.3	154.5	41	0	4.84	500	88	58	60	0.85
	RCCI OEM	8.85	0.44	122.5	124.0	34	0	3.11	500	—	68	0	0.88
	CDC OEM	6.82	0.46	157.8	166.8	64	15	11.6	1100	20	8	3	0

^a FTP modal points.

blanks (on the order of 2 cm³). Comparisons of the piston bowls are shown in Fig. 81.

4.3.3. Experimental results of optimized LD RCCI pistons

Experiments were conducted by Hanson et al. [96] on the multi-cylinder test engine at the three operating points mentioned earlier with the optimized RCCI piston. The details of the operating

conditions at each point are given in Table 41. Hanson et al. [96] conducted the test with three different engine configurations of Fig. 81 and compared the results. The 1500 rev/min operating point is a typical light-load cruising point in the LD FTP test. Hanson et al. used a single injection strategy for the RCCI OEM piston double injection strategy and the OEM injection strategy for the CDC OE piston. Combustion phasing for all cases was advanced as far as

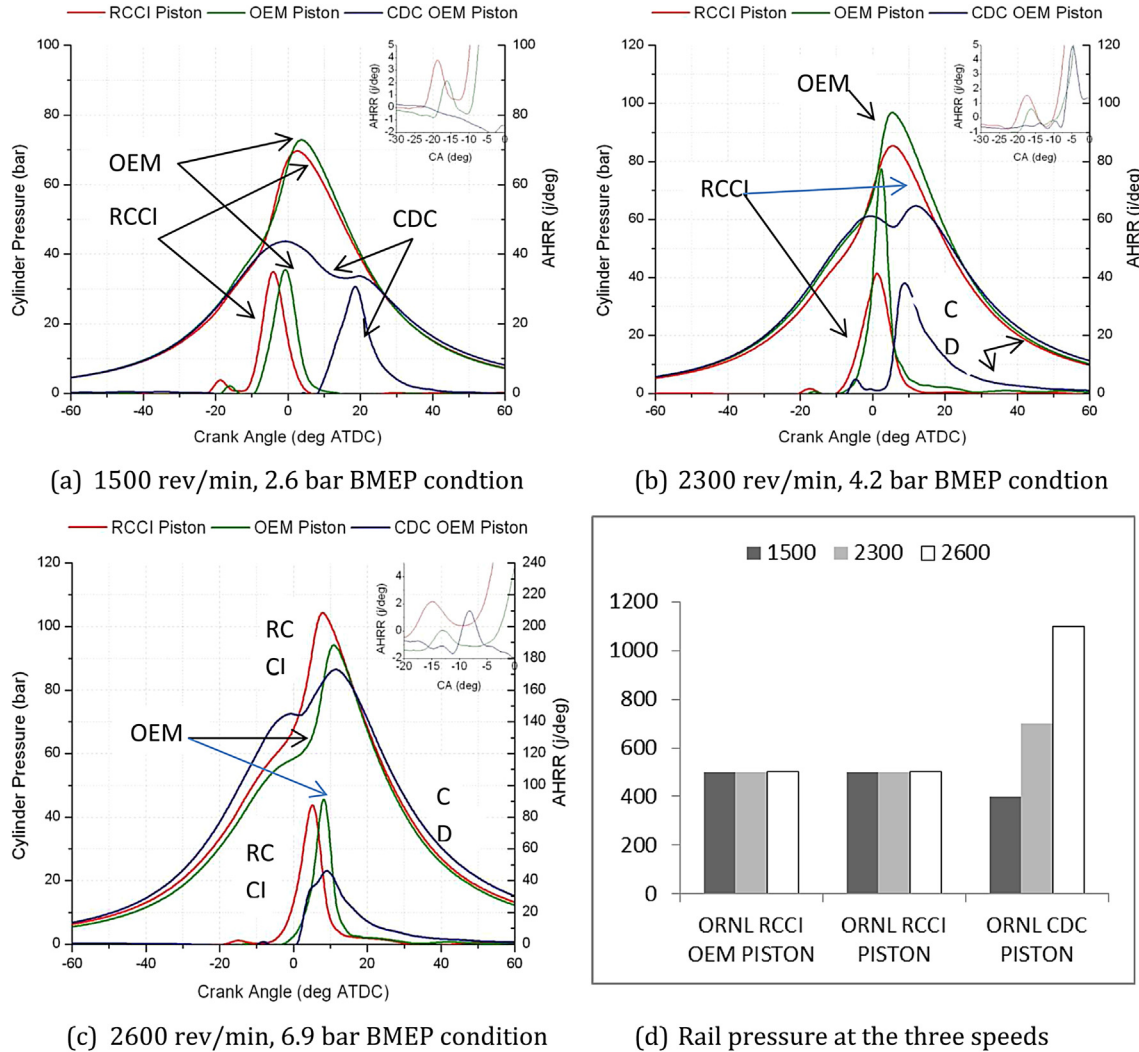


Fig. 82. Cylinder pressure, heat release rates and rail pressure at the three speeds [96].

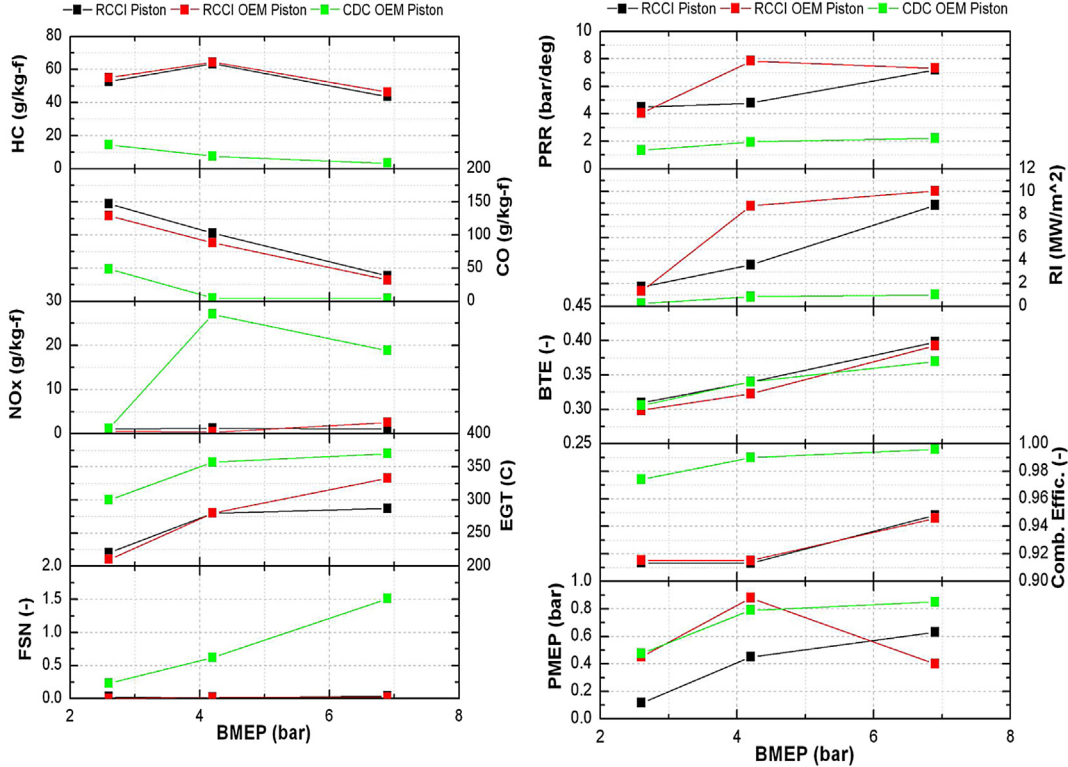


Fig. 83. Engine out emissions, combustion and performance for the three cases of Table 40 [96].

possible to reduce HC and CO emissions while keeping the maximum PRR below 10 bar/degCA and maintaining the highest possible brake thermal efficiency. Comparisons of heat release rate, cylinder pressure traces and rail pressure at all three speeds are given in Fig. 82.

From Fig. 82a,b,c it is noticed that the combustion is faster and occurs earlier for the RCCI piston than for CDC combustion. The CDC case has late combustion, which resulted in reduced cylinder pressure and heat release rates compared to the RCCI combustion case. The combustion phasing is observed to be same for all three speed conditions. The rail pressure used in the three cases is also shown in Fig. 82(d). It is interesting note that the OEM case actually uses lower rail pressure than for the RCCI at 1500 rev/min case. Engine-out emissions for all the cases are shown in Fig. 83. As expected, HC and CO were higher with NO_x and PM being lower than CDC with RCCI operation. This is in agreement with previous RCCI studies [8,26,29,99].

As seen in the previous RCCI studies, the increased HC and CO emissions were thought to be caused by a combination of the low combustion temperatures and crevice volumes that can trap unburned PFI fuel. The custom RCCI piston was designed to lower HC emissions by reducing the squish area and crevice volume. However, the RCCI piston was unable to significantly reduce HC compared to RCCI operation with the OEM piston in the MCE. This suggests that the squish area may not be the main source of HC emissions. The next possible source of HC is likely to be the piston-to-liner crevice volume.

More work is needed to definitively determine the source of HC emissions. CO emissions from RCCI generally follow the peak combustion chamber temperature, and this is seen by the reduction of CO with increased load. HC emissions were not found to be as sensitive to the combustion chamber temperature (i.e., load) as CO, again suggesting they are mainly a function of unburned fuel escaping combustion in the engine crevices. The temperature effect



Fig. 84. Modified RCCI piston (left) and OEM piston (right) [101].

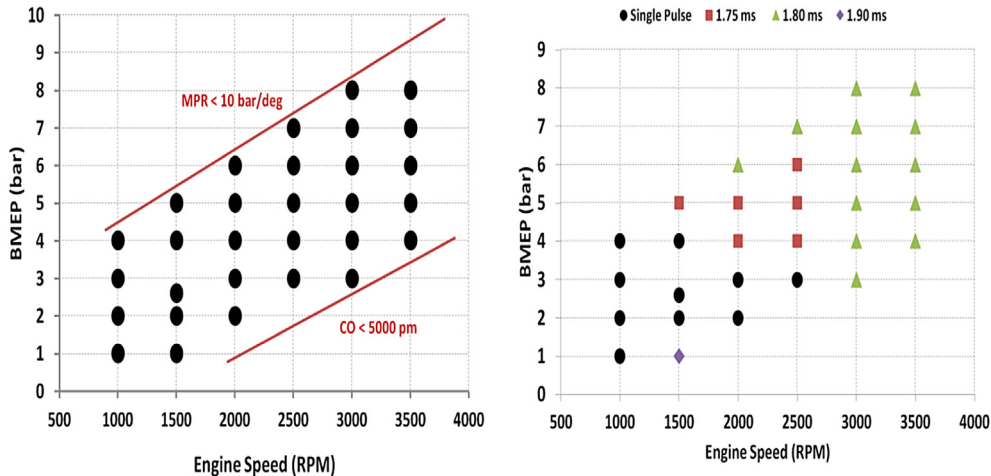


Fig. 85. RCCI operating points and injection strategy [101].

was also seen with the RCCI piston having higher CO than the OEM piston due to the lower in-cylinder temperatures with the reduced compression ratio of the custom piston.

In summary, Hanson et al. [96] demonstrated that RCCI combustion can be operated in multi-cylinder engines over a wide speed/load range, and that RCCI optimized pistons offer emissions and efficiency benefits compared to operating with a piston designed for CDC. In the experiments it was proved that the RCCI piston was successful in reducing NO_x and PM emissions, but the efficiency gains were lower than expected based on the single cylinder engine results.

4.4. Efficiency and emissions mapping of RCCI in the LD diesel engine

Curran et al. [101] explored the efficiency, emissions and combustion characteristics of RCCI with gasoline and diesel fuel over a wide speed and load range in the LD multi-cylinder diesel engine leading to the creation of an RCCI engine map. The RCCI map was developed under self-imposed constraints, which included a maximum cylinder pressure rise rate of 10 bar/deg CA and a CO emission limit of 5000 ppm. The RCCI map was developed using a mix of single and split diesel injections without the use of EGR for best brake thermal efficiency with the lowest possible NO_x emissions. The engine used for this study was shown in Fig. 2. The original equipment manufacturer (OEM) pistons were replaced with pistons modified for RCCI [101], shown in Fig. 84.

For the RCCI map exploration, the maximum cylinder pressure rise rate and CO constraints were observed during the RCCI operating procedure. RCCI operating points at intervals of 500 rev/min and every 1 bar BMEP were explored. The engine speed and load points explored are shown in Fig. 85, along with the constraints for MPR and CO. The DI injection strategy varied between a single DI pulse at the lower engine loads and lower speeds, and a split pulse at higher engine loads. The different injection strategies were implemented to minimize the NO_x and HC emissions tradeoffs. The split strategy was characterized by the majority of fuel in the pilot pulse occurring between 1.75 and 1.9 ms before the main injection, which varied between 28 and 61 CAD before TDC. The DI injection strategies are also shown in Fig. 84.

The contour plots presented for BTE, NO_x and Soot as function of engine load and speed shown in Fig. 86 were created using steady-state experimental data from the multi-cylinder engine (MCE). The maximum RCCI BTE for this map was 40.6% at

3000 rev/min, 8 bar which is 5% better than CDC operation at the same point with BTE of 38.6%. RCCI NO_x emissions were very low over the explored RCCI operating map and are approximately an order of magnitude less than CDC for all but the lowest engine loads. The engine performance and emission trends also show clear benefits and challenges for the application of RCCI on LD diesel engine in a road application.

4.5. Use of low pressure direct injection for RCCI LD engine operation

Walker et al. [102] used a single cylinder version of the same GM 1.9 L DI single-cylinder, four stroke diesel engine to improve efficiency and emissions via in-cylinder fuel blending with low pressure GDI technology and compared it against high pressure injection RCCI experiments. The experiments were carried out to examine the performance and emission characteristics of the base engine under the RCCI combustion strategy. Most previous RCCI studies used higher injection pressures greater than 500 bar with Common Rail Injection (CRI) hardware. Considering the broad market adoption of Gasoline Direct Injection (GDI) fueling systems, and the cost and weight of the hardware when compared to CRI hardware, a market type GDI injector was chosen for the study.

Diesel and gasoline were used as the high reactivity and low reactivity fuels, respectively. The low reactivity fuel gasoline (85%) was delivered by an automotive type Port Fuel Injection (PFI) system at -200 °CA aTDC during the intake stroke for the premixed charge. The high reactivity fuel diesel (15%) was delivered using the CRI system or the GDI system. Since the in-cylinder fuel distributions are the key factors for RCCI operation, the high reactivity fuel injection timing, pressure, spray angle, piston geometry, type of injector and the type of fuel play a vital role in the proper mixing of the premixed fuel and Direct Injected fuel.

Two injectors (the CRI (for 250 bar and 500 bar) and the GDI (for 150 bar and 200 bar)) were used for delivering the high reactivity fuel with injection sweeps from -115 degCA aTDC to -35 degCA aTDC. It was found that the GDI Injector provided a broader SOI range compared to the CRI injector. Nevertheless the CRI Injector offered a longer achievable combustion phasing range. The overall combustion efficiency was in the range of 90–93% and the CRI injector provided a 1% increase in combustion efficiency over the GDI Injector. From close observation of the results it was argued that deposition of unburned premixed gasoline in the squish and crevice regions of the cylinder was the major contributor to the

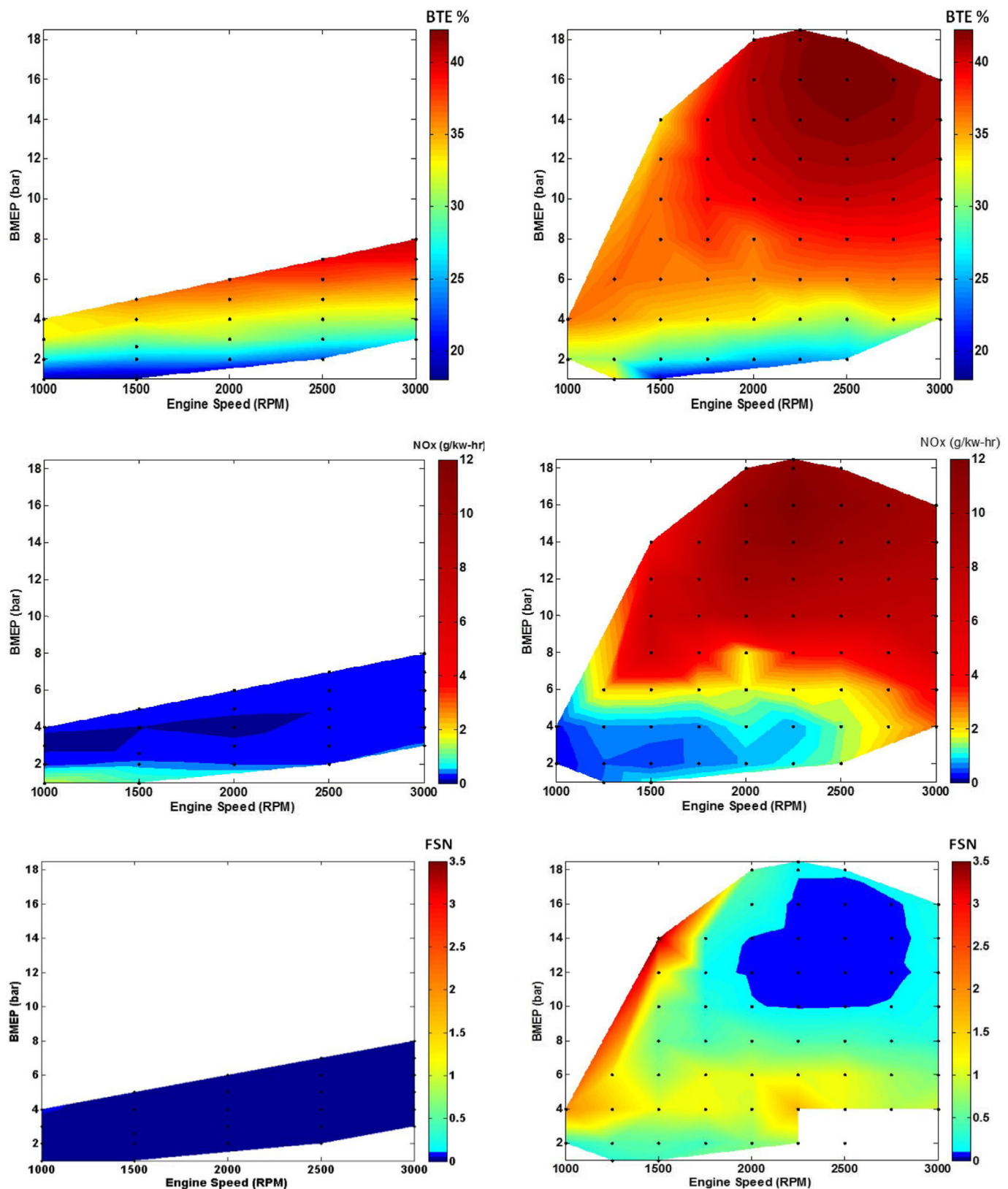


Fig. 86. Comparison of BTE, NO_x and soot between RCCI and CDC (right) [101].

relatively low combustion efficiency. This was resolved by optimizing the piston geometry for RCCI operation.

The modified RCCI piston had a TDC combustion chamber surface area of 152.5 cm^2 compared to the conventional diesel combustion piston's surface area of 174.01 cm^2 . The reduction in piston surface area indeed helped resolve the low combustion efficiency issues. NO_x and soot levels were found to be within the US EPA 2010 limits (0.27 g/kW-h and 0.013 g/kW-h). It was noticed that at late injection timings only the CRI injector with 500 bar met the NO_x limit, but at the earliest injection timings both injectors met the limits. HC was higher with the GDI injector compared to the CRI injector. CO levels were high for the 500 bar CRI injector sweep and the combustion stability was reduced slightly at the boundaries of proper mixture preparation and led to incomplete combustion.

To understand the results, a CFD investigation of the in-cylinder fuel distributions was conducted and it was found that with a given injection pressure, a wider spray angle increased the mixing of the direct injection fuel spray. For a given spray angle, use of a higher injection pressure also increased the mixing of the direct injection fuel spray. Further experiments were carried out with the optimized piston geometry (TDC surface area reduction of 12.45 cm^2 with the RCCI piston), wider spray angle (142°) and the GDI low injection pressure (150 bar) injector, which yielded a 5% (absolute) increase in thermal efficiencies compared to the CRI injector. In the final stage of the work, high-load RCCI engine operation was explored with the use of low-pressure direct-injection, and at 9 bar IMEP, equivalent performance and emissions characteristics were seen. Gross indicated thermal efficiencies greater than 47% and combustion efficiencies in excess of 95% were observed.

4.6. Effect of biodiesel blends on RCCI combustion in an LD multi-cylinder diesel engine

Hanson et al. [103], performed additional experiments in the GM 1.9 L light duty, multi-cylinder diesel engine shown in Fig. 2 to study the effects of biofuel blends on RCCI combustion. Previous RCCI experiments used petroleum-based fuels, such as diesel (ULSD) and gasoline and some work was done with high percentage biofuels, namely E85. Hanson et al. chose E20 and B20 to examine RCCI performance. The RCCI engine experiments were performed using intake port fuel-injection of gasoline, E20 or E85 and direct-injection of ULSD or B20.

Hanson et al. compared the results with CDC in the 2007 model year Opel Astra, which features the same 1.9 L engine and a manual transmission. In order to show the impact of using E20 in place of gasoline, the operating map results obtained from the GM 1.9 L light duty, multi-cylinder diesel engine were compared using a similar engine mapping exercise with gasoline and diesel fuels [101]. The high load performance of E20 was the primary focus of the work and hence loads below 3 bar BMEP were not extensively studied, as was also discussed in detail by Curran et al. [101]. The experiments were conducted following the US EPA FTP75 cycle with E20/ULSD with the specific operating points shown in Table 42.

Hanson et al. replaced the diesel with B20 and conducted their experiments with gasoline as the PFI fuel and B20 as the direct injection fuel. Also, by using E85 as the PFI fuel instead of E20, it was possible to increase the peak load and stay within the MPRR limits. Table 43 shows the operating conditions of G/B20 RCCI operation (Fig. 88).

The E20/D RCCI results show that the MPRR and HRR were reduced, which allowed for a 2 bar increase in peak load (from 8 to 10 bar BMEP), while the use of E85 (E85/B20) allowed for an additional 1 bar increase in load (from 10 to 11 bar BMEP). An increase in combustion efficiency and decrease in heat transfer and

Table 42
Operating points [103].

Speed, Rev/min	BMEP, Bar	Intake pressure, bar	PFI fraction, %	Main SOI, degCA aTDC
1000	4	1.1	0.5	-43
1500	3, 5	1,1.2	0.4,0.55	-42,-45
2000	3,4,5,6	1,1,1,2,1,4	0.4,0.55,0.6,0.62	-42,-43,-45,-49
2500	4,5,7	1,1,1,2,1,5	0.55,0.6,0.7	-43,-45,-52
3000	4,5,6,7,8	1,1,1,2,1,4,1,5,1,8	0.55,0.6,0.62, 0.7,0.75	-43,-45,-49, -52,-55

exhaust losses was also observed. On average, the net gain in reduced heat transfer, pumping and exhaust losses, allowed for increased BTE, by up to 1.33% when using E20. Also, it was noticed that the required PFI fraction decreased with E20/D operation, which, in turn, increased NO_x emissions. Increased volumetric efficiency was observed with E20, which led to lower pumping losses.

A reduced PFI-to-DI fuel amount was observed with G/B20 RCCI operation, but unlike with the use of E20, this decreased NO_x emissions. G/B20 RCCI operation also increased combustion efficiency due to reduced UHC, but had higher CO. The gain in combustion efficiency helped to increase BTE by up to 1.68%. The reduced PFI fraction in case of G/B20 operation increased the DI fuel fraction, which increased the MPRR similarly to the E20 results. E85/B20 RCCI operation allowed the peak BTE of RCCI to increase from 40% to 43% compared to gasoline/diesel RCCI operation.

4.7. RCCI combustion phasing control during load transitions

The effect of transient intake manifold conditions on RCCI engine combustion phasing control during load transitions was studied by Wu et al. [104]. The multi-dimensional computational fluid dynamics (CFD) code coupled with detailed chemistry, KIVA-CHEMKIN, was applied to develop a strategy for phasing control during load transitions. Steady-state operating points at 1500 rev/min were calibrated from 0 to 5 BMEP. The load transitions considered in the study included a load-up and a load-down load change transient between 1 bar and 4 bar BMEP at 1500 rev/min. Experimental results obtained using a fast response dynamometer system and combustion fast response HC and NO_x instrumentation showed that during the load transitions, the diesel injection timing responded in 2 cycles, while around 5 cycles were needed for the diesel common-rail pressure to reach the target value. However, the intake manifold pressure lagged behind the pedal change for about 50 cycles due to the slower response of the turbocharger.

The effect of these transients on RCCI engine combustion phasing was studied. Strategies for phasing control were adopted that changed the direct port fuel injection (PFI) amount during the load transitions. Specific engine operating cycles during the load transitions (6 cycles for the load-up transition and 7 cycles for the load-down transition) were selected based on the measured change of intake manifold pressure to represent the transition processes. Each cycle was studied separately to find the correct PFI-to-diesel fuel ratio for the desired CA50 (the crank angle at

Table 43
G/B20 operating condition [103].

Speed, Rev/min	BMEP, bar	Intake pressure, bar	PFI fraction, %	Equivalence ratio, ϕ
2000	2	1	0.3	0.267
1500	2.6	1	0.15	0.31
2300	4.2	1.2	0.62	0.34

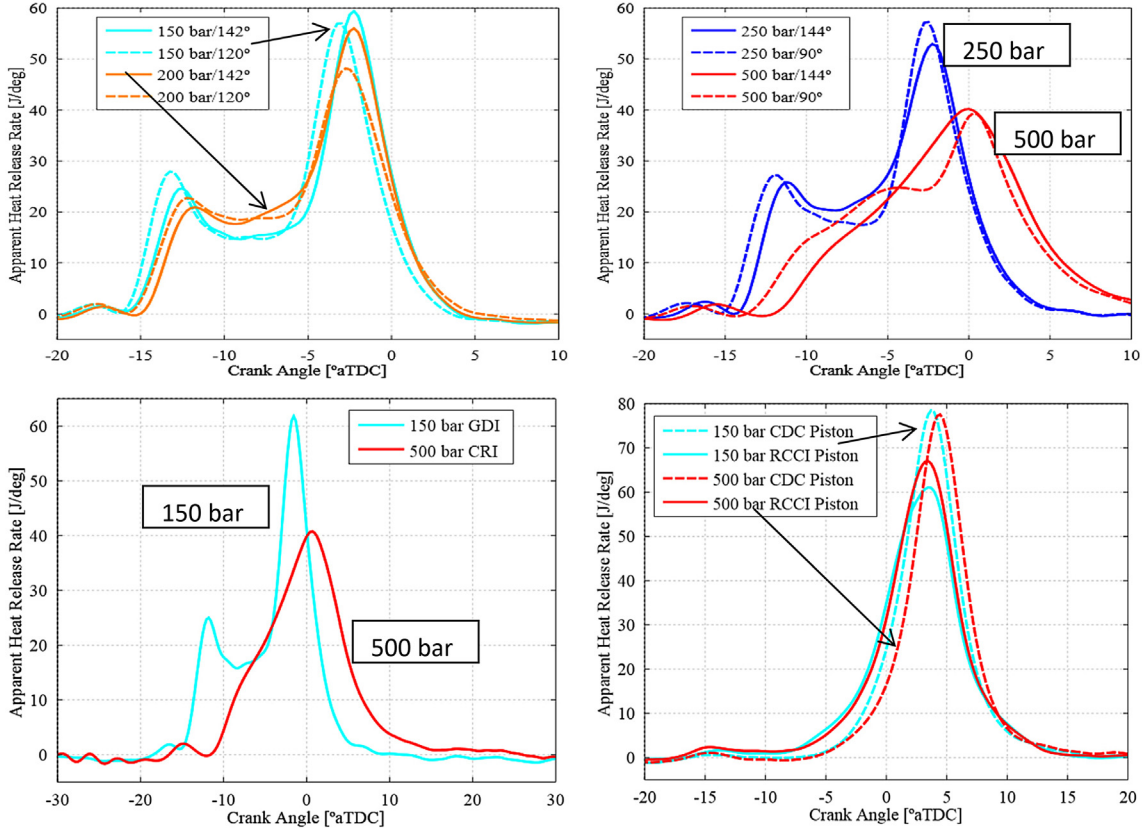


Fig. 87. Comparison of heat release rates between, GDI/CRI and RCCI/CDC piston [102].

which 50% of total heat release occurs). The simulation results showed that CA50 was delayed by 7–15° for the load up transition and advanced by around 5° during the load-down transition if the pre-calibrated steady-state PFI table was used. By decreasing the PFI ratio by 10%–15% during the load-up transition and increasing the PFI ratio by around 40% during the load-down transition, the CA50 could be controlled at a reasonable value during transitions. The proposed control strategy can also be used for closed-loop control during engine transient operating conditions (Hanson et al. [105]).

5. Conclusions and scope for future work

A review of experimental and modeling work in the field of high efficiency, low emissions engines has been conducted. Dual fuel

reactivity controlled compression ignition combustion in HD and LD diesel engines was focused on, due to its demonstrated superior control, compared to other strategies with discussion of the operating range, thermal efficiency and emission benefits. Experimental work on a single-cylinder HD diesel engine with the dual fuel strategy and a “single fuel” strategy (with the use of an additive) were presented, including low load to high load operation. Next, RCCI combustion in LD and HD engines was compared and combustion in an LD multi-cylinder diesel engine was discussed. Finally, RCCI combustion in an LD single-cylinder engine was reviewed.

In each section, the effects of fuel, injection pressure, injection timings, IVC timings, PFI fractions, piston geometry, intake temperature and intake pressure on heat transfer, combustion timing, thermal efficiency, combustion efficiency and emissions were discussed in detail. It was observed that simulation and modeling

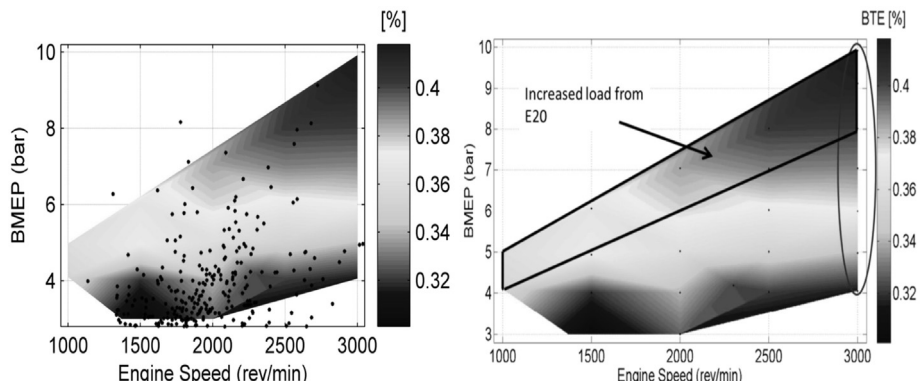


Fig. 88. E20/D operating map with CDC LD FTP points and load range extension with use of E20 [103].

works were extremely effective to guide the experimental studies work in order to achieve high efficiency and high load operation. CFD studies have been used to optimize the piston geometry for both HD and LD RCCI applications and have yielded further improved results. An optimized piston, which had less surface area compared to the stock piston, that minimized heat transfer losses and improved combustion efficiency, was described. The new piston design also helped in reducing HC emissions.

In summary, the experiments conducted using the RCCI strategy on the HD and LD diesel engines revealed the following achievements,

- The studies demonstrated that RCCI is a promising strategy to meet current and future emissions regulations without relying on NO_x and soot after-treatment.
- Gasoline/diesel RCCI provided high thermal efficiency over a wide range of engine loads, with a peak gross indicated efficiency of 56% at a 9.3 bar IMEP operating point on an HD engine. Operation over the load range from 2 bar IMEP to 14.6 bar IMEP (i.e., light load to mid-high-load operation) operation at 1300 rev/min was demonstrated.
- The HD engine experiments also clearly explained the reasons for the improved performance of RCCI combustion over conventional diesel combustion. The improved efficiency was found to be largely due to reduced heat transfer losses. Nearly three orders of magnitude of NO_x reduction, six times lower soot, and 16.4% higher gross indicated efficiency were also achieved using RCCI compared conventional diesel combustion without EGR.
- CFD modeling was used to compare RCCI and high EGR diesel combustion. In agreement with the experiments, it was found that at identical operating points, NO_x was reduced by two orders of magnitude, soot was reduced by factor of ten, and gross indicated efficiency was improved by 11.5%.
- RCCI experiments using a “single fuel strategy” (gasoline plus gasoline doped with a small amount of DTBP/2-EHN) exhibited nearly identical emissions to those obtained by the gasoline/diesel dual-fuel strategy. The comparison of the “single fuel” strategy with the dual fuel strategy also revealed that a decreased low temperature heat release magnitude decreased compression work, and resulted in approximately a 1% gain in gross indicated thermal efficiency.
- RCCI experiments on the HD engine demonstrated that ~60% gross engine efficiencies were possible through optimized combustion management and thermodynamic conditions, and thus provides a pathway to meet the DOE Super Truck 50% brake thermal efficiency goal, as well as a pathway for reaching the 55% brake thermal efficiency goal. These ultra-high efficiencies were reached by operating with a higher compression ratio (18.7) and without piston oil cooling.
- Natural gas/diesel RCCI operation on HD engine yielded clean, quiet, and efficient combustion throughout the tested load and speed range. Very low NO_x and soot emissions up to 13.5 bar IMEP load were attained without use of EGR, and with use of EGR up to full load. Also the study suggests that different injector configurations could allow further improvements for RCCI operation (e.g., smaller hole diameters, and use of optimized triple injections).
- The use of natural gas as the low reactivity fuel allowed extending the load limit and the combustion process, and emissions results were found to be sensitive to the injection mass split. The results showed that by equalizing the mass split in double injections, the peak pressure rise rate and ringing intensity were decreased substantially. Therefore, to properly condition the squish region with diesel fuel from the first

injection while maintaining reasonable combustion noise, precise injector control is needed, especially at high load.

- RCCI operation with E85-diesel was successful at engine loads as high as 16.5 bar IMEP_g. E85-diesel operation also enabled lower rates of EGR use at all engine loads. The lower EGR rates were found to be more beneficial for increasing thermal efficiency. The maximum thermal efficiency measured with E85-diesel fueling was 59% compared to 56% of gasoline-diesel.
- Low emissions RCCI operation (without the need for NO_x and PM after-treatment) was successful in a production type multi-cylinder engine utilizing the OEM diesel injection system and turbo-machinery over the engine speed and load range typical of light duty vehicles.
- RCCI operation was successful with both the stock high compression ratio OEM piston and an optimized RCCI piston. The brake thermal efficiency of RCCI was equal to or higher than the OEM brake thermal efficiency at three representative steady state operating conditions studied using the optimized RCCI piston. NO_x and PM were reduced by at least one order of magnitude compared to the OEM EURO IV calibration. However, HC and CO were increased by one order of magnitude over the OEM calibration indicating the need for an oxidation catalyst.
- Use of E20 as a low reactivity fuel in the LD multi-cylinder engine allowed for a 2 bar increase in the peak load from 8 to 10 bar BMEP, while the use of 85 allowed for an additional 1 bar increase in load from 10 to 11 bar BMEP.
- Use of B20 as the high reactivity fuel increased combustion efficiency due to reduced HC, but had higher CO. This gain in combustion efficiency increased the brake thermal efficiency by up to 1.68%. In addition, the use of B20 reduced the required PFI fuel fraction. However, unlike with the use of E20, this reduced NO_x emissions. The use of E85 and B20 allowed the peak brake thermal efficiency of RCCI with the OEM piston to be increased from 40% with gasoline-diesel operation to 43%.

5.1. Scope for future work

The present review demonstrates that achieving high efficiency and low NO_x and soot emissions in-cylinder is possible using the low temperature combustion RCCI strategy. From the presented literature it is inferred that there is scope for further improvements in RCCI, as listed below.

- Further optimization of engine parameters is needed to fully realize the potential of dual-fuel RCCI operation. Of paramount interest is the feasibility of cycle-to-cycle control of dual fuel RCCI operation over a wide range of loads and during transient operation. The next steps in operating parameter optimizations should include other load points.
- The need for increased understanding of the performance of turbo-machinery for low temperature combustion is also apparent. The relatively low exhaust temperatures imply that high turbocharger efficiencies will be needed.
- Future work will help define the level of after-treatment required for meeting LD federal-emission standards and will need to address other design elements of interest, including the relative sizes of the direct-injected diesel fuel tank and the PFI fuel tank needed in a vehicle.
- The lower exhaust temperatures with RCCI also offer challenges for after treatment systems. Developments in oxidation catalyst after-treatment systems are required to treat HC and CO emissions at the available exhaust temperature. More research is required in the direction of low temperature catalysts.
- Fuel injection strategy modifications may be required. In the current injection strategies: 70–90% of the total fuel mass was

injected in the intake port and the remaining 10% was injected into the cylinder with the help of GDI or CRI injectors at pressures of 150–800 bar. Instead, the order of blending could be changed/optimized, i.e., inject a certain portion of the low reactivity fuel first, followed by the high reactivity fuel and then inject the remaining low reactivity fuel. This could help in controlling the combustion phasing at higher load operation, but will require two in-cylinder direct injectors, as described by Wissink et al. [62] and Lim and Reitz [63].

- Choosing an inferior low reactivity fuel compared to gasoline may also be advantageous. Experiments conducted with ethanol as the low reactivity fuel show that it requires more high reactivity fuel at high load operation. This was also utilized to extend the load range in the LD multi-cylinder RCCI engine. Other potential of low reactivity fuels could also be investigated. Similarly, instead of diesel, biofuels (including neat biodiesel) could also be used as the DI fuel.
- More experiments are needed at higher speeds and loads to transfer the RCCI concept toward other applications (e.g., automotive/stationary).

Acknowledgments

The authors gratefully acknowledge the many colleagues in the Engine Research Center for their insights regarding the RCCI combustion technology discussed in this article. Support for the research from Caterpillar, the U.S. Department of Energy (DOE), the Sandia and Oak Ridge laboratories, the Direct-injection Engine Research Consortium (DERC), the Princeton CEFRC and the University Grants Commission (UGC)-Government of India is gratefully acknowledged.

References

- [1] Johnson TV. Review of diesel emissions and control. *Int J Engine Res* 2009;10: 275–85.
- [2] Reitz RD. <http://www.sae.org/mags/aei/power/8388>; 2010.
- [3] National Science Foundation Directorate for Engineering, NSF/DOE partnership on advanced combustion engines. NSF Solicitation 12-559; 2012.
- [4] Turns SR. An introduction to combustion: concepts and applications. 2nd ed. Boston, Massachusetts: WCB/McGraw-Hill; 1999.
- [5] Dempsey A, Walker N, Gingrich E, Reitz RD. Comparison of low temperature combustion strategies for advanced compression ignition engines with a focus on controllability. *Combust Sci Technol* 2014;86(2):210–41.
- [6] Manente V, Tunestal P, Johansson B. Partially premixed combustion at high load using gasoline and ethanol, a comparison with diesel. SAE paper 2009; 2009-01-0944.
- [7] Splitter DA, Hanson RM, Kokjohn SL, Reitz RD. Improving engine performance by optimizing fuel reactivity with a dual fuel PCCI strategy. Conference on Thermo and Fluid Dynamic Processes in Diesel Engines 2010; Valencia, Spain.
- [8] Kokjohn SL, Splitter DA, Hanson RM, Reitz RD. Experiments and modeling of dual fuel HCCI and PCCI combustion using in-cylinder fuel blending. *SAE Int J Engines* 2010;2(2):24–39.
- [9] Manente V, Johansson B, Tunestal P, Cannella W. Effects of ethanol and different type of gasoline fuels on partially premixed combustion from low to high load. SAE paper 2010; 2010-01-0871.
- [10] Hasegawa R, Yanagihara H. HCCI combustion in DI diesel engine. SAE paper 2003; 2003-01-0745.
- [11] Hardy WL, Reitz RD. A study of the effects of high EGR, high equivalence ratio, and mixing time on emissions levels in a heavy-duty diesel engine for PCCI combustion. SAE paper 2006; 2006-01-0026.
- [12] Opat R, Ra Y, Gonzalez MA, Krieger R, Reitz RD, Foster DE, et al. Investigation of mixing and temperature effects on HC/CO emissions for highly dilute low temperature combustion in a light duty diesel engine. SAE paper 2007; 2007-01-0193.
- [13] Dec JE, Yang Y. Boosted HCCI for high power without engine knock and with ultra-low NO_x emissions using conventional gasoline. *SAE Int J Engines* 2010;3(1):750–67.
- [14] Manente V, Johansson B, Tunestal P, Cannella W. Influence of inlet pressure, EGR, combustion phasing, speed and pilot ratio on high load gasoline partially premixed combustion. SAE paper 2010; 2010-01-1471.
- [15] Saxena S, Ivan DB. Fundamental phenomena affecting low temperature combustion and HCCI engines, high load limits and strategies for extending these limits. *Prog Energy Combust Sci* 2013;39:457–88.
- [16] Musculus PBM, Paul CM, Lyle MP. Conceptual models for partially premixed low temperature diesel combustion. *Prog Energy Combust Sci* 2013;39: 246–83.
- [17] Dec JE, Yang Y, Dronniou N. Boosted HCCI – controlling pressure-rise rates for performance improvements using partial fuel stratification with conventional gasoline. *SAE Int J Engines* 2011;4. 2011-01-0897.
- [18] Noehre C, Anderson M, Johnson B, Hultqvist A. Characterization of partially premixed combustion. SAE Technical Paper 2006; 2006-01-3412.
- [19] Kalghatgi GT, Risberg P, Angstrom H. Advantages of fuels with high resistance to auto-ignition in late-injection low temperature compression ignition combustion. SAE Technical Paper 2006; 2006-01-3385.
- [20] Dec J, Hwang W, Sjöberg M. An investigation of thermal stratification in HCCI engines using chemiluminescence imaging. SAE Technical Paper 2006; 2006-01-1518.
- [21] Dempsey A, Reitz RD. Computational optimization of reactivity controlled compression ignition in a heavy-duty engine with ultra low compression ratio. *SAE Int J Engines* 2011;4(2):2222–39.
- [22] Bessonette PW, Schleyer CH, Duffy KP, Hardy WL, Liechty MP. Effects of fuel property changes on heavy-duty HCCI combustion. SAE paper 2007; 2007-01-0191.
- [23] Park SH, Youn IM, Lim Y, Lee CS. Influence of the mixture of gasoline and diesel fuels on droplet atomization, combustion, and exhaust emission characteristics in a compression ignition engine. *Fuel Process Technol* 2013;106:392–401.
- [24] Valentino G, Corcione FE, Iannuzzi SE, Serra S. Experimental study on performance and emissions of a high speed diesel engine fuelled with n-butanol/diesel blends under premixed low temperature combustion. *Fuel* 2012;92(1):295–307.
- [25] Inagaki K, Fuyuto T, Nishikawa K, Nakakita K, Sakata I. Dual-fuel PCI combustion controlled by in-cylinder stratification of ignitability. SAE paper 2006; 2006-01-0028.
- [26] Kokjohn SL, Hanson RM, Splitter DA, Reitz RD. Experiments and modeling of dual-fuel HCCI and PCCI combustion using In-Cylinder fuel blending. SAE paper 2009; 2009-01-2647.
- [27] Amsden AA. KIVA-3V, Release 2, improvements to KIVA-3V. LA-UR-99-915. Los Alamos National Laboratory; 1999.
- [28] Beale JC, Reitz RD. Modeling spray atomization with the Kelvin–Helmholtz/Rayleigh–Taylor hybrid model. *Atom Sprays* 1999;9(6):623–50.
- [29] Abani N, Munnannur A, Reitz RD. Reduction of numerical parameter dependencies in diesel spray models. *Trans ASME J Eng Gas Turbines Power* 2008;130(3):1–9.
- [30] Abani N, Kokjohn SL, Park SW, Bergin M, Munnannur A, Ning W, et al. An improved spray model for reducing numerical parameters dependencies in diesel engine CFD simulations. SAE paper 2008; 2008-01-0970.
- [31] Kong SC, Sun Y, Reitz RD. Modeling diesel spray flame lift-off, sooty tendency and NO_x emissions using detailed chemistry with a phenomenological soot model. *Trans ASME J Eng Gas Turbines Power* 2007;129: 245–51.
- [32] Ra Y, Reitz RD. A reduced chemical kinetic model for IC engine combustion simulations with primary reference fuels. *Combust Flame* 2008;155(4): 713–38.
- [33] Ra Y, Reitz RD. The application of a multicomponent droplet vaporization model to gasoline direct injection engines. *Int J Engine Res* 2003;4(3): 193–218.
- [34] Hanson RM, Kokjohn SL, Splitter DA, Reitz RD. An experimental investigation of fuel reactivity controlled PCCI combustion in a heavy-duty engine. SAE paper 2010; 2010-01-0864.
- [35] Splitter DA, Hanson RM, Kokjohn SL, Rein K, Sanders, Reitz RD. An optical investigation of ignition processes in fuel reactivity controlled PCCI combustion. SAE paper 2010-01-0345, 2010.
- [36] Hiroyasu H, Kadota T. Models for combustion and formation of nitric oxide and soot in DI diesel engines. SAE paper 760129, 1976.
- [37] Sun Y. Diesel combustion optimization and emissions reduction using adaptive injection strategies (AIS) with improved numerical models. PhD thesis. Department of Mechanical Engineering, University of Wisconsin-Madison; 2007.
- [38] O'Rourke PJ, Amsden AA. A spray/wall interaction sub-model for the KIVA-3 wall film model. SAE paper 2000; 2000-01-0271.
- [39] O'Rourke PJ, Amsden AA. A particle numerical model for wall dynamics in port injected engines. SAE paper 1996; 961961.
- [40] Munnannur A. Droplet collisions modeling in multi-dimensional engine spray computations. PhD Thesis. Department of Mechanical Engineering, University of Wisconsin-Madison; 2007.
- [41] Yu C, Wang JX, Wang Z, Shuai SJ. Comparative study on gasoline homogeneous charge induced ignition (HCII) by diesel and gasoline/diesel blend fuels (GDBF) combustion. *Fuel* 2013;106:470–7.
- [42] Yang B, Yao M, Cheng WK, Li Y, Zheng Z, Li S. Experimental and numerical study on different dual-fuel combustion modes fuelled with gasoline and diesel. *Appl Energy* 2014;113:722–33.
- [43] Nevin RM, Sun Y, Gonzalez MA, Reitz RD. PCCI investigation using variable intake valve closing in a heavy duty diesel engine. SAE Technical Paper 2007; 2007-01-0903.

- [44] Szybist J, Bunting B, Manente V, Tunestal P. The effects of fuel composition and compression ratio on thermal efficiency in an HCCI engine. SAE paper 2007; 2007-01-4076.
- [45] Ma S, Zheng Z, Liu H, Zhang Q, Yao M. Experimental investigation of the effects of diesel injection strategy on gasoline/diesel dual-fuel combustion. *Appl Energy* 2013;109:202–12.
- [46] Benajes J, Molina S, Garcia A, Belarte E, Vanvolsem M. An Investigation on RCCI combustion in a heavy duty diesel engine using in-cylinder blending of diesel and gasoline fuels. *Appl Therm Eng* 2014;63:66–76.
- [47] Arregle J, Lopez JJ, Garcia JM, Fenollosa C. Development of a zero-dimension diesel combustion model, part 2: analysis of the transient initial and final diffusion combustion phases. *Appl Therm Eng* 2013;23:1319–31.
- [48] Pastor JV, Lopez JJ, Garcia JM, Pastor JM. A 1 D model for the description of mixing controlled inert diesel sprays. *Fuel* 2008;87:2871–85.
- [49] Papagiannakis RG, Hountalas DT. Experimental investigation concerning the effect of natural gas percentage on performance and emissions of a DI dual fuel diesel engine. *Appl Therm Eng* 2003;23(3):353–65.
- [50] Splitter D, Reitz RD, Hanson RM. High efficiency, low emissions RCCI combustion by use of a fuel additive. *SAE Int J Fuel Lubric* 2010;3(2):742–56.
- [51] Tanaka S, Ayala F, Keck JC, Heywood JB. Two stage ignition in HCCI combustion and HCCI control by fuels and additives. *Cambust Flame* 2003;132: 219–39.
- [52] Pohlkamp K, Reitz RD. Reactivity controlled compression ignition (RCCI) in a single cylinder air-cooled HSDI diesel engine. SAE paper 2012; 2012-32-0074.
- [53] Eng JA, Leppard WR, Sloane TM. The effect of di-tertiary butyl peroxide (DTBP) addition to gasoline on HCCI combustion. SAE Technical Paper 2003; 2003-01-3170.
- [54] Hanson RM, Kokjohn SL, Splitter DA, Reitz RD. An experimental investigation of fuel reactivity controlled PCCI combustion in a heavy-duty engine. *SAE Int J Engines* 2010;3(1):700–16.
- [55] Hanson RM, Kokjohn SL, Splitter DA, Reitz RD. Fuel effects on reactivity controlled compression ignition (RCCI) combustion at low load. SAE paper 2011; 2011-01-0361.
- [56] Thompson AA, Lambert SW, Mulqueen SC. Prediction and precision of cetane number improver response equations. SAE Technical Paper 1997; 972901.
- [57] Oxley JC, Smith JL, Rogers E, Ye W, Aradi AA, Henly TJ. Fuel combustion additives: a study of their thermal stabilities and decomposition pathways. *Energy Fuels* 2000;14:1252–64.
- [58] Ickes AM, Bohac SV, Assanis DN. Effect of 2-Ethylhexyl nitrate cetane improver on NO_x emissions from premixed low-temperature diesel combustion. *Energy Fuels* 2009;23(10):4943–8.
- [59] Bunting BG, Wildman CB, Szybist JP, Lewis S, Storey J. Fuel chemistry and cetane effects on diesel homogeneous charge compression ignition performance, combustion, and emissions. *J Engine Res* 2007;8(1):15–27.
- [60] Kokjohn SL, Hanson RM, Splitter DA, Reitz RD. Fuel reactivity controlled compression ignition (RCCI): a pathway to controlled high-efficiency clean combustion. *Int J Engine Res* 2011;12:209–26.
- [61] De Ojeda W, Yu Zhang Y, Xie K, Han X, Wang M, Zheng M. Exhaust hydrocarbon speciation from a single-cylinder compression ignition engine operating with In-Cylinder blending of gasoline and diesel fuels. SAE Technical Paper 2012; 2012-01-0683.
- [62] Wissink ML, Lim JH, Splitter DA, Hanson RM, Reitz RD. Investigation of injection strategies to improve high efficiency RCCI combustion with diesel and gasoline direct injection. In: Proceedings of ASME Internal Combustion Engine Division Fall Technical Conference 2012; 2012. Paper No ICEF2012-92107, September 23–26, Vancouver, BC, Canada.
- [63] Lim JH, Reitz RD. High load (21Bar IMEP) dual fuel RCCI combustion using dual direct injection. In: Proceedings of the ASME 2013 internal combustion engine division fall technical conference; 2013. Paper ICEF2013-19140, October 13–16, Dearborn, Michigan.
- [64] Tess M, Reitz RD. Diesel engine combustion size scaling at medium load without EGR. SAE paper 2011; 2011-01-1384.
- [65] Akihama K, Takatori Y, Inagaki K, Sasaki S, Dean AM. Mechanism of the smokeless rich diesel combustion by reducing temperature. SAE paper 2001; 2001-01-0655.
- [66] Splitter DA, Martin Wissink, Dan DeVescovo, Reitz RD. RCCI engine operation towards 60% thermal efficiency. SAE paper 2013; 2013-01-0279.
- [67] Foster DE. Low temperature combustion-a thermodynamic pathway to high efficiency engines. National Petroleum Council Fuels Study; 2012.
- [68] Grandin B, Denbratt I, Boord I, Brackmann C. The effect of knock on the heat transfer in an SI engine: thermal boundary layer investigation using CARS temperature measurements and heat flux measurements. SAE Technical Paper 2000; 2000-01-2831 2000.
- [69] Shibata G, Oyama K, Urushihara T, Nakano T. Correlation of low temperature heat release with fuel composition and HCCI engine combustion. SAE Technical Paper 2005; 2005-01-0138.
- [70] Shibata G, Urushihara T. Realization of dual phase high temperature heat release combustion of base gasoline blends from oil refineries and a study of HCCI combustion processes. *SAE Int J Engines* 2009;2(1):145–63.
- [71] Sjöberg M, Dec J, Cernansky N. Potential of thermal stratification and combustion retard for reducing pressure-rise rates in HCCI engines, based on multi-zone modeling and experiments. SAE Technical Paper 2005; 2005-01-0113.
- [72] Herold R, Krasselt J, Foster D, Ghandhi J. Investigations into the effects of thermal and compositional stratification on HCCI combustion – Part II: optical engine results. *SAE Int J Engines* 2009;2(1):1034–53.
- [73] Sjöberg M, Dec J. Smoothing HCCI heat-release rates using partial fuel stratification with two-stage ignition fuels. SAE Technical Paper 2006; 2006-01-0629.
- [74] Yang Y, Dec J, Droniou N, Sjöberg M. Partial fuel stratification to control HCCI heat release rates: fuel composition and other factors affecting pre-ignition reactions of two-stage ignition fuels. *SAE Int J Engines* 2011;4(1): 1903–20.
- [75] Kokjohn SL, Reitz RD. Characterization of dual-fuel PCCI combustion in a light-duty engine. International Multidimensional Engine Modeling User's Group Meeting 2010; Meeting-2010/7, USA.
- [76] Kokjohn SL, Musculus M, Splitter DA, Reitz RD. Investigation of fuel reactivity stratification for controlling PCI heat-release rates using high-speed chemiluminescence imaging and fuel tracer fluorescence. *SAE Int J Engines* 2012;5(2):248–69.
- [77] Splitter DA, Kokjohn SL, Rein K, Hanson RM. An optical investigation of ignition processes in fuel reactivity controlled PCCI combustion. *SAE Int J Engines* 2010;3(1):142–62.
- [78] Splitter DA, Hanson RM, Kokjohn SL, Reitz RD. Reactivity controlled compression ignition (RCCI) heavy-duty engine operation at mid-and high-loads with conventional and alternative fuels. SAE paper 2011; 2011-01-0363.
- [79] Heywood JB. Internal combustion engine fundamentals. New York: McGraw-Hill; 1988.
- [80] Hashimoto K. Inhibition effect of ethanol on homogeneous charge compression ignition of heptane. SAE Technical Paper 2008; 2008-01-2504.
- [81] Shi Y. Optimization of a compression ignition engine fueled with diesel and gasoline-like fuels. PhD Thesis. University of Wisconsin-Madison; 2009.
- [82] Srinivas P, Woo Y, Koo S, Hawkes ER. Ethanol utilisation in a diesel engine using dual-fuelling technology. *Fuel* 2013;109:597–607.
- [83] Zhang Y, De Ojeda W, Wickman D. Computational study of combustion optimization in a heavy-duty diesel engine using In-Cylinder blending of gasoline and diesel fuels. SAE Technical Paper 2012; 2012-01-1977.
- [84] Zhang Y, Sagalovich I, De Ojeda W, Ickes A, Wallner T, Wickman D. Development of dual-fuel low temperature combustion strategy in a multi-cylinder heavy-duty compression ignition engine using conventional and alternative fuels. SAE Technical Paper 2013; 2013-01-2422.
- [85] Li Y, Jia M, Liu Y, Xie M. Numerical study on the combustion and emission characteristics of a methanol/diesel reactivity controlled compression ignition (RCCI) engine. *Appl Energy* 2013;106:184–97.
- [86] Li Y, Jia M, Chang Y, Liu Y, Xie M, Wang T, et al. Parametric study and optimization of a RCCI (Reactivity controlled compression ignition) engine fueled with methanol and diesel. *Energy* 2014;65:319–32.
- [87] Liu J, Yang F, Wang H, Ouyang M. Numerical study of hydrogen addition to DME/CH₄ dual fuel RCCI engine. *Int J Hydrogen Energy* 2012;37(10): 8688–97.
- [88] Kokjohn SL, Hanson RM, Splitter DA, Kadatz J, Reitz RD. Fuel reactivity controlled compression ignition (RCCI) combustion in light- and heavy-duty engines. SAE paper 2011; 2011-01-0357.
- [89] Shi Y, Reitz RD. Study of diesel engine size-scaling relationships based on turbulence and chemistry scales. SAE Technical Paper 2008; 2008-01-0955.
- [90] Curran SJ, Prikhodko VY, Cho K, Sluder C, Parks JE, Wagner RM, et al. In-Cylinder fuel blending of gasoline/diesel for improved efficiency and lowest possible emissions on a multi-cylinder light-duty diesel engine. SAE paper 2010; 2010-01-2206.
- [91] Nieman D, Dempsey AB, Reitz RD. Heavy-duty RCCI operation using natural gas and diesel. SAE Paper 2012; 2012-01-0379.
- [92] Nieman D. Computational study and optimization of heavy-duty natural gas/diesel RCCI operation. MS thesis. University of Wisconsin-Madison; 2012.
- [93] Curran S, Hanson RM, Wagner RM. Effect of E85 on RCCI performance and emissions on a Multi-Cylinder light-duty diesel engine. SAE paper 2012; 2012-01-0376.
- [94] Prikhodko VY, Curran SJ, Barone TL, Lewis SA, Storey JM, Kukwon Cho, et al. Emission characteristics of a diesel engine operating with In-Cylinder gasoline and diesel fuel blending. SAE paper 2010; 2010-01-2266.
- [95] Splitter DA, Reitz RD. Fuel reactivity effects on the efficiency and operational window of dual-fuel compression ignition engines. *Fuel* 2014;118: 163–75.
- [96] Hanson RM, Curran SJ, Wagner RM, Kokjohn SL, Splitter DA, Reitz RD. Piston bowl optimization for RCCI combustion in a light-duty multi-cylinder engine. SAE paper 2012; 2012-01-0380.
- [97] Sluder C, Wagner R. An estimate of diesel high-efficiency clean combustion impacts on FTP-75 aftertreatment requirements. SAE Technical Paper 2006; 2006-01-3311.
- [98] Kenney T, Gardner T, Low S, Eckstrom J, Wolf LR, Korn SJ, et al. Overall results: phase-I ad hoc diesel fuel test program. SAE Technical Paper 2001; 2001-01-0151.
- [99] Splitter DA, Wissink M, Kokjohn SL, Reitz RD. Effect of compression ratio and piston geometry on RCCI load limits and efficiency. SAE Technical Paper 2012; 2012-01-0383, 2012.
- [100] Reitz RD, Kokjohn SL, Hanson RM, Splitter DA. Engine combustion control via fuel reactivity stratification. United states Patent 8,616,177 B2, 2013.

- [101] Curran S, Hanson RM, Wagner RM, Reitz RD. Efficiency and emissions mapping of RCCI in a light-duty diesel engine. SAE Paper 2013; 2013-01-0289.
- [102] Walker NR, Dempsey AB, Andrie MJ, Reitz RD. Use of low pressure direct-injection for reactivity controlled compression ignition (RCCI) light-duty engine operation. SAE paper 2013; 2013-01-1605.
- [103] Hanson RM, Curran S, Wagner RM, Reitz RD. Effects of biofuel blends on RCCI combustion in a light-duty, multi-cylinder diesel engine. SAE paper 2013; 2013-01-1653.
- [104] Wu Y, Hanson RM, Reitz RD. Investigation of combustion phasing control during reactivity controlled compression ignition (RCCI) multi-cylinder engine load transitions. J Eng Gas Turbines Power 2014;136(10):10. 091511-1.
- [105] Hanson RM. Experimental investigation of transient RCCI combustion in a light duty diesel engine. PhD thesis. University of Wisconsin-Madison; 2013.